



**NORTHERN COMMITTEE  
SIXTEENTH REGULAR SESSION**

ELECTRONIC MEETING  
[To be confirmed]

---

**Stock Assessment of Albacore Tuna in the North Pacific Ocean in 2020**

---

**WCPFC-NC16-2020/IP-03**

**ISC<sup>1</sup>**

---

<sup>1</sup> International Scientific Committee for Tuna and Tuna-like Species in the North Pacific Ocean

FINAL

ISC/20/ANNEX/12



## ANNEX 12

*20<sup>th</sup> Meeting of the  
International Scientific Committee for Tuna  
and Tuna-Like Species in the North Pacific Ocean  
Held Virtually  
July 15-20, 2020*

# **STOCK ASSESSMENT OF ALBACORE TUNA IN THE NORTH PACIFIC OCEAN IN 2020**

**July 2020**

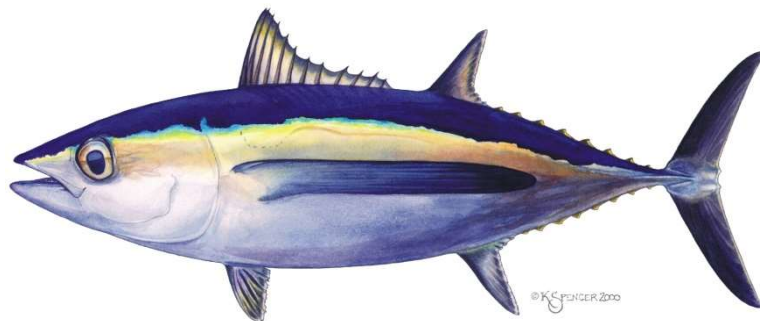
Left Blank for Printing

**FINAL**

**STOCK ASSESSMENT OF ALBACORE TUNA IN THE NORTH  
PACIFIC OCEAN IN 2020**

**REPORT OF THE ALBACORE WORKING GROUP**

**International Scientific Committee for Tuna and Tuna-like Species in  
the North Pacific Ocean**



**15 - 20 July 2020  
Web Meeting**

## TABLE OF CONTENTS

ACKNOWLEDGEMENTS.....	4
EXECUTIVE SUMMARY .....	5
1.0 INTRODUCTION.....	17
2.0 BACKGROUND .....	18
2.1 Biology.....	18
2.1.1 Stock structure.....	18
2.1.2 Reproduction.....	18
2.1.3 Growth.....	19
2.1.4 Movements .....	19
2.2 Fisheries.....	20
2.3 Important Changes from 2017 Assessment.....	20
2.3.1 Input sample sizes of size composition data .....	20
2.3.2 Japan pole-and-line fisheries .....	21
2.3.3 Japanese longline fisheries.....	21
3.0 DATA .....	21
3.1 Spatial Stratification .....	22
3.2 Temporal Stratification .....	22
3.3 Fishery Definitions .....	22
3.4 Catch.....	23
3.5 Relative Abundance Indices .....	23
3.5.1 F09 – Japanese longline index (1996 – 2018).....	23
3.5.2 F01 – Japanese longline index (1996 – 2018; sensitivity run).....	24
3.6 Size Composition.....	24
3.6 Sex Composition.....	25
4.0 MODEL DESCRIPTION.....	25
4.1 Stock Synthesis .....	25
4.2 Biological and Demographic Assumptions.....	26
4.2.1 Maximum age.....	26
4.2.2 Growth.....	26
4.2.3 Weight-at-length .....	27
4.2.4 Natural mortality .....	27
4.2.5 Sex specificity .....	27
4.2.6 Movement .....	27
4.2.7 Stock structure.....	28

4.2.8 Recruitment and reproduction .....	28
4.2.9 Initial conditions .....	29
4.3 Fishery Dynamics.....	29
4.3.1 Selectivity .....	29
4.3.2 Catchability.....	31
4.4 Data Observation Models .....	31
4.5 Data Weighting .....	32
4.6 Model Diagnostics.....	32
4.6.1 Model convergence .....	32
4.6.2 Age-Structured Production Model (ASPM) diagnostic.....	33
4.6.3 Likelihood profile on virgin recruitment ( $R_0$ ).....	33
4.6.4 Residual analysis.....	33
4.6.5 Retrospective Analysis .....	33
4.7 Sensitivity to Model Assumptions.....	33
4.8 Fishery Impact Analysis.....	34
4.9 Future Projections.....	34
5.0 STOCK ASSESSMENT MODELLING RESULTS.....	35
5.1 Model Convergence.....	35
5.2 Model Diagnostics.....	35
5.2.1 Model fit of abundance indices.....	35
5.2.2 Model fit of size composition data .....	35
5.2.3 Age-structured production model (ASPM) diagnostic .....	36
5.2.4 Likelihood Profiles on Virgin Recruitment ( $R_0$ ) .....	36
5.2.5 Retrospective Analysis .....	37
5.3 Model Parameter Estimates .....	37
5.3.1 Selectivity .....	37
5.3.2 Catch-at-Age.....	37
5.3.3 Sex Ratio .....	37
5.4 Stock Assessment Results .....	38
5.4.1 Biomass.....	38
5.4.2 Recruitment.....	38
5.4.3 Fishing intensity.....	38
5.5 Biological Reference Points .....	39
5.6 Sensitivity to Model Assumptions.....	39
5.6.1 Sensitivity 01 – Natural mortality.....	39
5.6.2 Sensitivity 02 – Steepness .....	40

5.6.3 Sensitivity 03 – Growth ..... 40

5.6.4 Sensitivity 04 – Catch estimates for F30, F31, and F32..... 40

5.6.5 Sensitivity 05 – Catch estimates for F33 during 2016 - 2018 ..... 40

5.6.6 Sensitivity 06 – Extended F09 index..... 41

5.6.7 Sensitivity 07 – Fit to F01 index..... 41

5.6.8 Sensitivity 08 – Size composition data weighting ..... 41

5.6.9 Sensitivity 09 – US longline asymptotic selectivity ..... 42

5.6.10 Sensitivity 10 – Equilibrium catch ..... 42

5.6.11 Sensitivity 11 – Start year ..... 42

5.6.12 Sensitivity 12 – 2017 base case model structure..... 43

5.7 Fishery Impact Analysis ..... 43

5.8 Future Projections ..... 43

6.0 STOCK STATUS..... 44

    6.1 Current Status ..... 44

    6.2 Conservation Information..... 45

7.0 KEY UNCERTAINTIES AND RESEARCH RECOMMENDATIONS..... 46

8.0 LITERATURE CITED..... 47

TABLES ..... 52

FIGURES..... 67

## **ACKNOWLEDGEMENTS**

The 2020 stock assessment of north Pacific albacore tuna is the result of a collaborative effort of the Albacore Working Group. Members of the Albacore Working Group who contributed to this assessment include Hidetada Kiyofuji (Chair), Akiko Aoki, Carolina Minte-Vera, Chiee-Young Chen, Daichi Ochi, Desiree Tommasi, Hirotaka Ijima, Hui-hua Lee, Kelsey James, Kevin Piner, Ko Fujioka, Mi Kyung Lee, Naoto Matusbara, Peter Kuriyama, Steve Teo, Yoshinori Aoki, and Zane Zhang. Steve Teo, with assistance from Hirotaka Ijima, and Kevin Piner, was the lead modeller on this assessment.



## EXECUTIVE SUMMARY

**Stock Identification and Distribution:** The north Pacific albacore tuna (*Thunnus alalunga*) stock area consists of all waters in the Pacific Ocean north of the equator to 55 °N. All available fishery data from this area were used for the stock assessment, under the assumption that there is instantaneous mixing of albacore on a quarterly basis, i.e., a single well-mixed stock.

**Important Changes from the 2017 Assessment:** There were three important changes to the base case model compared to the previous assessment in 2017. However, these changes were relatively minor compared to the changes between the 2014 and 2017 assessments. The three important changes were: **1)** Input sample sizes of the size composition data were allowed to vary between fisheries and over time, depending on the sampling that occurred, because of improvements in data preparation; **2)** The primary Japan pole-and-line fisheries were subdivided into seasonal fisheries, and the selectivity of the two most important Japanese pole-and-line fisheries were allowed to vary annually, if data were available. This approach substantially improved the model fits to the size composition data of these important fisheries; and **3)** The Japan longline fisheries that caught albacore in the main spawning area were also subdivided into seasonal fisheries with separate selectivity patterns, which improved fit to the size composition data. Sensitivity of assessment results to the model structure changes listed above are illustrated with a model using a similar structure to the base case model in the 2017 assessment, albeit with the same data as this assessment (Table ES1).

**Catches:** During the modeling period (1994-2018), the total reported catch of north Pacific albacore reached a peak of about 119,000 t in 1999 and then declined in the early 2000s, followed by a recovery in later years. However, catches have dropped to low levels during the last three years of the time series (2016 – 2018), with catches fluctuating between about 52,000 and 57,000 t (Fig. ES1). Surface gears (troll, pole-and-line), which primarily harvest juvenile albacore, have accounted for approximately twice as much albacore catch as longline gear (Fig. ES2)

**Data and Assessment:** All north Pacific albacore catch and size composition data from ISC member (Canada, China, Chinese Taipei, Japan, Korea, Mexico, and USA) and non-member countries were compiled for the assessment. Coherent fishery definitions, especially for the Japan longline and pole-and-line fisheries, improved model fits to the data and model diagnostics. Seven relative abundance indices (standardized catch-per-unit-effort) were provided by Japan and Chinese Taipei. Based on a thorough review of all fishery data and preliminary model runs, the Albacore Working Group (ALBWG) fitted the base case model to one abundance index, the Japanese longline index (F09 index) from the fishery operating south of 30°N and west of 160 °E (1996-2018). The F09 index was chosen because it represented the best information on trends for the adult age-classes of female albacore, had good contrast, and the results of age-structured production model (ASPM) analyses provided evidence that the F09 index was informative on both population trend and scale. The same primary index was used in the 2017 assessment.

The north Pacific albacore tuna stock was assessed using a length-based, age-, and sex-structured Stock Synthesis (SS Version 3.30.14.08) model over the 1994-2018 period. Biological parameters like growth and natural mortality ( $M$ ), were the same as for the 2017 assessment. Sex-specific growth curves were used because of evidence of sexually dimorphic growth, with adult males attaining a larger size-at-age than females after maturity. Sex-specific  $M$ -at-age vectors were developed from a meta-analysis, with a sex-combined  $M$  that scaled with size for ages 0-2, and sex-specific  $M$  fixed at 0.48 and 0.39  $y^{-1}$  for age-3+ females and males, respectively. The steepness of the Beverton-Holt stock-recruitment relationship was assumed to be 0.9, based on two prior analyses.

The assessment model was fitted to the F09 index (1996-2018) and all representative size composition data in a likelihood-based statistical framework. All fisheries were assumed to have dome-shaped length selectivity curves, and age-based selectivity for ages 1-5 were also estimated for surface fisheries (troll and pole-and-line) to address age-based changes in juvenile albacore availability and movement. Selectivity curves of the two fisheries with the largest catches (Japan pole-and-line in Area 3 during Q2 and Q3; F21 and F22 respectively) were allowed to have annually varying age-based selectivity, if data were available, to better represent variability in fishing operations and availability of juvenile age-classes, and hence improve model fits to the size composition data. Selectivity curves were also assumed to vary over time for fleets with important changes in fishing operations. Maximum likelihood estimates of model parameters, derived outputs, and their uncertainties were used to characterize stock status. Several sensitivity analyses were conducted to evaluate model performance or the range of uncertainty resulting from changes in model parameters, including natural mortality, stock-recruitment steepness, growth, starting year, selectivity patterns, and weighting of size composition data.

An ASPM diagnostic analysis, showed that the estimated catch-at-age and fixed productivity parameters (growth, mortality and stock-recruitment relationship without annual recruitment deviates) were able to explain trends in the F09 index. Based on these findings, the ALBWG concluded that the base case model was able to estimate the stock production function and the effect of fishing on the abundance of the north Pacific albacore stock. Similar to the 2017 assessment, the link between catch-at-age and the F09 index adds confidence to the data used and the results of the assessment. Due to the moderate exploitation levels relative to stock productivity, the production function was weakly informative about north Pacific albacore stock size, resulting in asymmetric uncertainty in the stock's absolute scale, with more uncertainty in the upper limit of the stock than the lower limit. It is important to note that the primary aim of estimating the female spawning biomass (SSB) in this assessment was to determine whether the estimated SSB was lower than the limit reference point (i.e., determine whether the stock is in an overfished condition). Since the lower bound is better defined, it adds confidence to the evaluation of stock condition relative to the limit reference point.

**Stock Status:** Estimated total stock biomass (males and female at age-1+) declines at the beginning of the time series until 2000, after which biomass becomes relatively stable (Fig. ES3A). Estimated female SSB exhibits a similar population trend, with an initial decline until 2003 followed by fluctuations without a clear trend through 2018 (Fig. ES3B). However, estimated recruitment reached historical lows in 2014 (~125 million fish; 95% CI: 69 – 180 million fish) and 2015 (~113 million fish; 95% CI: 56 – 170 million fish) (Fig. ES3C), which may have contributed to relatively low catches of fisheries catching juvenile albacore in recent years. It is currently unclear whether recruitment improved after 2015 because recruitment during the terminal years of the assessment (2016 – 2018) have large uncertainties (Fig. ES3C).

The estimated average SPR (spawners per recruit relative to the unfished population) during 2015 – 2017 is 0.50 (95% CI: 0.36 – 0.64), which corresponds to a moderate fishing intensity (i.e.,  $1-SPR = 0.50$ ). Instantaneous fishing mortality at age (F-at-age) is similar in both sexes through age-5, peaking at age-4 and declining to a low at age-6, after which males experience higher F-at-age than females up to age 12 (Fig. ES4). Juvenile albacore aged 2 to 4 years comprised approximately 70% of the annual catch between 1994 and 2018 (Fig. ES5). This is also reflected in the larger impact of the surface fisheries (primarily troll, pole-and-line), which remove juvenile fish, relative to longline fisheries, which primarily remove adult fish (Fig. ES6).

The Northern Committee (NC) of the Western and Central Pacific Fisheries Commission (WCPFC), which manages this stock together with the Inter American Tropical Tuna Commission (IATTC),

adopted a biomass-based limit reference point (LRP) in 2014 (<https://www.wcpfc.int/harvest-strategy>) of 20% of the current spawning stock biomass when  $F=0$  ( $20\%SSB_{\text{current}, F=0}$ ). The  $20\%SSB_{\text{current}, F=0}$  LRP is based on dynamic biomass and fluctuates depending on changes in recruitment. For north Pacific albacore tuna, this LRP is calculated as 20% of the unfished dynamic female spawning biomass in the terminal year of this assessment (i.e., 2018) (<https://www.wcpfc.int/meetings/nc13>). However, neither the IATTC nor the WCPFC have adopted F-based limit reference points for the north Pacific albacore stock.

Stock status is depicted in relation to the limit reference point (LRP;  $20\%SSB_{\text{current}, F=0}$ ) for the stock and the equivalent fishing intensity ( $F_{20\%}$ ; calculated as  $1-SPR_{20\%}$ ) (Fig. ES7A). Fishing intensity ( $F$ , calculated as  $1-SPR$ ) is a measure of fishing mortality expressed as the decline in the proportion of the spawning biomass produced by each recruit relative to the unfished state. For example, a fishing intensity of 0.8 is equivalent to fishing at  $F_{20\%}$  and will result in a SSB of approximately 20% of  $SSB_0$  over the long run. Fishing intensity is considered a proxy of fishing mortality.

The Kobe plot shows that the estimated female SSB has never fallen below the LRP since 1994, albeit with large uncertainty in the terminal year (2018) estimates. Even when alternative hypotheses about key model uncertainties such as growth were evaluated, the point estimate of female SSB in 2018 ( $SSB_{2018}$ ) did not fall below the LRP, although the risk increases with this more extreme assumption (Fig. ES7B). The  $SSB_{2018}$  was estimated to be 58,858 t (95% CI: 27,751 – 89,966 t) and 2.30 (95% CI: 1.49 – 3.11) times greater than the estimated LRP threshold of 25,573 t (95% CI: 19,150 – 31,997 t) (Table ES1). Current fishing intensity,  $F_{2015-2017}$  (0.50; 95% CI: 0.36 – 0.64; calculated as  $1-SPR_{2015-2017}$ ), was at or lower than all seven potential F-based reference points identified for the north Pacific albacore stock (Table ES1).

Based on these findings, the following information on the status of the north Pacific albacore stock is provided:

1. The stock is likely not overfished relative to the limit reference point adopted by the Western and Central Pacific Fisheries Commission ( $20\%SSB_{\text{current}, F=0}$ ), and
2. No F-based reference points have been adopted to evaluate overfishing. Stock status was evaluated against seven potential reference points. Current fishing intensity ( $F_{2015-2017}$ ) is likely at or below all seven potential reference points (see ratios in Table ES1).

**Biological Reference Points:** Biological reference points were computed with the base case model (Table ES1). It should be noted that the  $20\%SSB_{\text{current}, F=0}$  LRP is based on dynamic biomass and fluctuates depending on changes in recruitment. This LRP is calculated as 20% of the unfished dynamic female spawning biomass in the terminal year of this assessment (i.e., 2018). The coefficients of variation of the ratios of SSB/LRP were assumed to be the same as for SSB/ $SSB_0$ . In addition, all F-based reference points were calculated as the fishing intensity ( $1-SPR$ ) equivalents of the reference points. The point estimate of maximum sustainable yield (MSY; includes male and female of all age classes removed by fisheries) was 102,236 t (95% CI: 77,027 – 127,444 t) and the point estimate of female SSB to produce MSY ( $SSB_{\text{MSY}}$ ) was 19,535 t (95% CI: 14,840 – 24,229 t). The ratio of  $F_{2015-2017}/F_{\text{MSY}}$  was estimated to be 0.60 (95% CI: 0.43 – 0.77) and the ratio of  $SSB_{2018}/20\%SSB_{\text{current}, F=0}$  was estimated to be 2.30 (95% CI: 1.49 – 3.11). Current fishing intensity ( $F_{2015-2017}$ ) is at or below  $F_{\text{MSY}}$  and all MSY-proxy reference points, and  $SSB_{2018}$  is well above the LRP threshold (Table ES1).

**Future Projections:** Two 10-yr projection scenarios were conducted externally to the base case model to evaluate impacts on future female SSB: 1) F constant at the  $F_{2015-2017}$  level, and 2) constant catch at the average of 2013-2017 (69,354 t). Projections started in 2019 and continued for 10 years through 2028. Future recruitment was based on the expected recruitment variability ( $\sigma_R =$

0.3) of the recruitment time series (1994 – 2018) in the base case model. The overall sex-specific F-at-age was estimated from the base case model and used (scaled to the appropriate catch in the constant catch scenario) to remove albacore from the appropriate age and sex in the projected populations. There are two main sources of uncertainty in the projections: 1) uncertainty in the estimates of numbers-at-age in the terminal year; and 2) uncertainty in future recruitment.

Under the current fishing intensity ( $F_{2015-2017}$ ) scenario, female SSB is expected to increase to 62,873 t (95%CI: 45,123 – 80,622 t) by 2028, with a 0.2 % and <0.01 % probability of being below the LRP by 2020 and 2028, respectively (Fig. ES8). Similarly, employing the constant catch harvest scenario is expected to lead to an increased female spawning biomass of 66,313 t (CI: 33,463 – 99,164 t) by 2028. The probability that female SSB will be below the LRP in the constant catch scenario is higher than the constant  $F_{2015-2017}$  scenario but is still below 0.5% for all years (Fig. ES9). It should be noted that the projections, especially the constant  $F_{2015-2017}$  scenario, appear to underestimate the uncertainty due to a fixed F-at-age over time and a relatively low recruitment variability. Therefore, it is advisable to use the estimated future probabilities of breaching the LRP in a qualitative manner for management purposes until the projection software is improved. It also should be noted that the constant catch scenario is inconsistent with current management approaches for north Pacific albacore tuna adopted by the IATTC and the WCPFC.

**Conservation Information:** Two harvest scenarios were projected to evaluate impacts on future female SSB: F constant at the 2015-2017 rate over 10 years ( $F_{2015-2017}$ ) and constant catch<sup>1</sup> (average of 2013-2017 = 69,354 t) over 10 years. Median female SSB is expected to increase to 62,873 t (95% CI: 45,123 - 80,622 t) by 2028, with a low probability of being below the LRP by 2028, if fishing intensity remains at the 2015-2017 level (Fig. ES8). If future catch is held constant at 69,354 t, the female SSB is expected to increase to 66,313 t (95% CI: 33,463 - 99,164 t) by 2028 and the probability that female SSB will be below the LRP by 2028 is slightly higher than the constant F scenario (Fig. ES9). Although the projections appear to underestimate the future uncertainty in female SSB trends, the probability of breaching the LRP in the future is likely small if the future fishing intensity is around current levels.

Based on these findings, the following information is provided:

1. If a constant fishing intensity ( $F_{2015-2017}$ ) is applied to the stock, then median female spawning biomass is expected to increase to 62,873 t and there will be a low probability of falling below the limit reference point established by the WCPFC by 2028.
2. If a constant average catch ( $C_{2013-2017} = 69,354$  t) is removed from the stock in the future, then the median female spawning biomass is expected to increase to 66,313 t and the probability that SSB falls below the LRP by 2028 will be slightly higher than the constant fishing intensity scenario.

**Key Uncertainties:** The ALBWG notes that the lack of sex-specific size and age data, uncertainty in growth, and the simplified treatment of the spatial structure of north Pacific albacore population dynamics are important sources of uncertainty in the assessment.

---

<sup>1</sup> It should be noted that the constant catch scenario is inconsistent with current management approaches for north Pacific albacore tuna adopted by the Inter-American Tropical Tuna Commission (IATTC) and the Western and Central Pacific Fisheries Commission (WCPFC).

**Table ES1.** Estimates of maximum sustainable yield (MSY), female spawning biomass (SSB), and fishing intensity (F) based reference point ratios for north Pacific albacore tuna for: 1) the base case model; 2) an important sensitivity model due to uncertainty in growth parameters; and 3) a model representing an update of the 2017 base case model to 2020 data.  $SSB_0$  and  $SSB_{MSY}$  are the unfished biomass of mature female fish and at MSY, respectively. The Fs in this table are indicators of fishing intensity based on SPR and calculated as  $1-SPR$  so that the Fs reflect changes in fishing mortality (e.g.,  $F_{20\%}$  is calculated as  $1-SPR_{20\%}$ ). SPR is the equilibrium SSB per recruit that would result from the current year's pattern and intensity of fishing mortality. Current fishing intensity is based on the average fishing intensity during 2015-2017 ( $F_{2015-2017}$ ).  $20\%SSB_{current, F=0}$  is 20% of the current unfished dynamic female spawning biomass, where current refers to the terminal year of this assessment (i.e., 2018). The model representing an update of the 2017 base case model is highly similar to but not identical to the 2017 base case model due to changes in data preparation and model structure.

Quantity	Base Case	Growth CV = 0.06 for $L_{inf}$	Update of 2017 base case model to 2020 data
MSY (t) <sup>A</sup>	102,236	84,385	113,522
$SSB_{MSY}$ (t) <sup>B</sup>	19,535	16,404	21,431
$SSB_0$ (t) <sup>B</sup>	136,833	113,331	152,301
$SSB_{2018}$ (t) <sup>B</sup>	58,858	34,872	77,077
$SSB_{2018}/20\%SSB_{current, F=0}$ <sup>B</sup>	2.30	1.63	2.63
$F_{2015-2017}$	0.50	0.64	0.43
$F_{2015-2017}/F_{MSY}$	0.60	0.77	0.52
$F_{2015-2017}/F_{0.1}$	0.57	0.75	0.49
$F_{2015-2017}/F_{10\%}$	0.55	0.71	0.48
$F_{2015-2017}/F_{20\%}$	0.62	0.80	0.54
$F_{2015-2017}/F_{30\%}$	0.71	0.91	0.62
$F_{2015-2017}/F_{40\%}$	0.83	1.06	0.72
$F_{2015-2017}/F_{50\%}$	1.00	1.27	0.86

A – MSY includes male and female juvenile and adult fish

B – Spawning stock biomass (SSB) in this assessment refers to mature female biomass only.

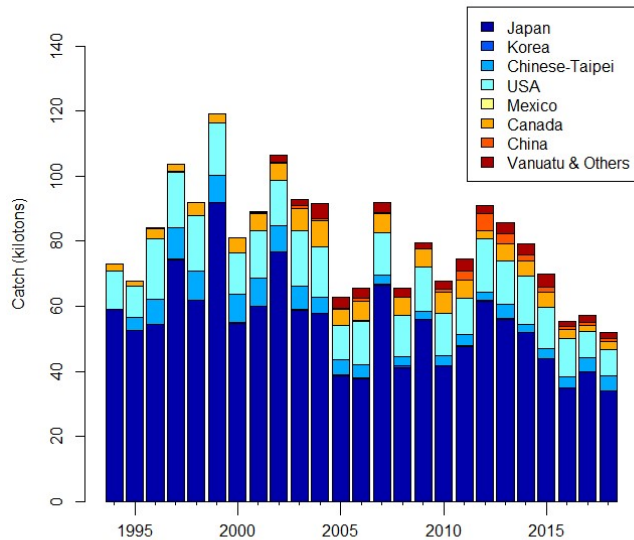


**Figure ES1.** Estimated total annual catch of north Pacific albacore (*Thunnus alalunga*) by all countries harvesting the stock, 1994-2018. Catches by Vanuatu and other countries includes small amounts of catch by other countries, including Tonga, Belize, Cook Islands, and Marshall Islands.

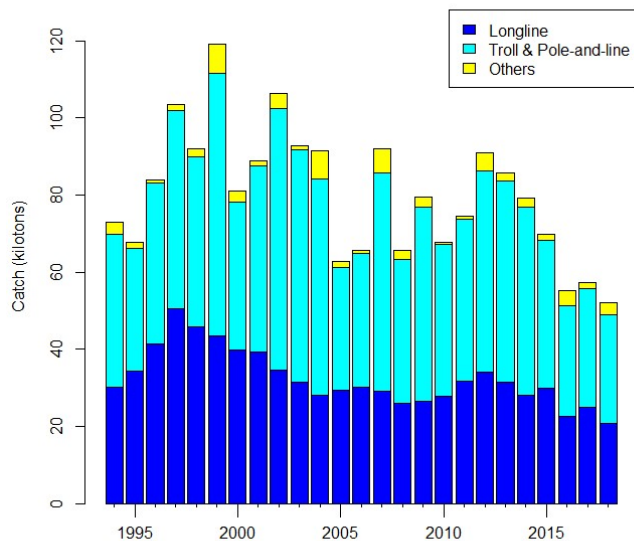
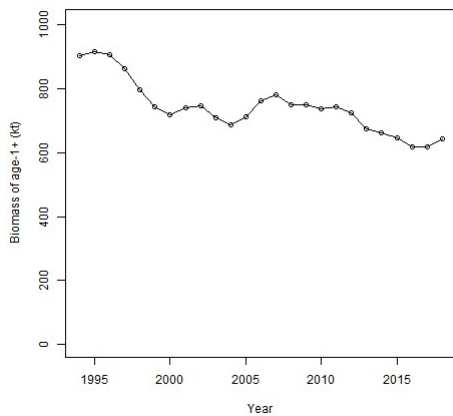
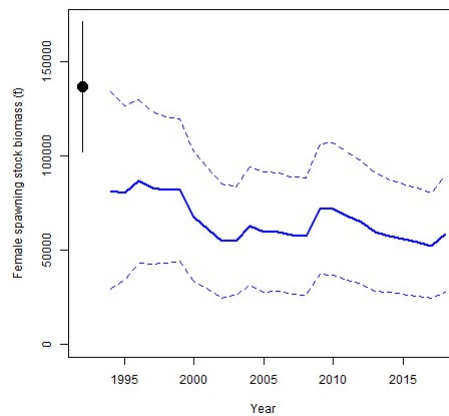


**Figure ES2.** Estimated catches of north Pacific albacore (*Thunnus alalunga*) by major gear types, 1994-2018. The Other gear category includes catches with purse seine, gillnet, hand lines, and harpoons.

A.



B.



C.

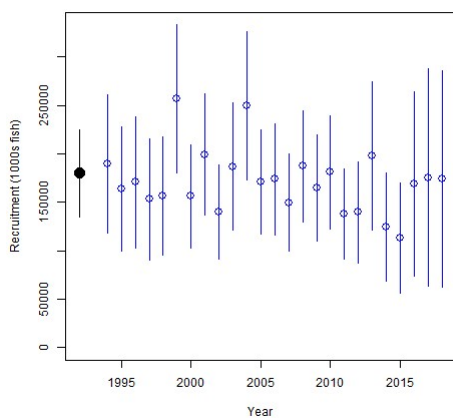


**Figure ES3.** Maximum likelihood estimates of (A) total age-1+ biomass (B), female spawning biomass (SSB) (solid blue line), and (C) age-0 recruitment (open circles) of north Pacific albacore tuna (*Thunnus alalunga*). Dashed lines (B) and vertical bars (C) indicate 95% confidence intervals of the female SSB and recruitment estimates respectively. Closed black circle and error bars in (B) are the maximum likelihood estimate and 95% confidence intervals of unfished female spawning biomass,  $SSB_0$ . Estimates of total biomass (A) are based on estimates from Quarter 1 of each year. Estimates of female SSB (B) and age-0 recruitment (C) are based on estimates from Quarter 2 of each year.

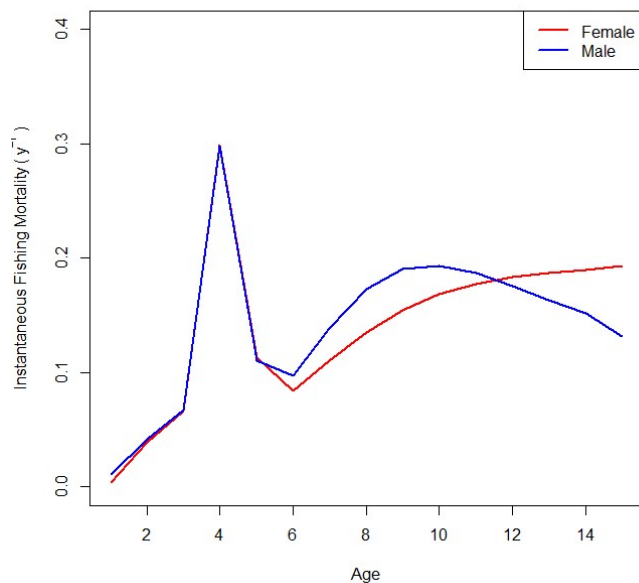


**Figure ES4.** Estimated sex-specific instantaneous fishing mortality-at-age (F-at-age) for the 2020 base case model, averaged across 2015-2017.

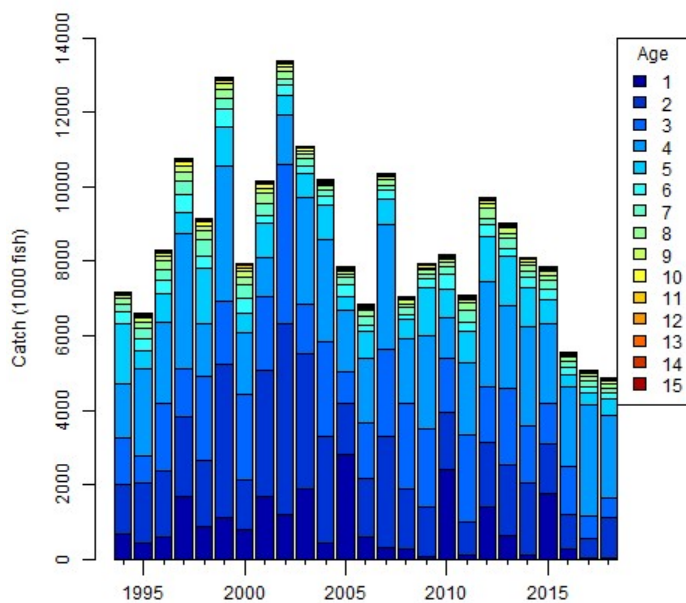


**Figure ES5.** Historical catch-at-age of north Pacific albacore (*Thunnus alalunga*) estimated by the 2020 base case model.



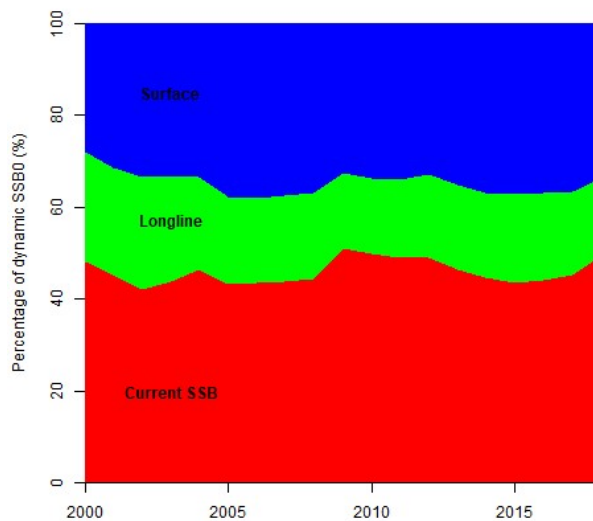


**Figure ES6.** Fishery impact analysis on north Pacific albacore (*Thunnus alalunga*) showing female spawning biomass (SSB) (red) estimated by the 2020 base case model as a percentage of dynamic unfished female SSB (SSB<sub>0</sub>). Colored areas show the relative proportion of fishing impact attributed to longline (USA, Japan, Chinese-Taipei, Korea, China, Vanuatu and others) (green) and surface (USA, Canada, and Japan) (blue) fisheries (primarily troll and pole-and-line gear, but including all other gears except longline).

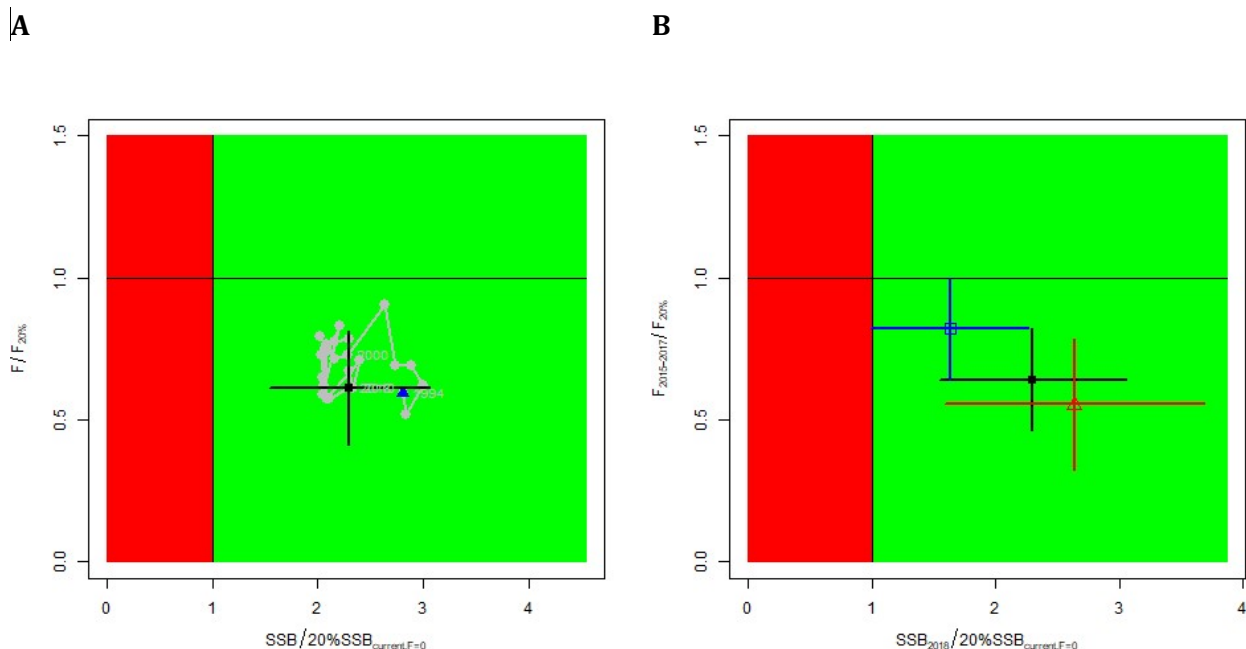


**Figure ES7.** (A) Kobe plot showing the status of the north Pacific albacore (*Thunnus alalunga*) stock relative to the  $20\%SSB_{current, F=0}$  biomass-based limit reference point, and equivalent fishing intensity ( $F_{20\%}$ ; calculated as  $1-SPR_{20\%}$ ) over the base case modeling period (1994-2018). Blue triangle indicates the start year (1994) and black circle with 95% confidence intervals indicates the terminal year (2018). (B) Kobe plot showing current stock status and 95% confidence intervals of the base case model (black; closed circle), an important sensitivity run of  $CV = 0.06$  for  $L_{inf}$  in the growth model (blue; open square), and a model representing an update of the 2017 base case model to 2020 data (red; open triangle). The coefficients of variation of the  $SSB/20\%SSB_{current, F=0}$  ratios are assumed to be the same as for the  $SSB/20\%SSB_0$  ratios.  $F_s$  in this figure are not based on instantaneous fishing mortality. Instead, the  $F_s$  are indicators of fishing intensity based on SPR and calculated as  $1-SPR$  so that the  $F_s$  reflects changes in fishing mortality. SPR is the equilibrium SSB per recruit that would result from the current year's pattern and intensity of fishing mortality. Current fishing intensity is calculated as the average fishing intensity during 2015-2017 ( $F_{2015-2017}$ ), while current female spawning biomass refers to the terminal year of this assessment (i.e., 2018). The model representing an update of the 2017 base case model is highly similar to but not identical to the 2017 base case model due to changes in data preparation and model structure.

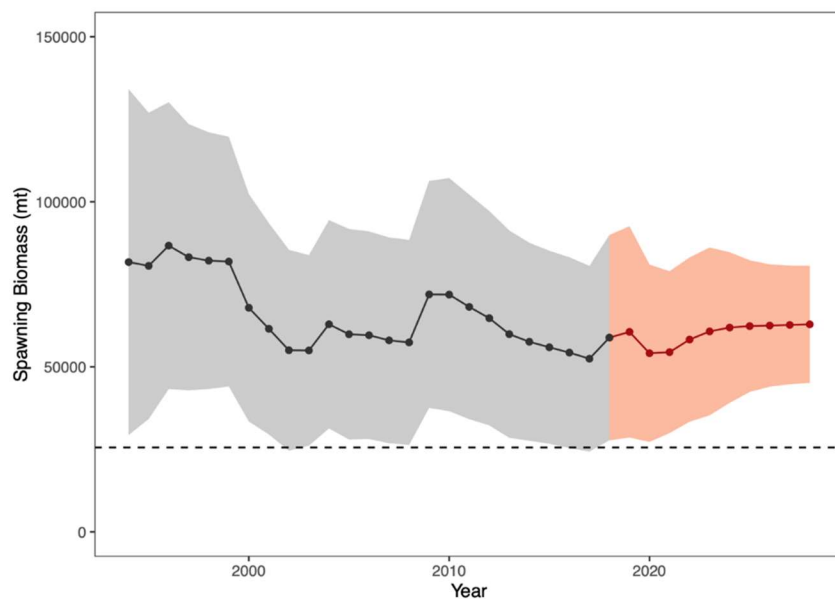


**Figure ES8.** Historical and future trajectory of north Pacific albacore (*Thunnus alalunga*) female spawning biomass (SSB) under a constant fishing intensity ( $F_{2015-2017}$ ) harvest scenario. Future recruitment is based on the expected recruitment variability. Black line and gray area indicates maximum likelihood estimates and 95% confidence intervals (CI), respectively, of historical female SSB, which includes parameter uncertainty. Red line and red area indicates mean value and 95% CI of projected female SSB, which only includes future recruitment variability and SSB uncertainty in the terminal year. Dashed black line indicates the  $20\%SSB_{\text{current } F=0}$  limit reference point for 2018 (25,573 t).

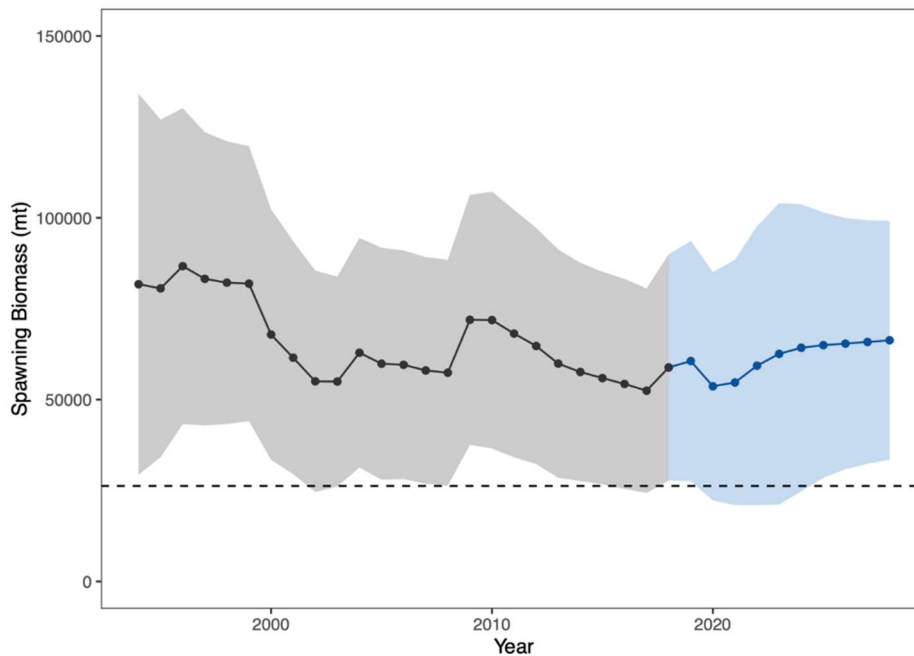


**Figure ES9.** Historical and future trajectory of north Pacific albacore (*Thunnus alalunga*) female spawning biomass (SSB) under a constant catch (average 2013-2017 = 69,354 t) harvest scenario. Future recruitment is based on the expected recruitment variability. Black line and blue area indicates maximum likelihood estimates and 95% confidence intervals (CI), respectively, of historical female SSB, which includes parameter uncertainty. Blue line and blue area indicates mean value and 95% CI of projected female SSB, which only includes future recruitment variability and SSB uncertainty in the terminal year. Dashed black line indicates the 20%SSB<sub>current F=0</sub> limit reference point for 2018 (25,573 t).

## 1.0 INTRODUCTION

The Albacore Working Group (ALBWG) of the International Scientific Committee for Tuna and Tuna-like Species in the North Pacific Ocean (ISC) is tasked with conducting regular stock assessments of north Pacific albacore tuna (*Thunnus alalunga*) to estimate population parameters, summarize stock status, and develop scientific advice on conservation needs for fisheries managers. The origins of the ALBWG date to 2005 when the *North Pacific Albacore Workshop*, which was established in 1974 to promote cooperative research and stock assessment analyses on north Pacific albacore, was integrated into the ISC. The ALBWG includes members from coastal states and fishing entities of the region (Canada, China, Chinese-Taipei, Japan, Korea, Mexico, USA) and members from relevant intergovernmental fishery and marine science organizations (e.g., Inter-American Tropical Tuna Commission, Secretariat of the Pacific Community).

The Northern Committee (NC) of the Western and Central Pacific Fisheries Commission (WCPFC), which manages this stock together with the Inter American Tropical Tuna Commission (IATTC), adopted a biomass-based limit reference point (LRP) of 20% of the current spawning stock biomass without fishing ( $20\%SSB_{\text{current}, F=0}$ ) (WCPFC 2014). The  $20\%SSB_{\text{current}, F=0}$  LRP is based on dynamic biomass and fluctuates depending on changes in recruitment. For north Pacific albacore tuna, this LRP is calculated as 20% of the unfished dynamic female spawning biomass in the terminal year of the assessment (<https://www.wcpfc.int/meetings/nc13>). However, neither the IATTC nor the WCPFC have adopted limit reference points based on fishing intensity or mortality for the north Pacific albacore stock.

The previous stock assessment in 2017 (ALBWG 2017) used an integrated, length-based, and age- and sex-structured forward-simulating statistical stock assessment model in the Stock Synthesis (SS) modeling framework (Methot and Wetzel 2013) to assess stock status. The ALBWG recognized that the adoption of the  $20\%SSB_{\text{current}, F=0}$  LRP emphasized the importance of estimating population scale from the assessment model. Based on this recognition, the ALBWG included three major changes in the 2017 base case model that were major improvements over the previous assessment in 2014. Most importantly, the ALBWG developed a new adult albacore abundance index that had good contrast and, based on Age-Structured Production Model (ASPM) diagnostic analyses (Maunder and Piner 2015a), was informative on both population trend and scale. Secondly, the start year of the base case model was changed from 1966 (in 2014) to 1993 (in 2017), which eliminated the influence of poorly fit size composition data from the Japanese longline fleets during 1975 – 1992, and eliminated the conflict between these size composition data and the primary adult albacore indices. Thirdly, the 2017 base case model used new sex-specific natural mortality ( $M$ ) at age vectors that were developed from a meta-analysis (Kinney and Teo 2016; Teo 2017), with a sex-combined  $M$  that scaled with size for ages 0-2, and sex-specific  $M$  fixed at 0.48 and 0.39  $y^{-1}$  for age-3+ females and males, respectively. Although biomass scale was uncertain, female spawning stock biomass (SSB) in the terminal year of the assessment (2015) was estimated to be 46.9 % of unfished SSB and fishing intensity on the stock was relatively low (i.e.,  $1-SPR_{2012-2014} = 0.51$ ). In 2017, the ALBWG concluded that the north Pacific albacore stock was not likely in an overfished condition relative to the  $20\%SSB_{\text{current}, F=0}$  LRP adopted by the WCPFC. Although there were no adopted LRPs based on fishing intensity or mortality, the ALBWG evaluated the average fishing intensity during 2012 – 2014 against seven potential reference points during the 2017 assessment, and concluded that the stock was not likely experiencing overfishing.

The ALBWG made three important changes to the base case model in this assessment compared to the previous assessment in 2017 (Section 2.3). However, these changes were relatively minor compared to the changes between the 2014 and 2017 assessments (ALBWG 2014, 2017). First, the

input sample sizes of the size composition data were allowed to vary between fisheries and over time, depending on the sampling that occurred, because of improvements in data preparation. Second, the Japan pole-and-line fisheries on their primary fishing grounds were also subdivided into seasonal fisheries, and the selectivity of these seasonal fisheries were allowed to vary annually, if data were available. Third, the Japan longline fisheries that caught albacore in the main spawning area were subdivided into seasonal fisheries with separate selectivity patterns, which improved fit to the size composition data.

This report presents the results of the 2020 assessment of north Pacific albacore tuna, and provides scientific advice on stock status and conservation information to fisheries managers. The assessment uses updated fishery data through 2018 in a length-based, age- and sex-structured integrated statistical stock assessment model fitted to an abundance index derived from Japanese longline fisheries data that was considered to be representative of adult albacore abundance in the north Pacific Ocean. The assessment was conducted through an online meeting due to the COVID-19 pandemic during 5 – 14 and 20 April 2020 (California time), and supersedes the 2017 assessment (ALBWG 2017). The objectives of this assessment are to: 1) understand the population dynamics of the north Pacific albacore tuna stock by estimating population parameters such as time series of recruitment, biomass and fishing intensity; 2) determine stock status by summarizing results relative to a suite of biological reference points, including the 20%SSB<sub>current, F=0</sub> LRP and MSY-based reference points; and 3) to provide conservation information for fisheries managers based on projections using constant fishing intensity and constant catch scenarios.

## 2.0 BACKGROUND

### 2.1 Biology

#### 2.1.1 Stock structure

Albacore tuna in the Pacific Ocean consist of the north Pacific stock (focus of this assessment) and the south Pacific stock. The discreteness of these stocks is supported by fishery data [lower catch rates in equatorial regions; Suzuki et al. (1977)], tagging data [there are no south Pacific Ocean recoveries of fish tagged in the north Pacific Ocean; Ramon and Bailey (1996)], ecological data [albacore larvae are rare in samples from equatorial waters; Ueyanagi (1969)], and genetic data [genetic differentiation between north and south Pacific albacore; Takagi et al. (2001)]. In addition, a recent study of single nucleotide polymorphisms of north Pacific albacore from a wide range of locations suggested that the north Pacific albacore stock is best thought of as a single, well-mixed stock with limited amounts of mixture from the south Pacific albacore stock (Vaux et al. in prep). Thus, north Pacific albacore is assumed to be a discrete, reproductively isolated stock, with no internal sub-group structure within the stock.

#### 2.1.2 Reproduction

Albacore are batch spawners, shedding hydrated oocytes, in separate spawning events, directly into the sea where fertilization occurs. Spawning frequency is estimated to be 1.7 d in the western Pacific Ocean (Chen et al. 2010), and batch fecundity ranges between 0.17 and 2.6 million eggs (Ueyanagi 1957; Otsu and Uchida 1959; Chen et al. 2010). Female albacore mature at lengths ranging from 83 cm fork length (FL) in the western Pacific Ocean (Chen et al. 2010) to 90 cm FL in the central Pacific Ocean (Ueyanagi 1957), and 93 cm FL in waters north of Hawaii (Otsu and Uchida 1959).

Spawning occurs primarily in tropical and sub-tropical waters between Hawaii (155°W) and the east coast of Taiwan and the Philippines (120°E) and between 10 and 25°N latitudes at depths exceeding 90 m (Ueyanagi 1957, 1969; Otsu and Uchida 1959; Yoshida 1966; Chen et al. 2010). Although spawning probably occurs over an extended period from March through September in the western and central Pacific Oceans, recent evidence based on a histological assessments of gonadal status and maturity (Chen et al. 2010) shows that spawning peaks in the March-April period in the western Pacific Ocean, which is consistent with evidence from larval sampling surveys in the same region (Nishikawa et al. 1985). In contrast, studies of albacore reproductive biology in the central Pacific Ocean have concluded that there was a probable peak spawning period between June and August (Ueyanagi 1957; Otsu and Uchida 1959), but these studies are based on indirect observation methods, are more than 50 years old, and have not been updated using modern histological techniques (e.g., see Chen et al. 2010).

### 2.1.3 Growth

Growth of albacore tuna is commonly modeled by a von Bertalanffy growth function, with rapid growth in immature fish followed by a slowing of growth rates at maturity and through the adult period. Growth in the first year of life is uncertain since these young fish are rarely captured in any of the active fisheries in the north Pacific Ocean. However, juvenile albacore recruit into intensive surface fisheries in both the eastern and western Pacific Oceans at age-2 and as a result, much better size-at-age and growth information is available. Early growth models combined both sexes because sex-specific fishery data were not collected, although it was known that adult males attained a larger size than females (Otsu and Uchida 1959; Yoshida 1966; Otsu and Sumida 1968). Chen et al. (2012) provided clear evidence of sexually dimorphic growth functions for males and females after they reach sexual maturity and reported that males attained a larger size and older age than females (114 cm FL and 14 years vs. 103.5 cm FL and 10 years, respectively).

A re-examination of the age and growth data compiled by Wells et al. (2013), some of which were used as conditional age-at-length data in the 2011 assessment, showed that for those individuals in which sex was recorded, there was clear evidence of sexually dimorphic growth between males and females (Xu et al. 2014). Given the clear evidence of sexual dimorphism in the growth and longevity of north Pacific albacore, the ALBWG used the same sex-specific male and female von Bertalanffy growth functions in this assessment as used in the 2014 and 2017 assessments. These growth parameters were estimated externally to the stock assessment model by Xu et al. (2014), who combined the sex-specific datasets compiled by Chen et al. (2012) and Wells et al. (2013). James et al. (2020a) concurred that the current sex-specific growth parameters are the best available scientific information but also suggested that the ALBWG collect sex-specific age-length samples using a coordinated biological sampling plan (James et al. 2020b) to improve current growth curves, and examine regional and temporal differences in length-at-age.

### 2.1.4 Movements

North Pacific albacore are highly migratory, with and these movements are influenced by oceanic conditions (e.g., Polovina et al. 2001; Zainuddin et al. 2006, 2008). The majority of the migrating population is believed to be composed of juvenile fish (i.e., immature animals that are less than 5 years old and 85 cm FL), which generally inhabit surface waters (0-50 m) in the Pacific Ocean. Some juvenile albacore undertake trans-Pacific movements and display seasonal movements between the eastern or western and central Pacific Ocean (Ichinokawa et al. 2008; Childers et al. 2011). The trans-Pacific movements track the position of the transition zone chlorophyll front (Polovina et al. 2001; Zainuddin et al. 2006, 2008) and increase when large meanders in the Kuroshio current occur, increasing albacore prey availability in the transition zone (Kimura et al. 1997; Watanabe et

al. 2004). Westward movements of juveniles tend to be more frequent than eastward movements (Ichinokawa et al. 2008), corresponding to the recruitment of juvenile fish into fisheries in the western and eastern Pacific Ocean and are followed by a gradual movement of older juveniles and mature fish to low latitude spawning grounds in the western and central Pacific Ocean. These general patterns may be complicated by seasonal movements of juvenile and adult fish, as well as sex-related movements of large adult fish, which may be predominately male, to areas south of 20°N. The significance of sex-related movements on the population dynamics of this stock is uncertain at present.

## 2.2 Fisheries

Albacore tuna is a valuable species with a long history of exploitation in the north Pacific Ocean (e.g., Clemens 1961). The total reported catch of north Pacific albacore for all nations combined (Figure 2.1) peaked at a 127,227 metric tonnes (t) in 1976 and then declined to a lowest observed catch in the time series (37,274 t) in 1991. Following this low point, total catch recovered to a second peak of 119,212 t by 1999. Total catch has generally fluctuated without a trend since 2000 but has declined to under 60,000 t in recent years (2016-2018). Average catch over the model time frame (1994-2018) was 79,951 t. Over the last five years (2014-2018), Japanese fisheries accounted for 65.3 % of the annual total harvest on average, followed by fisheries from the United States (17.5 %), Chinese-Taipei (6.0 %), Canada (5.2 %), China (1.8 %), Korea (0.2 %), and Mexico (0.0 %). During the same five year period, non-ISC countries, primarily Vanuatu, harvested an average of 4.0 % of the total annual catch.

The main gears deployed to harvest albacore in the north Pacific Ocean are longline, and troll and pole-and-line (Fig. 2.2). Surface fisheries capture smaller, juvenile fish, and include the USA and Canada troll and pole-and-line fisheries and Japanese pole-and-line fisheries. Over the model time frame (1994 – 2018), surface fisheries have harvested approximately 56.0 % of the north Pacific albacore catch. Longline fisheries, which fish deeper in the water column and tend to capture larger, mature albacore, were responsible for harvesting about 40.6 % of the albacore during the same period, with major fleets from Japan, USA, Chinese-Taipei, and recently China and Vanuatu. Pole-and-line catches in the 2000s exhibited greater year-to-year variability than other gear types due to target switching between skipjack (*Katsuwonus pelamis*) and albacore by some vessels on the fishing grounds off the east coast of Japan (Kiyofuji and Uosaki 2010). High gillnet catches of albacore in the 1980s reflect data from high seas driftnet fisheries that began in 1978 and ceased operations in 1993 as a result of United Nations General Assembly Resolution 44/225, which put in place a moratorium on the use of high seas driftnets (Uosaki et al. 2011).

## 2.3 Important Changes from 2017 Assessment

### 2.3.1 Input sample sizes of size composition data

In the 2017 base case model, the input sample sizes for each fishery were rescaled by a multiplier so that the average input sample size for each fishery was approximately the same as for the US longline fisheries (~7), which had the lowest number of fish sampled. This was in part due to inconsistent data preparation between fisheries, with size composition data of some fisheries being raised to the catch but not others. However, rescaling all fisheries to the same average input sample size resulted in the relatively low weighting per sample for well-sampled fisheries as compared with less sampled fisheries. For example, weighting per sample for one of the US longline fisheries was approximately 146x higher than for the best-sampled fishery, one of the Japan longline fisheries. Subsequently, the size composition data of the US longline fisheries and some Japanese longline fisheries were found to have relatively poor model fits, and were additionally down-



weighted with lambda factors of 0.1 to reduce the influence of their size composition data on the estimated population scale.

For the 2020 assessment, the ALBWG improved the data preparation by raising the size composition data statistically to represent the catch in numbers for all the fisheries that were fitted in the model. Based on this improvement, the input sample sizes were allowed to vary between fisheries and over time, depending on the sampling that occurred. The input sample sizes of the best-sampled fishery were rescaled by a multiplier such that the average input sample size for the fishery was  $\sim 30$  and the same multiplier was then used for all fisheries (see Section 4.4 for more details).

### **2.3.2 Japan pole-and-line fisheries**

The Japan pole-and-line fisheries are the largest source of removals for north Pacific albacore and the size composition data are highly variable. During the 2017 assessment, it was unclear if variability was due to inadequate sampling of the fisheries or the result of variability in fishery operations and/or availability of the fish. Therefore, the ALBWG focused on modeling the average selectivity of the fisheries and not allowing misfits to the size composition data to influence the estimated population scale. This resulted in adequate fits to the average size composition data from these fisheries but some individual strata had large misfits.

One of the foci in the 2020 assessment was to improve the fit to the size composition data of the Japanese pole-and-line fisheries because subsequent analysis suggested that the sampling of these fisheries was adequate to provide representative size composition data. The high variability of the size composition data was thought to be due to the variability in fishery operations and/or availability of different age classes of albacore in different areas at different times. For the 2020 assessment, the Japanese pole-and-line fisheries on the main fishing grounds were subdivided into seasonal fisheries. The selectivity curves of the Japanese pole-and-line fisheries were assumed to be a product of size selectivity and age selectivity because their size composition data exhibited very strong modes approximating juvenile age classes. In addition, the age-selectivity parameters of the two most important Japanese pole-and-line fisheries were allowed to vary annually, if the size composition data were available. These changes resulted in substantially improved model fits to the size composition data of the Japanese pole-and-line fisheries.

### **2.3.3 Japanese longline fisheries**

The movements of adult north Pacific albacore are poorly known but changes in the size composition data suggest that they exhibit seasonal movements between regions of the North Pacific Ocean. In the 2017 assessment, the Japanese longline fisheries on the main fishing grounds and the largest catches were subdivided into seasonal fisheries with separate selectivity patterns, which improved fit to the size composition data. In the 2020 assessment, the Japanese longline fisheries on the main spawning grounds were also subdivided into seasonal fisheries with separate selectivity patterns, which improved fit to the size composition data.

## **3.0 DATA**

Three types of data were used in this assessment: fishery-specific catches, size compositions, and abundance indices. These data were originally compiled from 1966 through 2018, but the ALBWG agreed to follow the decision made for the 2017 assessment (ALBWG 2017) and start the base case model in 1994 (Section 3.2). Therefore, only data from 1994 – 2018 are shown in this section. Data sources and temporal coverage of the available datasets are summarized in Figure 3.1.

### 3.1 Spatial Stratification

The geographic area of this assessment is the Pacific Ocean north of the equator (0°) to 55°N and from 120°E to 100°W (Fig. 3.2). This area includes all of the known catches of north Pacific albacore from 1994 through 2018. The base case model is not spatially explicit but fisheries were defined using multiple criteria, including fishing area, and therefore implicitly included spatial inferences (Table 3.1). Analyses of fishing operations and size composition data from Japanese and US longline vessels in the north Pacific showed that there were five areas with relatively consistent size distributions of albacore (ALBWG 2016; Ochi et al. 2016; Teo 2016) (Fig 3.2). These five fishing areas were used to define fisheries in the base case model (Section 3.3).

### 3.2 Temporal Stratification

The time frame of the 2020 assessment was 1994–2018. Catch and size composition data were compiled into quarters (Jan–Mar, Apr–Jun, Jul–Sep, Oct–Dec) and a quarterly time step was used in the base case model.

The 1994–2018 time frame for this assessment is an extension of the 2017 assessment (1993–2015) (ALBWG 2017) but is substantially shorter than the time frames used for earlier assessments, which had start years of 1966 (e.g., ALBWG 2014). Although the catch time series extended back to at least 1952 for some fisheries, a start year of 1994 was used because previous assessments had identified issues with the data and model parameters prior to 1994, especially during the 1980s and early 1990s (ALBWG 2014, 2017). These issues, still unresolved, included: 1) a large proportion of size samples from Japanese longline vessels during the 1980s and early 1990s consisted of large albacore ( $\geq 100$  cm FL) that were poorly fit with reasonable selectivity processes; 2) these observations of large albacore may be due differences in growth, especially the  $L_{inf}$  parameter, during the 1980s and early 1990s; 3) conflicts between poorly fit size composition data and the primary longline indices during the 1980s and early 1990s; and 4) uncertainty in the catch and bycatch of high seas driftnet vessels during the 1980s and early 1990s. Most importantly, starting the base case model in 1994 allowed the ALBWG to estimate population scale from the adult albacore index, which was informative on population scale. In addition, starting the model in 1994 allowed the ALBWG to avoid modelling potentially unrepresentative size composition data from the 1980s and early 1990s that may be misinformative on population scale. The start year of the base case model for the 2017 assessment (1993) was also meant to be congruent with major changes in logbook regulations for Japanese fisheries (Ijima et al. 2016). However, the ALBWG subsequently noted that 1994 was a more appropriate start year because 1994 was the year when the major changes in logbook regulations occurred (ALBWG 2019). Additional model runs were conducted to help the ALBWG understand the base case model structure of this assessment and evaluate the effect of different starting years on estimated quantities (Sections 4.7 and 5.6.10).

### 3.3 Fishery Definitions

Thirty-five (35) fisheries were defined for the assessment on the basis of gear, fishing area, season, and unit of catch (numbers or weight), and all catch and effort data were allocated to these fisheries (Table 3.1). The aim was to define relatively homogeneous fisheries with greater differences in selectivity and catchability between fisheries than temporal changes in these parameters within fisheries. This approach allowed the ALBWG to use differences in selectivity between fisheries as proxies for movement between fishing areas (Hurtado-Ferro et al. 2014a; Waterhouse et al. 2014) since movement information is not available. These fisheries consisted primarily of 27 longline fisheries from Japan (F01 – F19), USA (F25 & F26), Chinese-Taipei (F27 & F28), Korea (F29), China (F30 & F31), and Vanuatu (F32) (Table 3.1). There were also five pole-and-line fisheries from Japan

(F20 – F24), and the surface gears (primarily troll and pole-and-line) from Canada, Mexico, and the USA, which were combined into a single surface gear fishery (F33). In addition, high seas drift net catches from Japan, Korea, and Chinese-Taipei were combined into a single fishery (F34), which was important in the past but had zero catch during the modeling period; and catch from all other miscellaneous gears (e.g., purse-seine) from Japan and Chinese-Taipei were combined into a single miscellaneous fishery (F35). The approximate fishing area of each fishery can be deduced from Table 3.1 and Figure 3.2.

### 3.4 Catch

Estimates of total catch in each fishery were compiled by calendar quarter for 1966-2018 but only catch during 1994 – 2018 were used for the base case model (Fig. 3.3). Catch was reported and compiled in original units consisting of weight in metric tons (t) or 1000s of fish (Table 3.1).

### 3.5 Relative Abundance Indices

The ALBWG reviewed seven abundance indices, including Japanese longline (Fujioka et al. 2019, 2020), Japanese pole-and-line (Matsubara et al. 2019, 2020), Taiwanese longline (Chen and Cheng 2019) fisheries (ALBWG 2019). Based on this review and experience from the 2017 assessment, the ALBWG decided to continue using the abundance index from the Japanese longline fishery in Area 2 and Quarter 1 (F09; 1996-2018) as the index of adult albacore abundance (Fujioka et al. 2020). This index is highly similar to the adult index (S1 index) used in the 2017 assessment, albeit with three additional terminal years of data. The F09 index is an appropriate index for adult albacore in the north Pacific because the majority of the adult female albacore population in the north Pacific Ocean is thought to be in the western Pacific, especially Area 2. In addition, the F09 index had good contrast and preliminary ASPM analysis results showed that an ASPM was able to fit well to the index, which the ALBWG interpreted as an indication that the F09 index was informative on both population trend and scale.

The abundance index from the Japanese longline fishery in Areas 1 and 3 during Quarter 1 (F01; 1996-2018) was also investigated as a potential index of juvenile/subadult albacore abundance (Fujioka et al. 2020) but eventually rejected (ALBWG 2020). Visual comparison of the F01 and F09 indices suggested the F01 index was similar to the F09 index but with a lead of about 3 years. However, ASPM analysis and other model diagnostics of preliminary models fitting both F01 and F09 indices indicated a conflict between the indices. These preliminary model runs suggested that the F01 fishery was a mixture of two fleets, with two apparent size modes (one each for juvenile and adult fish) and variable proportions of each fleet over time. The ALBWG therefore decided to not fit to the F01 index in the base case model, but instead in a sensitivity run. Other indices were not considered in this assessment based on the experience from previous assessments.

Standardized annual values and input coefficients of variation (CVs) for the F09 index used in the base case model and F01 index used in sensitivity runs are shown in Table 3.2 and Figure 3.4. The relative weighting of the indices was controlled by adjusting the input CVs (Section 4.4).

#### 3.5.1 F09 – Japanese longline index (1996 – 2018)

The only index that was fitted in the base case model was developed by Fujioka et al. (2019, 2020) using set-by-set catch (number of albacore) and effort (1000s of hooks) data from logbooks of Japanese longline vessels operating in Area 2 in Quarter 1 (F09; Table 3.1) during 1996–2018. A Bayesian zero-inflated negative binomial generalized linear mixed effects model (Bayesian ZINB GLMM) was used to standardize the catch and effort data. Year, quarter, hooks-per-basket, and

fleet-type (distant-water, offshore, coastal) were used as fixed explanatory factors while location ( $5^{\circ} \times 5^{\circ}$  strata) and vessel were used as random effects (Fujioka et al. 2019, 2020). The ALBWG observed that the proportion of sets with zero albacore catch, species composition, and Pearson residuals were biased in 1994 and 1995 (ALBWG 2019; Fujioka et al. 2020). Therefore, similar to the 2017 assessment, the ALBWG decided to start the index in 1996 instead of 1994 (ALBWG 2019). Fujioka et al. (2020) had also developed indices for 1975–1993 but this index was not considered because the start year of the base case model was 1994. Further details on the data and standardization model can be found in Fujioka et al. (2019, 2020).

### **3.5.2 F01 – Japanese longline index (1996 – 2018; sensitivity run)**

The ALBWG investigated the F01 index as a potential index of juvenile/subadult albacore abundance but eventually rejected it for the base case model and instead only used this index in a sensitivity run (Section 3.5). The model (Bayesian ZINB GLMM), explanatory variables, and data source used for the F01 index were highly similar to the F09 index except for the fishing areas (Areas 1 and 3 instead of Area 2) (F01; Table 3.1). Following the F09 index, the start year of the F01 index was also 1996 (ALBWG 2019). Further details on the data and standardization model can be found in Fujioka et al. (2019, 2020).

## **3.6 Size Composition**

Quarterly length composition data from 1994 through 2018 were used in this assessment. Length data were available for 22 of the 35 fisheries in the base case model (Table 3.1 and Fig. 3.5) and were compiled into 2-cm size bins, ranging from 26 to 142 cm FL, where the labels are the lower boundary of each bin. Most of these fisheries exhibited clear modes when lengths were aggregated across quarters and years (Fig. 3.5). The length data for the Japanese pole-and-line fisheries (F20 – F24) exhibited exceptionally high variability in the number of modes and mean sizes between quarters and years.

The length frequency observations were the estimated catch-at-size (i.e., size compositions were raised to the catch) for 19 of the fisheries with size composition data and these size composition data were fitted in the base case model (Table 3.1). However, the size composition data from three of the fisheries (F30 – F32) were not raised to the catch and the base case model was not fitted to these data. Instead, it was assumed that the selectivity of these fisheries were the same as other longline fisheries with similar fishing operations and fishing area (Section 4.3.1).

The majority of albacore length composition data were collected through port sampling or on-board sampling by vessel crews or observers. Length data for the Japanese longline (F01 – F04; F09 – F12; F17; & F19) and pole-and-line fisheries (F20 – F24) were measured to the nearest cm at the landing ports or onboard fishing vessels from which catch-at-size data were derived (Ijima et al. 2017). Fork lengths of albacore in the EPO surface fishery (F33) were compiled from port samples of the US troll and pole-and-line fisheries (Teo et al. 2019). Although length composition data were available for the Canadian component of this fishery (2008-present), these data were not used because the USA and Canada components of the fishery overlap greatly in their fishing areas and size composition plots of both fisheries are very similar. The data from the USA component were thus considered representative of the entire fishery. Length compositions for the US longline fishery were collected by observers (Teo 2019). Albacore lengths for the Taiwanese longline fishery (F27) were measured onboard fishing vessels and compiled for 1995-2018 by the Overseas Fisheries Development Council (OFDC) of Chinese-Taipei (Chen and Cheng 2019). Length composition data prior to 2003 were not considered representative of catches by this fishery because they were sampled from a restricted geographic area and shorter annual time period than

the spatial and temporal scope at which the fishery was operating (ALBWG 2014). Thus, only the 2003-2018 size composition data were fitted in the base case model.

### 3.6 Sex Composition

Size composition data from Japanese longline training and research vessels are currently the primary source of sex ratio information for north Pacific albacore because sex composition data are not commonly collected by commercial fisheries. Although sample sizes of sexed individuals only ranged from about 10 to 300 fish per year, the sex composition data show that males reach larger sizes than females (Figure 3.6), and that the sex ratio of males to females becomes heavily biased towards males at large sizes (>100 cm FL) (Ashida et al. 2016). This bias towards males at large sizes has also been observed in south Pacific albacore (Farley et al. 2013), and is likely due to the sex-specific differences in growth (Williams et al. 2012; Chen et al. 2012) and/or natural mortality (Kinney and Teo 2016). Although sex composition data from Japanese training and research vessels were collected, the data were undocumented and not considered for the assessment. The sex composition data were instead used as a visual reference to the expected sex ratio from the base case model.

Japanese and US scientists have made substantial progress towards a polymerase chain reaction (PCR) based sex identification method for albacore tuna (Craig and Hyde 2020). Once the precision of this sex identification method has been established, the ALBWG would endeavour to collect sex ratio data from commercial fisheries for future assessments.

## 4.0 MODEL DESCRIPTION

The 2020 stock assessment of north Pacific albacore tuna was conducted using the Stock Synthesis (SS) modeling platform (Methot 2000; Methot and Wetzel 2013). A sex-specific, length-based, age-structured, forward-simulating, fully-integrated, statistical model was developed for the stock assessment. The specification of the base case model for north Pacific albacore followed several steps. First, the spatial and temporal extent of fisheries in the assessment were defined based on analyses of the biology and historical fishing operations of albacore fisheries (ALBWG 2016, 2019). Second, the data sources and inputs for these fisheries in the model, including total catch, indices of relative abundance, and size compositions were identified, collated and reviewed for completeness, trends, and outliers or unusual behaviour. Third, important biological parameters (e.g., growth, stock-recruitment relationship) were obtained from previous studies after review by the ALBWG and included in the model as fixed parameters, or estimated within the assessment model (Table 4.1). Based on these inputs, preliminary models were developed and iteratively refined through an analysis of model fits (e.g., total and component negative log-likelihoods) and diagnostic outputs (e.g., ASPM,  $R_0$  profiles, Pearson residuals) (ALBWG 2020), resulting in a base case model with several differences from the base case model in the 2017 stock assessment (ALBWG 2017). These differences included improvements in the data preparation and input sample sizes of size composition data, annually varying selectivity for the two most important Japanese pole-and-line fisheries, and subdividing the Japanese longline fisheries in the main spawning grounds into seasonal fisheries (Section 2.3).

### 4.1 Stock Synthesis

Stock Synthesis is a highly flexible, statistical age-structured population modeling platform that can incorporate multiple data types and account for a variety of biological, fishery, and environmental processes (Methot and Wetzel 2013). Importantly for this assessment, SS can model sex-specific

growth but fit to non-sex-specific observations. Although SS was initially developed for and used in US domestic stock assessments, particularly groundfish assessments on the US west coast, its use has spread to stock assessments of large pelagic fish like tunas and sharks because of the flexibility it provides for modelling multiple data types and processes.

The SS platform consists of three subcomponents: 1) a population dynamics subcomponent that simulates the assessed population (i.e., population numbers and biomass at age) using processes such as natural and fishing mortality, and the stock-recruitment relationship; 2) an observational subcomponent that relates the modeled population dynamics to observed quantities including abundance indices and size composition data; and 3) a statistical subcomponent that quantifies the fit of the observations to the simulated population using maximum likelihood methods. The 2020 north Pacific albacore assessment model was implemented using SS version 3.30.14.08, which is publicly available from NOAA (<https://vlab.ncep.noaa.gov/web/stock-synthesis/document-library>) (Methot 2000; Methot and Wetzel 2013).

## 4.2 Biological and Demographic Assumptions

### 4.2.1 Maximum age

The maximum age bin in the model was 15 years based on the maximum observed age (Wells et al. 2013). This bin served as the accumulator for all older ages. To avoid potential biases associated with the approximation of dynamics in the accumulator age, the maximum longevity was set at an age sufficient to result in near zero fish in this age bin ( $\approx 1$  percent of an unfished cohort).

### 4.2.2 Growth

The 2020 assessment used the same sex-specific growth curves as the base case model for the previous assessments in 2014 and 2017, which were based on the study by Xu et al (2014). Sex-specific growth curves were used because studies have found that north Pacific albacore tuna exhibit sex-specific growth, with male albacore exhibiting larger size at age after maturing and growing to larger size (Chen et al. 2012; Xu et al. 2014). Xu et al. (2014) combined age-at-length data from Chen et al. (2012), who primarily aged otolith samples from the northwestern Pacific, and Wells et al. (2013), who primarily obtained samples from the central and eastern North Pacific, to develop sex-specific growth curves covering the entire north Pacific Ocean.

A von Bertalanffy growth function, as parameterized by Schnute (1981), was used to model the relationship between fork length (cm) and age for north Pacific albacore:

$$L_2 = L_{inf} + (L_1 - L_{inf})e^{-K(A_2 - A_1)}$$

where  $L_1$  and  $L_2$  are the sizes associated with ages,  $A_1$  and  $A_2$ , respectively,  $L_{inf}$  is the asymptotic length, and  $K$  is the growth coefficient.

In this assessment,  $L_1$  was fixed at 43.504 and 47.563 cm for females and males at age 1, respectively (Table 4.1). The  $L_{inf}$  and  $K$  parameters were also fixed at sex-specific values from Xu et al. (2014) ( $L_{inf}$  - female: 106.570 cm, male: 119.150 cm;  $K$  - female: 0.2976  $y^{-1}$ , male: 0.2077  $y^{-1}$ ) (Fig. 4.1). The coefficients of variation (CVs) of size-at-age at  $L_1$  ( $CV_1$ ) and  $L_{inf}$  ( $CV_2$ ) were fixed at 0.06 and 0.04 for both female and male albacore in the base case model, based on estimates of these CVs during preliminary runs of the 2017 assessment. The  $CV_1$  parameter was well estimated in the preliminary runs because of the clear modal structure in juvenile size composition data and the model results were not highly sensitive to this parameter. However, the  $CV_2$  parameter was highly influential in the preliminary model results because of an interaction with the  $L_{inf}$  parameter. An

analysis of conditional age-at-length data found that the variability of size-at-age for older albacore was similar to juvenile albacore and that the CV was approximately 0.04 (Xu et al. 2014). Sensitivity analyses on the  $CV_2$  parameter and alternative growth models were performed (Table 4.6 and Section 5.6.3).

#### 4.2.3 Weight-at-length

Non sex-specific weight-length relationships are used to convert catch-at-length to weight-at-length data (Fig. 4.2). A previous study (Watanabe et al. 2006) reported that there were seasonal differences in the relationship between weight (kg) and fork length (cm) of north Pacific albacore. These non sex-specific seasonal weight-at-length relationships were used in this assessment (Table 4.1) and previous assessments in 2014 and 2017 (ALBWG 2014, 2017) because there were no previous studies documenting sex-specific differences in the weight-length relationships of north Pacific albacore.

#### 4.2.4 Natural mortality

The 2020 assessment used the same age and sex-specific parameters for  $M$  as the base model for the previous assessment in 2017, which were based on study by Teo (2017) (Table 4.1). In assessments prior to 2017,  $M$  was assumed to be  $0.3 \text{ y}^{-1}$  for both sexes at all ages but this assumption was not well supported (Kinney and Teo 2016). First, the ALBWG incorporated results from studies that used meta-analytical methods on a range of empirical relationships between  $M$  and life history parameters (Hamel 2015; Then et al. 2015; Kinney and Teo 2016; Teo 2017), which identified an  $M$  of  $0.38$  and  $0.49 \text{ y}^{-1}$  for adult male and female albacore tuna, respectively. These results corresponded well to an independent study of tagging data, which estimated a non sex-specific  $M$  of  $0.45 - 0.5 \text{ y}^{-1}$  for north Pacific albacore (Ichinokawa et al. 2008). Based on these results, the ALBWG assumed that the  $M$  of juvenile north Pacific albacore tuna followed a Lorenzen (1996) relationship between size and  $M$  for age-0 to age-2, with no difference between the sexes until age-3. Upon reaching age-3, the  $M$  for male albacore is assumed to be  $0.38 \text{ y}^{-1}$  and the  $M$  for female albacore is assumed to be higher, reaching  $0.49 \text{ y}^{-1}$ , which may reflect the cost of reproduction. Sensitivity analyses on the  $M$  parameters were performed (Table 4.6 and Section 5.6.1).

#### 4.2.5 Sex specificity

A sex-specific (two sex) model was used for this assessment because of sex-specific differences in growth (Chen et al. 2012; Xu et al. 2014) and natural mortality (Kinney and Teo 2016; Teo 2017) of north Pacific albacore. In addition, males predominate in longline catches of large, mature albacore from Japanese research and training vessels, while juveniles <85 cm generally have a sex ratio of 1:1 (Ashida et al. 2016). However, there are currently no data on the sex of individual fish caught by commercial fisheries. As described above, sex-specific growth curves and natural mortality were used in the base case model. However, the base case model did not include sex-specific selectivity, and sex ratio at birth was assumed to be 1:1.

#### 4.2.6 Movement

This stock assessment did not have explicit spatial structure and did not explicitly model the movements of north Pacific albacore. North Pacific albacore are known to exhibit seasonal and ontogenetic movements (e.g., Ichinokawa et al. 2008; Childers et al. 2011), but it is not currently feasible to develop a spatially explicit assessment model due to the lack of well designed, and consistent tagging data. Instead, selectivity patterns for fisheries were used as a proxy for spatial structure, which helps to compensate for potential biases caused by the lack of explicit spatial

structure in the assessment model (Hurtado-Ferro et al. 2014a). The collection and pre-processing of fishery data in this assessment are area-specific, especially Japanese longline fisheries, and therefore contain spatial inference (Section 3.3).

#### 4.2.7 Stock structure

The current stock assessment assumes a single stock of albacore in the north Pacific Ocean from the equator to 55°N latitude and between 120°E and 100°W longitude (Fig. 3.2). This assumption is supported by evidence from tagging, and seasonal fishing pattern studies (Suzuki et al. 1977; Ichinokawa et al. 2008; Childers et al. 2011). Studies of albacore population genetics (Chow and Ushiyama 1995; Takagi et al. 2001; Montes et al. 2012) support the hypothesis of two stocks in the Pacific Ocean, but do not provide conclusive results on finer scale structure. More recently, a study of single nucleotide polymorphisms of north Pacific albacore from a wide range of locations suggested that the north Pacific albacore stock is best thought of as a single, well-mixed stock with limited amounts of mixture from the south Pacific albacore stock (Vaux et al. in prep).

#### 4.2.8 Recruitment and reproduction

North Pacific albacore were assumed to have one spawning and recruitment period in the second quarter of the year (Q2) based on recent histological assessments of gonadal status and maturity from the western Pacific Ocean (Chen et al. 2010; Ashida et al. 2016). Although historical circumstantial evidence supported spawning in the central Pacific Ocean near Hawaii through the third quarter of the year (e.g., Otsu and Uchida 1959), there is no recent confirmation of this spawning segment so it was not considered in the assessment. Ashida et al. (2016) also recently estimated the length at 50% maturity for female north Pacific albacore at 86 cm, which was approximately the expected length at age-5. Based on this finding, the ALBWG assumed that 50% of the albacore at age-5 were mature and that all fish age-6+ were mature (Fig. 4.3). This maturity ogive has been used in the previous assessments since 2006 (ALBWG 2014).

A standard Beverton-Holt stock recruitment relationship was used in this assessment. The expected annual recruitment was a function of spawning biomass with steepness ( $h$ ), virgin recruitment ( $R_0$ ), and unfished equilibrium spawning biomass ( $SSB_0$ ) corresponding to  $R_0$ , and was assumed to follow a lognormal distribution with standard deviation  $\sigma_R$  (Methot 2000; Methot and Wetzel 2013). Annual recruitment deviations were estimated based on the information available in the data and the central tendency that penalizes the log (recruitment) deviations. A log-bias adjustment factor was used to assure that the estimated log-normally distributed recruitments were mean unbiased (Methot and Taylor 2011).

Recruitment variability ( $\sigma_R$ ) was fixed at 0.3 to approximate the expected variability of preliminary models, which had recruitment variability ranging from 0.25 to 0.30 depending on model configuration. The log of  $R_0$ , annual recruitment deviates, and the offset for the initial recruitment relative to virgin recruitment,  $R_I$ , were estimated in the base case model. The choice of estimating years with information on recruitment was based on a preliminary model run with all recruitment deviations estimated (1994 – 2018). The first few years of size composition data often contain some information on recruitment from early cohorts before 1994 and the variability of recruitment deviations often increases as the information content decreases the further back in time prior to starting year examined (Methot and Taylor 2011). The number of years for which recruitments may be observed from the early cohorts was selected and the initial recruitment deviances were estimated in the model. Ten annual deviations were estimated prior to the start of the model in 1994 (i.e., 1984-1993). The 10-year period was chosen because early model runs showed negligible information on deviates more than 10 years prior to the beginning of the data. Bias adjustment was



used to account for the reduction in information content from the data on recruitment deviations during the early and late periods. This adjustment mostly affects the estimation of uncertainty and not the population trajectory.

Steepness of the stock-recruitment relationship ( $h$ ) was defined as the fraction of recruitment from a virgin population ( $R_0$ ) when the spawning stock biomass is 20% of its unfished level ( $SSB_0$ ). Recently, Lee et al. (2012) concluded that if the model is correctly specified, then steepness is estimable for relatively low productivity stocks with good contrast in spawning stock biomass. However, estimating  $h$  within the assessment model for north Pacific albacore is likely to be imprecise and biased because contrast in the spawning biomass over the assessment period is relatively poor. Two independent estimates of steepness for north Pacific albacore (Brodziak et al. 2011; Iwata et al. 2011), based on the life history approach of Mangel et al. (2010), reported values of  $h$  ranging from 0.84 to 0.95. Therefore, the ALBWG assumed a  $h$  of 0.9 in this assessment, which was the same as the 2014 and 2017 assessments, and performed sensitivity analyses within a plausible range of  $h$ , and estimating  $h$  with a prior (Section 5.6.2). Nevertheless, the ALBWG notes that these steepness estimates are subject to considerable uncertainty and further work is needed to evaluate steepness estimates.

#### 4.2.9 Initial conditions

A model must assume something about the period prior to the start of the main population dynamics period. Typically, two approaches are used to achieve this assumption. The first approach starts the model as far back as necessary to satisfy the notion that the period prior to the estimation of dynamics was in an unfished or near unfished state. However, this approach is not viable for this assessment because the base case model started in 1994 (Section 3.2). Instead, a second approach was used in which initial conditions were estimated (where possible) assuming equilibrium catch. The equilibrium catch is the catch taken from a fish stock when it is in equilibrium with fishery removals and natural mortality balanced by stable recruitment and growth. The initial fishing mortality rates in the assessment model that remove these equilibrium catches were estimated to allow the model to start at an appropriate depletion level. Initial fishing mortality rates were estimated for the F27 (Taiwanese longline in Areas 3 & 5) because it captures a wide size range of albacore, but the initial fishing mortality rates were not fitted to historical catches prior to 1994. This approach allowed the model to start in 1994 at a depletion level that was consistent with the adult abundance index and size composition data without being overly constrained. In addition, the model included estimation of 10 recruitment deviations prior to 1994 to develop a non-equilibrium age structure at the start of the model time frame.

### 4.3 Fishery Dynamics

#### 4.3.1 Selectivity

The base case model has a sex-specific structure, with sex-specific growth curves. However, it was assumed that female and male albacore have identical size selectivity for each fishery because sex-specific size composition data were not available. Selectivity curves were fishery-specific and assumed to be a function of only size for all but five fisheries (Table 4.1). Preliminary model runs indicated that size composition data of the Japanese pole-and-line fisheries in Area 3 (F20, F21, F22, F23) and the EPO surface fishery (F33) had very strong modes corresponding to juvenile age classes and could not be adequately fit using only size selectivity curves. Therefore, the selectivity curves of F20, F21, F22, F23, and F33 were assumed to be a product of size and age, which improved model fits. The age-based selectivity was intended to capture differences in the availability of juvenile fish to the fishing gear based on movement patterns, which may vary

between seasons and years. Selectivity curves were estimated for all fisheries with representative size composition data while selectivity curves for fisheries without representative size composition data were assumed to be the same as fisheries with similar operating characteristics (season, area, gear) and estimated selectivity curves. If specific fisheries had changes in fishery operations or exhibited changes in size composition data consistent with changes in movement patterns, then selectivity was allowed to vary with time to account for these changes. Highlights of the parameterization of the selectivity curves are briefly described below but more details can be found in Tables 4.2, 4.3, 4.4, and 4.5.

Selectivity curves for longline fisheries and the Japanese pole-and-line fishery in Area 2 (F24) were assumed to be dome-shaped, and were modeled using either double-normal functions (F02, F04, F09, F10, F11, F12, F19, F24, F25, F26, and F27) or spline functions (F01, F03, and F17), depending on the size data and model fit. (Table 4.2) Fisheries were first fitted with double-normal functions but F1, F3, and F13 were found to have inadequate model fits with this approach. These three fisheries were subsequently fit with spline functions, which are substantially more flexible. The double-normal selectivity functions were configured to use four parameters: 1) peak, which is the initial length at which albacore were fully selected; 2) width of the plateau at the top; 3) width of the ascending limb of the curve; and 4) width of the descending limb of the curve. If the estimated width of the plateau at the top was negligible and tended to hit the lower bounds, then that parameter was fixed at a small value. The spline selectivity functions were configured to be three knot splines. The first and third knots were generally located near the edges of the respective size compositions, while the second knot was typically located near the midpoint between the first and third knot. However, the locations of the knots were subject to some trial and error. The values of two of the three knots were estimated relative to the value of the third knot, which was fixed at an arbitrary value. The gradients before the first knot and after the third knot were also estimated.

Selectivity curves of the Japanese pole-and-line fisheries in Area 3 (F20, F21, F22, and F23) and the EPO surface fishery (F33) were assumed to be a product of size and age because their size composition data exhibited very strong modes corresponding to juvenile age classes (Table 4.3 and 4.4). The size selectivity curves for these fisheries were assumed to be dome-shaped and were modeled using double normal functions, which were configured as described above. The age selectivity of the juvenile age-classes (age-1 through age-5) of these three fisheries were estimated as free parameters. If the age selectivity parameter of an age class hit the upper or lower bound, that parameter was fixed at the upper or lower bound during the final model run to stabilize the optimization of the model. The interactions between the age and size selectivity functions for these three fisheries were difficult to visualize but resulted in substantially improved fits to their size composition data.

The selectivity curves for fisheries lacking representative size composition data (F05, F06, F07, F08, F13, F14, F15, F16, F18, F28, F29, F30, F31, F32, F34, and F35) were assumed to be the same as (i.e., mirrored to) closely related fisheries or fisheries operating in the same area (Table 4.5). For example, the selectivity of F05 was assumed to be the same as F01 because F05 was identical to F01 except for their catch units (Table 3.1).

Selectivity curves for relative abundance indices were assumed to be the same as the fishery from which each respective index was derived. Size selectivity for the F09 and F01 indices were assumed to be the same as the F09 and F01 longline fisheries, respectively.

Selectivity curves were allowed to vary over time for fisheries exhibiting important changes in fishery operations or if large changes in fish availability during certain periods were observed as changes in the size composition data. The Japanese pole-and-line fisheries exhibited highly variable

size composition data, which was thought to be due to the variability in fishery operations and/or availability of different age classes of albacore in different areas at different times. The age-selectivity parameters of the two most important Japanese pole-and-line fisheries (F21 and F22) were allowed to vary annually, if the size composition data were available (Table 4.4). The US longline fisheries (F25 and F26) had major regulatory changes during 2001 to 2005 to mitigate turtle bycatch, which likely affected fishing operations after 2005 (Table 4.2). The fishing operations of the EPO surface fishery (F33) were found to have changed after 1998, with the fishery moving closer to the US West Coast during and after 1999 (Xu et al. 2013) (Table 4.4).

#### 4.3.2 Catchability

Catchability,  $q$ , was estimated (solved analytically) assuming the abundance index was proportional to vulnerable biomass with a scaling factor of  $q$ . It was assumed that  $q$  was constant over time for each index.

### 4.4 Data Observation Models

The current assessment model fitted three data components: 1) total catch, 2) relative abundance indices, and 3) size composition data. The observed total catches were assumed to be unbiased and relatively precise, and were fitted assuming a lognormal error distribution with standard error (SE) of 0.05.

The relative abundance indices were assumed to have lognormally distributed errors with SE in log space, which is approximately equivalent to CV ( $SE/estimate$ ) in natural space. The estimated CVs of each index in this assessment were described in Fujioka et al. (2019, 2020) (Table 3.2). However, the reported CVs for the abundance indices only capture observation errors within the standardization model and do not reflect process errors that are inherent in the link between the unobserved vulnerable population and observed abundance indices. The longline indices were fitted to a second-degree loess smoother with a span of 0.75 and the CV of the indices relative to the loess smoother was calculated ( $CV_{loess}$ ). An additional constant was added to the CVs of the indices, such that the average CV for any index was equivalent 0.2 or the estimated  $CV_{loess}$ , whichever was greater. Therefore, a constant of 0.100 was added to the CVs of the F9 index in the base case model, and 0.165 to the CVs of the F1 index in sensitivity model runs.

The size composition data were assumed to have multinomial error distributions with the error variance determined by the effective sample size ( $effN$ ). Size measurements of fish are usually not random samples of fish from the entire population, but are instead highly correlated within each set or trip (Pennington et al. 2002). The effective sample size is usually substantially lower than the actual number of fish measured because the variance within each set or trip is substantially lower than the variance within a population. The initial effective sample size was set to the number of trips from which fish were measured to account for the lower variance within a trip relative to the population. Since most albacore fisheries only record the number of fish, an analysis of the EPO surface fishery (F33) was used to relate the number of fish sampled to the number of trips. Based on this analysis, we assumed that 100 fish sampled were equivalent to a sampled trip. Size composition records with sample size of  $<1$  were considered unrepresentative and removed. The input sample sizes for each fishery were further rescaled by a multiplier (0.1626) so that the average input sample size for fishery with the most fish sampled (F01) was approximately 30. Therefore, the input sample sizes varied between fishery and over time, depending on the sampling that occurred for that fishery and period.

## 4.5 Data Weighting

Statistical stock assessment models fit a variety of data components, including abundance indices and size composition data. The results of these models can depend substantially on the relative weighting between different data components (Francis 2011). A statistical approach using the maximum likelihood estimates of variances or effective sample sizes to weight each data component by model fit (Deriso et al. 2007; Maunder 2011) tends to put too much weight on size composition data because numerous important processes such as variability in movements and selectivity are often not modeled or mis-specified. As a result, many assessments now weight different components based on expert knowledge of the data sampling, fishery operations, and biology of the stock, in order to balance or prioritize information from various data components.

Relative abundance indices were prioritized in this assessment based on the principle that relative abundance indices should be fitted well and that other data components such as size composition data should not induce poor fits to the abundance indices because abundance indices are a direct measure of population trends and scale (Francis 2011). Preliminary models indicated that the size composition data from the F09 longline fishery degraded the fit of the F09 abundance index, especially relative to the ASPM model fit to the index (ALBWG 2020). The weighting to the size composition data from the F09 fishery were down-weighted by reducing the size composition sample size multiplier from 0.1626 (Section 4.4) to 0.01626, which is in effect multiplying the likelihoods of these data by 0.1. Down-weighting these size compositions resulted in improved model fits to the F09 abundance index. The effect of these data weightings on model results was investigated using sensitivity runs.

In addition, the ALBWG used the Francis data weighting method (TA1.8 in Francis 2011) to examine the weighting of each fishery's size composition data relative to how well the model fitted to the data. Results from preliminary models indicated that three fisheries (F01, F23, and F27) had size composition data that were over-weighted (i.e., Francis weighting multiplier of  $<1.0$ ). The weighting to the size composition data from the F01, F23, and F27 fishery were down-weighted by reducing the size composition sample size multiplier from 0.1626 (Section 4.4) to 0.09756, 0.14634, and 0.13008, respectively. These sample size multipliers correspond to down-weighting the size composition data of these fisheries by 40, 10, and 20%, respectively, resulting in Francis weighting multipliers of these three fisheries in the base case model of approximately 1.

## 4.6 Model Diagnostics

Model diagnostics were used to assess issues associated with convergence, model structure, parameter mis-specification, and data conflicts in the 2020 base case model. The following diagnostic tools were employed in this assessment: 1) model convergence tests, 2) Age-Structured Production Model (ASPM) diagnostic, 3)  $R_0$  likelihood profiles, 4) residual analysis, and 5) retrospective analysis.

### 4.6.1 Model convergence

Convergence to the global minima was examined by changing initial parameter values and the order of phases used in the optimization procedure. Particular attention was placed on the initial value and estimation phase of parameters, such as  $R_0$ , that influence population scale because these changes force the model to search over a vastly expanded portion of the likelihood surface. In addition, all initial parameter values were randomly jittered by sampling from a uniform distribution centered at input parameter values with upper and lower bounds of  $\pm 10\%$ . The

optimized likelihood and  $R_0$  values were examined from 50 such model runs to ensure that these model runs did not find a solution with better likelihoods.

#### **4.6.2 Age-Structured Production Model (ASPM) diagnostic**

Following the proposal by Maunder and Piner (2015b), the base case model was modified into an ASPM to identify whether the catch and F09 abundance index were consistent with the estimated scale and trends in the population. Maunder and Piner (2015b) stated that “When catch does explain indices with good contrast (e.g., declining and increasing trends), it suggests that a production function is apparent in the data, therefore providing evidence that the index is a reasonable proxy of stock trend”. In this assessment, the base case model was modified by fixing the stock-recruitment relationship, sex-specific growth curves, and selectivities of all fleets to those estimated in the base case model, not estimating annual recruitment deviates so that recruitment follows the stock recruitment curve, and not fitting to the size composition data.

#### **4.6.3 Likelihood profile on virgin recruitment ( $R_0$ )**

Likelihood profiling over virgin recruitment ( $R_0$ ) was used to examine the influence of each data component on the overall population scale (Lee et al. 2014). The unfished level of recruitment ( $R_0$ ) is a global scaling parameter in an SS model because it is proportional to unfished biomass. This process is used to assess whether the relative data weightings are appropriate and/or whether the model is mis-specified. The likelihood profile consisted of running a series of models with the  $\ln(R_0)$  parameter fixed at a range of values above and below that estimated within the model, and examining the likelihoods of the various data components.

#### **4.6.4 Residual analysis**

Model residuals (i.e., differences between observed data and expected values) were examined to evaluate model fit and performance. The residuals were first visually examined for patterns. The variances of residuals were also compared to evaluate the statistical assumptions of the observation model. If the variance of the residuals differs substantially from the assumed variance, then the relative data weightings likely were not appropriate. However, a lack of residual patterns does not ensure that the model is not mis-specified because parameter estimates can change to compensate for the mis-specification (Maunder and Punt 2013).

#### **4.6.5 Retrospective Analysis**

Retrospective analysis was used to identify systemic inconsistencies in population estimates given increasing or decreasing data periods. In this assessment, we performed a within-model retrospective analysis by systematically removing the terminal year of data from successive models (1 to 5 years), while maintaining the same model structure between models.

### **4.7 Sensitivity to Model Assumptions**

A series of sensitivity runs were performed to examine the effects of plausible alternative model assumptions on the assessment results, and to help identify the major axes of uncertainty in this assessment. The sensitivity analyses conducted in this assessment (Table 4.6) can be categorized into three main themes: 1) biology (e.g., natural mortality, steepness); and 2) data (e.g., data weighting, start year, alternative indices); and 3) model structure (e.g., selectivity, equilibrium catch). For each sensitivity run, female spawning stock biomass (SSB), fishing intensity (1-SPR) trajectories, and where appropriate, model fits to the data, were compared.

## 4.8 Fishery Impact Analysis

The impact of the surface and longline fisheries on SSB was evaluated. The fishery impact analysis was conducted using the parameterization and assumptions of the base case model and dropping the annual catches (1994-2018) from the SS base case data file one-by-one and calculating the SSB time series for each scenario. The magnitude of differences in the simulated SSB trajectories with and without fishing indicates the impact of the major fishery types on the female SSB. Due to the assumed selectivities of the gillnet (F34) and miscellaneous (F35) fisheries, both fisheries are included as part of the surface fisheries.

## 4.9 Future Projections

Stock projections were used to assess the impact of current fishing intensity and catch on future harvest and stock status. In this assessment, a new version of the software package (SSfuture C++; sscpp; sscpp20191125.cpp) was developed to perform the future projections (Ijima 2020). The sscpp software package is similar in principle to the SS base case model and is highly similar to the sscpp package used in the 2017 assessment. In general, the sscpp uses the estimated sex-specific N-at-age from the base case model and projects the population forward using either a fixed F-at-age (constant F scenarios) or total catch (constant catch scenarios), and a recruitment deviate vector sampled from a distribution consistent with the  $\sigma_R$  in the base case model. Details and code for the software package can be found in Ijima (2020). It should be noted that sscpp incorporates two main sources of uncertainty in the projections: 1) uncertainty of N-at-age estimates in the terminal year of the base case model; and 2) uncertainty in future recruitment. Thus, sscpp does not incorporate all of the estimated uncertainty from the base case model into projections. For example, in the constant F scenarios, the projections have a fixed F-at-age and the uncertainty in the projected population gradually become dominated by the uncertainty in future recruitment. Nevertheless, the current sscpp version is an improvement over the version used in the 2017 assessment because the 2017 version only accounted for the uncertainty in the total biomass estimates and the relative N-at-age in the terminal year was assumed to be known without error.

Two 10-yr projection scenarios, constant  $F_{2015-2017}$  and constant catch (average of 2013-2017; 69,354 t), were used to evaluate the impacts of fishing on future female SSB. Future recruitment was sampled from a distribution consistent with the expected recruitment variability ( $\sigma_R = 0.3$ ) of the recruitment time series (1994 – 2018) in the base case model. The overall sex-specific F-at-age was estimated from the base case model and used (scaled to the appropriate catch in the constant catch scenario) to remove albacore from the appropriate age and sex in the projected populations. Projections started in 2019 and continued for 10 years through 2028. The projected female SSB, catch, and F-multipliers were calculated for each projection. 100 initial populations were simulated by sampling from a multivariate normal distribution consistent with the estimated N-at-age in 2018 and its variance-covariance matrix. Each initial population was subsequently projected using 1,000 runs for 10 years. Each run used a 10-year recruitment vector that was sampled from the distribution of expected future recruitment, which incorporated the stock-recruitment relationship, and expected recruitment variability. A total of 100,000 (100 x 1,000) runs were therefore performed for each projection scenario.

## 5.0 STOCK ASSESSMENT MODELLING RESULTS

### 5.1 Model Convergence

All estimated parameters in the base case model were within the set bounds and the final gradient of the model was 8.486E-5, which is consistent with a model that converged onto a local or global minimum. Preliminary models results showed that the likelihood surface around the model convergence zone was bumpy and prone to converging onto local minima. The base case model was therefore run from the SS 'par' file, with highly precise initial values for parameters. Based on the results of 50 model runs with different phasing and initial values, the base case model likely converged to a global minimum (i.e., there was no evidence of a lack of convergence to a global minimum) (Fig. 5.1). Total negative log-likelihood from the model run using the phasing and initial parameters from the base case model was 419.555 and the lowest (best) among these runs, and 0 out of 50 model runs also obtained the same negative log-likelihood. In addition, the estimated virgin recruitments in log-scale [ $\ln(R_0)$ ] and the estimated female SSB in 2018 relative to the 20%SSB<sub>current, F=0</sub> LRP were also similar from runs with total negative log-likelihoods similar to the base case model (Fig. 5.1). Therefore, even if the base case model had not converged onto the global minima, the results of a model that converged onto the global minima would be highly similar to the base case model presented here.

### 5.2 Model Diagnostics

#### 5.2.1 Model fit of abundance indices

The base case model fitted the F09 adult abundance index well (Fig. 5.2 and Table 5.1). It was important that the root-mean-squared-error (RMSE) between observed and predicted abundance indices for the F09 index were  $<0.2$ , which was the input CV for these indices, because this was the primary index that provided information on the spawning stock biomass trends. The catchability coefficient ( $q$ ) was solved analytically in the base case model as a single value for each index (Table 5.1).

#### 5.2.2 Model fit of size composition data

Base case model fits to the size composition data were reasonably good. Overall, the model predicted size compositions matched the observations (Fig. 5.3). Examination of the input sample size (input N) and model estimated effective sample size ( $effN$ ) also show reasonably good model fits (Table 5.2). A higher  $effN$  is consistent with better model fit and a mean  $effN$  of  $>30$  is a sign of good overall model fit. In addition, the ratios of the harmonic mean of  $effN$  to the mean of input N were all  $>1$ , which is interpreted to mean that the base case input N did not assume less error than is evident in the model fits. The model fits to the size composition data of the F01 fishery, although adequate, had a ratio of the harmonic mean of  $effN$  to the mean of input N that was  $<2$  and could be improved upon in the next assessment. Preliminary model runs suggested that the F01 fishery was a mixture of two fleets, with two apparent size modes (one each for juvenile and adult fish) and variable proportions of each fleet over time. Francis weighting multipliers for all fisheries were  $\geq 1$ , indicating that the weighting for all fisheries were not greater than suggested by model fits (Table 5.2). Pearson residual plots of the model fit to the size composition data did not reveal substantial patterns in residuals (Fig. 5.4). Where patterns were evident visually, the scale of the residuals was generally small, mostly lying within  $\pm 2$  standard deviations.

### 5.2.3 Age-structured production model (ASPM) diagnostic

The ASPM had similar scale and populations trends to the base case model (Fig. 5.5). Model fit of the ASPM to the F09 index was also similar to the base case model, with both the RMSE and negative log-likelihood of the F09 index of the ASPM (0.161 RMSE; -29.6 log-likelihood units) being similar to the base case model (0.169 RMSE; -28.7 log-likelihood units). These results showed that the estimated catch-at-age and fixed productivity parameters (i.e., growth, natural mortality, and spawner-recruit relationship) were able to explain trends in the F09 index without the addition of process error in the form of annual recruitment deviates. This finding in turn means that the base case model was able to estimate the stock production function and the effect of fishing on the abundance of the north Pacific albacore stock. Similar to the 2017 assessment, the connection between catch-at-age and the F09 index adds confidence to the model and data used, and represents a major improvement from previous assessments.

### 5.2.4 Likelihood Profiles on Virgin Recruitment ( $R_0$ )

Results of the likelihood profiling on virgin recruitment,  $R_0$ , for the abundance indices and size composition data components of the model are shown in Fig. 5.6. Changes in the likelihood of each data component are a measure of how informative that data component is to the overall estimated population scale.

The ASPM diagnostic showed that the F09 index was informative on the estimated population scale, especially the status of the stock with respect to the 20%SSB<sub>current, F=0</sub> LRP. However, due to the moderate exploitation levels of this stock, the  $R_0$  profile of the F09 index showed that the changes in log-likelihood over the range of  $R_0$  examined was relatively small, which means that the estimated population scale was relatively uncertain. Nevertheless, it is important to note that the negative log-likelihood profile of the F09 index was asymmetrical, with increasing negative log-likelihoods when  $R_0$  was low and relatively little change when  $R_0$  was high. This finding is consistent with a F09 index that is particularly useful for providing information on whether the population is lower than a certain minimum level but less informative on the upper limit to the population scale (i.e., uncertainty was primarily on the high  $R_0$  side). The primary aim of estimating the SSB in this assessment was to determine whether the estimated SSB is lower than the LRP (i.e., determine whether the stock was in an overfished condition). Since the  $R_0$  profiles show that the lower bound is better defined, it adds confidence to the ALBWG's evaluation of stock condition relative to the limit reference point.

The information from the size composition data appeared to be relatively consistent with the index data. Importantly, the minima of the likelihood profile of the size composition data occurred around the same range of  $R_0$  as the minima of likelihood profile of the index data, which suggests that estimated population scales from both data sources were relatively consistent. In addition, the range of changes in the negative log-likelihood of the size composition data were only slightly larger than the range of the F09 index, which suggests that the size composition data are appropriately weighted.

Overall, the  $R_0$  likelihood profile showed that there was substantial uncertainty in the estimate of population scale of this assessment, which was reflected in the uncertainty in biomass estimates. Nevertheless, the  $R_0$  likelihood profile also showed that the estimated  $\ln(R_0)$  in the base case model was consistent with all the data components, especially the F09 index, that the ALBWG considered to be important for defining population scale in the assessment model and for defining the status of the stock.



Importantly, even when the fit to the F09 index was degraded (increase in log-likelihood of about 1.9) with a  $\ln(R_0)$  fixed at 11.0, the ratio of the estimated female SSB relative to unfished SSB remained higher than the 20%SSB<sub>current, F=0</sub> LRP (Fig. 5.7). Thus, the results of this assessment with respect to the status of the stock, are relatively robust.

### 5.2.5 Retrospective Analysis

Retrospective analysis did not reveal any important pattern in the estimates of spawning biomass and fishing intensity (1-SPR) with the successive elimination of terminal year data. Removing one to five years of terminal data resulted in negligible changes in the results of the model (Fig. 5.8). The annualized Mohn's rho (Mohn 1999) for female SSB, SSB depletion, and 1-SPR of the retrospective models were calculated using the method described by Hurtado-Ferro et al. (2014b) and found to be 0.018, -0.019, and 0.046  $y^{-1}$ , respectively, which indicate negligible retrospective patterns for these quantities. The estimated female SSB from all the models from this analysis remained above the 20%SSB<sub>current, F=0</sub> LRP, which is consistent with the conclusion that the results of this assessment are relatively robust.

## 5.3 Model Parameter Estimates

### 5.3.1 Selectivity

The estimated selectivity of fisheries assumed to have size-only selectivity or a product of size and age selectivity (F20, F21, F22, F23 and F33) are shown in Fig. 5.9 and 5.10, respectively. Although all fisheries with size-only selectivity have nominally dome-shaped selectivity, the peak of the selectivity of some fisheries were so large (e.g., F26) that they acted as fisheries with asymptotic selectivity (Fig. 5.9). The selectivity of the F20, F21, F22, F23 and F33 fisheries were relatively non-intuitive, especially the age selectivity, because the overall selectivities were products of both size and age selection.

The peak and width of the ascending slope parameters for the fisheries with dome-shaped selectivity are typically precisely estimated while the width of the plateau and descending slope parameters have high uncertainty (Table 4.2 and 4.3). The differences in uncertainty of parameters in a double normal selectivity curve is expected because the width of the plateau and descending slope parameters are highly correlated, which increases the uncertainty in these parameters. It should also be noted that most of the age selectivity parameters of the F20, F21, F22, F23 and F33 fisheries were also highly uncertain due to correlation between parameters (Table 4.3).

### 5.3.2 Catch-at-Age

Juvenile albacore aged 2, 3, and 4 were the largest components of north Pacific albacore catch (Figure 5.11) due to the importance of surface fisheries (primarily troll, pole-and-line, and including other miscellaneous gears).

### 5.3.3 Sex Ratio

The fraction of females in the population changes by age and length (Fig 5.12). Sex ratio is approximately 1:1 until albacore reach age-3+, after which males becomes more common due to the higher  $M$  in females at ages-3+. This change in sex ratio is further accentuated by the differences in growth such that the sex ratio is heavily biased for albacore >100 cm FL. The heavy bias towards males at large sizes (>100 cm) has been observed in this stock (Fig. 3.6) and in the south Pacific albacore stock (Farley et al. 2013). Although the heavily biased sex ratio of large albacore may have consequences in the estimated population dynamics of this stock, the implications of this bias on

estimates of management quantities, stock status determinations or the development of conservation advice, are not known.

## 5.4 Stock Assessment Results

### 5.4.1 Biomass

The estimated female SSB fluctuated between 1994 and 2018, with a high of  $86,715 \pm 22,168$  t ( $\pm$ SE) in 1996 and a low of  $52,466 \pm 14,342$  t in 2003 (Fig. 5.13 and Table 5.3). Estimated female SSB exhibited an initial decline until 2003 followed by fluctuations without a clear trend through 2018 (Fig. 5.13). In the terminal year of the assessment (2018), female SSB was estimated to be  $58,858 \pm 15,871$  t. The LRP ( $20\%SSB_{\text{current}, F=0}$ ) adopted by the WCPFC is based on dynamic  $SSB_0$  and has fluctuated between 24,870 to 31,001 t during the assessment period (Table 5.3). The maximum likelihood estimate of female SSB has therefore been above the LRP throughout the assessment period. However, it should be noted that uncertainties in the estimates of female SSB were relatively large. This was because the virgin recruitment parameter ( $R_0$ ), which largely determines the population scale, was estimated with a relatively large uncertainty.

The total biomass estimates in the first quarter, which includes all age-1+ male and female albacore, have also fluctuated during the assessment period, ranging from a low of 617,363 t in 2016 to a high of 916,529 t in 1995 (Fig. 5.13 and Table 5.3).

### 5.4.2 Recruitment

Estimated recruitment was generally consistent with the biology of the stock and assumptions in the base case model. Recruitment estimates did not show a substantial trend with respect to female SSB (Fig. 5.13), which was expected because albacore and other tunas have recruitment variability largely driven by environmental conditions, and a steepness of 0.9 was assumed in this assessment (Section 4.2.8). The estimated recruitments were consistent with the expected distribution of recruitment deviations ( $\sigma_R = 0.3$ ), where all recruitment estimates were within the expected distribution.

The estimated recruitments have fluctuated widely during the assessment period (1994 – 2018), ranging from historical lows of  $124.5 \pm 28.4$  million fish ( $\pm$  SD) in 2014 and  $112.8 \pm 29.1$  million fish in 2015 to a high of  $256.9 \pm 38.9$  million fish in 1999 (Figure 5.13 and Table 5.3). The low estimated recruitment in 2014 and 2015 may have contributed to the relatively low catches of fisheries catching juvenile albacore after 2016. The average recruitment during the 1994 – 2018 period was 171.2 million fish, which was slightly below virgin recruitment (180.1 million fish).

Uncertainty in the recruitment estimates was relatively large because uncertainty estimated for the virgin recruitment parameter, which largely determines the population scale, was relatively large. In addition, the uncertainty in the last three years (2016 – 2018) of the assessment were larger than the rest of the time series because the amount of information on recruitment declines towards the end of a model. Therefore, it is currently unclear if recruitment improved after 2015.

### 5.4.3 Fishing intensity

Spawning potential ratio (SPR) was used to describe the fishing intensity on this stock. The SPR of a population is the ratio of female SSB per recruit under fishing to the female SSB per recruit under virgin (or unfished) conditions. Therefore, 1-SPR is the reduction in female SSB per recruit due to fishing and can be used to describe the overall fishing intensity on a fish stock (Goodyear 1993). The fishing intensity (1-SPR) on the north Pacific albacore stock has fluctuated between 0.40 and

0.71 during the assessment period (1994 – 2018) (Table 5.3). The estimated mean fishing intensity during 2015 – 2017 was  $0.50 \pm 0.07$ , which corresponds to a moderate level of exploitation (Table 5.3).

Instantaneous fishing mortality-at-age (F-at-age) was estimated for female and male albacore in the base case model (Fig. 5.14). The F-at-age of juveniles was higher than most of the adult age classes, which corresponds to the larger catches of the surface fisheries. The F-at-age is highly similar in both sexes through age-5, peaking at age-4 and declining to a low at age-6, after which males experience higher F-at-age than females up to age 12. These sex and age-specific differences in F-at-age are due to sex-specific differences in natural mortality and size-at-age for adult albacore.

## 5.5 Biological Reference Points

Kobe plots are presented in Figure 5.15 to illustrate the stock status of the north Pacific albacore stock in relation to the biomass-based LRP adopted by the WCPFC ( $20\%SSB_{\text{current}, F=0}$ ) and the equivalent fishing intensity ( $1-SPR_{20\%}$ ) for the LRP. It should be noted that the  $20\%SSB_{\text{current}, F=0}$  LRP is based on dynamic biomass and fluctuates depending on changes in recruitment. This LRP is calculated as 20% of the unfished dynamic female spawning biomass in the terminal year of this assessment (i.e., 2018). The coefficients of variation of the ratios of SSB/LRP were assumed to be the same as for SSB/SSB<sub>0</sub>. Limit reference points for fishing intensity or F-based reference points for north Pacific albacore have not been adopted by either the IATTC or WCPFC. The Kobe plot for the base case model shows that the stock has not fallen below the LRP during the assessment period. However, there is substantial uncertainty in the estimated female SSB and accompanying stock status. Even when alternative hypotheses about key uncertainties such as growth are evaluated (Section 5.6), the point estimate of female spawning biomass does not fall below the LRP, although risk of being below increases with some assumptions (Fig. 5.15).

Biological reference points were computed from the base case model (Table 5.4). The point estimate ( $\pm$ SE) of maximum sustainable yield (MSY – which includes male and female juvenile and adult fish) was  $102,236 \pm 12,862$  t and the point estimate of female SSB to produce MSY ( $SSB_{\text{MSY}}$ ) is  $19,535 \pm 2,395$  t. Current F ( $F_{2015-2017}$ ) was defined as the average 1-SPR for the years 2015-2017 because terminal year estimates of fishing intensity were generally considered to be uncertain. Current SSB ( $SSB_{2018}$ ) was defined as the female SSB in 2018. The ratio of  $F_{2015-2017}/F_{\text{MSY}}$  was estimated to be  $0.60 \pm 0.09$ , and the ratio of  $SSB_{2018}/20\%SSB_{\text{current}, F=0}$  was estimated to be  $2.30 \pm 0.41$ . Current fishing intensity ( $F_{2015-2017}$ ) is likely at or below  $F_{\text{MSY}}$  and all MSY-proxy reference points, and  $SSB_{2018}$  is well above the LRP threshold (Table 5.4). Note that  $F_{2015-2017}$  and F-based reference points were not based on the average instantaneous fishing mortality. Instead,  $F_{2015-2017}$  and F-based reference points were indices of fishing intensity based on SPR and calculated as 1-SPR so that they reflected changes in fishing mortality.

## 5.6 Sensitivity to Model Assumptions

The following sensitivity analyses were performed to examine the effects of plausible alternative model assumptions on the assessment results, and help identify the major axes of uncertainty in this assessment (see Table 4.6 for details).

### 5.6.1 Sensitivity 01 – Natural mortality

Natural mortality is typically considered to be a major axis of uncertainty in most stock assessments. Sensitivity model runs were performed using a constant  $M$  of  $0.3 \text{ y}^{-1}$  for both sexes and all ages (as in the 2014 assessment); a constant  $M$  of 0.38 and  $0.49 \text{ y}^{-1}$  for males and females,

respectively, of all ages; and an estimated, single parameter, female  $M$  for all ages, with the prior from Teo (2017),  $M_{female} \sim \log N[-0.7258, (0.457)^2]$ , and a constant logscale offset (-0.21258) between male and female  $M$ . Changing the  $M$  from the sex-specific  $M$ -at-age vector in the base case model to the constant  $0.3 \text{ y}^{-1}$  in the 2014 assessment or estimating  $M$  with a prior resulted in major differences in the estimated spawning biomass depletion, and fishing intensity (1-SPR) of the assessment (Fig. 5.16). The estimated posterior for  $M_{female}$  was  $\log N[-0.3005, (0.078)^2]$ , leading to an estimated female  $M$  of  $0.74 \text{ y}^{-1}$  with a corresponding male  $M$  of  $0.60 \text{ y}^{-1}$ . The results of the model estimating female  $M$  with a prior suggests that there may be information on  $M$  in the data. However, substantial work needs to be done before estimating  $M$  in the base case model.

### 5.6.2 Sensitivity 02 – Steepness

Steepness of the Beverton-Holt stock-recruitment relationship is also often considered a major axis of uncertainty in most stock assessments. Sensitivity model runs were performed using alternative steepness values ( $h = 0.75$ ;  $0.80$ ; and  $0.85$ ) to the base case model ( $h = 0.90$ ), and an estimated  $h$  using a prior of  $h \sim N[0.9, (0.05)^2]$ . Changing the steepness values had very limited effect on the estimated scale or trends in female SSB, spawning biomass depletion, and fishing intensity (Fig. 5.17). A similar result was reported in previous assessments. The estimated posterior for  $h$  was  $N[0.896, (0.05)^2]$ , which suggests that there is a negligible amount of information on  $h$  in the data. This is not surprising because the north Pacific albacore stock is on the relatively flat part of the stock-recruitment curve and  $h$  is generally not well estimated in such cases (Lee et al. 2012).

### 5.6.3 Sensitivity 03 – Growth

Growth was considered an important axis of uncertainty in previous assessments because of uncertainty in the age and growth of this stock, as well as conflicts in the size composition data. The same sex-specific growth model from the 2014 assessment was used in this assessment. The model fits to the size composition data were substantially improved in this assessment, but there remained uncertainty in the growth model, especially the CV of the  $L_{inf}$  parameter. Sensitivity runs were performed with the CVs of the  $L_{inf}$  parameter (CV =  $0.06$ ; and  $0.08$ ) that were larger than those parameter values in the base case model (CV =  $0.04$ ). Changing the CVs on the  $L_{inf}$  parameter had major effects on the scale of estimated female SSB, spawning depletion, and fishing intensity, with larger CVs leading to lower estimated SSB (Fig. 5.18). Growth was considered by the ALBWG to be the most important axis of uncertainty in this assessment.

### 5.6.4 Sensitivity 04 – Catch estimates for F30, F31, and F32

The catch time series for three fisheries (F30, F31, and F32) had relatively large (up to  $\sim 4000 \text{ t}$ ) changes for this assessment compared to the 2017 assessment (Kiyofuji 2020). The reasons for the differences are currently unknown. Therefore, a sensitivity model run was conducted that used the catch time series from the 2017 assessment for the 1994 – 2015 period. Changing the catch time series for these three fisheries had very limited effect on the estimated scale or trends in female SSB, spawning biomass depletion, and fishing intensity (Fig. 5.19).

### 5.6.5 Sensitivity 05 – Catch estimates for F33 during 2016 - 2018

The ALBWG noticed that the observed catch for the EPO surface fishery (F33) during 2016 – 2018 was substantially lower than for previous years. The ALBWG was interested in understanding the effect on the model results if the catch of F33 was approximately the same as previous years ( $\sim 2x$ ). Therefore, a model run was performed with the catch for F33 being doubled during 2016 – 2018. It should be noted that this model run was not considered a sensitivity run because there was no evidence that the catch of F33 was substantially higher than reported during 2016 – 2018. Instead,

this model run is best viewed as a ‘what if’ scenario to help the ALBWG understand what if the catch of F33 was approximately the same as previous years. Doubling the catch for F33 during 2016 – 2018 increased the estimated fishing intensity during the terminal years of the model (Fig. 5.20). However, the impact on the estimated scale or trends in female SSB, and spawning biomass depletion were limited (Fig. 5.20).

#### **5.6.6 Sensitivity 06 – Extended F09 index**

In this assessment, the ALBWG decided to start the F09 index in 1996 instead of 1994 because the proportion of sets with zero albacore catch, species composition, and Pearson residuals were biased in 1994 and 1995 (Section 3.5.1). A sensitivity model run was performed by fitting to an extended F09 index that started in 1994, which was developed using the same methods (Fujioka et al. 2020). Fitting to the extended F09 resulted in highly similar estimates of female SSB, spawning biomass depletion, and fishing intensity for most years, especially the terminal years (Fig. 5.21). The main difference was in the initial years, which was expected because the extended F09 index had two extra initial years of data.

#### **5.6.7 Sensitivity 07 – Fit to F01 index**

In this assessment, the F01 index was investigated as a potential index of juvenile/subadult albacore abundance but was eventually rejected by the ALBWG for the base case model because ASPM analysis and other model diagnostics of preliminary models suggested a conflict between the F01 and F09 indices (Section 3.5). Instead, the base case model was fitted only to the F09 index as an adult abundance index, while the F01 index was fitted in a sensitivity model. Fitting to the F01 index resulted in slightly lower estimates of female SSB and spawning biomass depletion, and slightly higher estimates of fishing intensity (Fig. 5.22).

#### **5.6.8 Sensitivity 08 – Size composition data weighting**

In the base case model of this assessment, the size composition data of the F09 fishery were downweighted (0.1x) to minimize the conflict between the size composition data and the F09 index (Section 4.5). In addition, the size composition data of three fisheries (F01, F23, and F27) were downweighted by 0.6, 0.9 and 0.8 times, respectively (Table 5.2), such that the size composition data weightings for these fisheries were consistent with their model fit (i.e., Francis multiplier of ~1; Section 3.5). A sensitivity model was developed where the size composition data for the F09 fishery were fully weighted (1.0x). In addition, a series of sensitivity models were developed where the size composition data for each fishery, except for F09, were downweighted by 0.1x to understand the effect of data weighting on the size composition data. Results from only three sensitivity models are shown in Figure 5.23 to highlight the approximate range of model results, even though all fisheries were downweighted in turn. Allowing the size composition data of the F09 fishery to be fully weighted (1.0x) did not substantially affect either trends or scale of the estimated female SSB, spawning depletion, and fishing intensity (Fig. 5.23). Downweighting the F01 fishery (0.1x) resulted in an increased estimate of female spawning biomass in the initial years of the model (Fig. 5.23). In contrast, downweighting the F27 fishery (0.1x), resulted in a decreased estimate of female spawning biomass over the entire modelling period (Fig. 5.23). However, these differences were within the expected uncertainty of the model results (Fig. 5.13). The ALBWG concluded that the results of the assessment were robust to the weighting of the size composition data.

### 5.6.9 Sensitivity 09 – US longline asymptotic selectivity

In this assessment, all fisheries were allowed to have a dome-shaped selectivity and all estimated size selectivity appeared to be dome-shaped in the base case model. Stock assessments without a fishery assumed to have an asymptotic selectivity may result in an unrealistically large estimated SSB (i.e., cryptic biomass) because not all fish are selected. A sensitivity model was developed where the F26 US longline fishery, which catches the largest albacore, was assumed to have asymptotic selectivity instead of being allowed to estimate a dome-shaped selectivity. Assuming an asymptotic selectivity for the F26 US longline fishery resulted in negligible differences in the scale and trends of estimated female SSB, spawning depletion, and fishing intensity (Fig. 5.24).

### 5.6.10 Sensitivity 10 – Equilibrium catch

Initial conditions of the model in this assessment were relatively freely estimated from the data in the main model period (1994 – 2018). Although the initial fishing mortality of a fishery (F27) was estimated, the equilibrium catch prior to the modelling period was not fitted. A sensitivity model was developed where the initial fishing mortality of all major fisheries were estimated and the equilibrium catch of these fisheries were fitted. The equilibrium of each fishery was calculated as the average of 10 years of annual catch during 1984 – 1993. The sensitivity model fitting to equilibrium catch failed to converge, and the ALBWG did not further consider the results from this sensitivity run.

### 5.6.11 Sensitivity 11 – Start year

The 1994 – 2018 time frame for this assessment is an extension of the 2017 assessment (1993 – 2015) (ALBWG 2017) but is substantially shorter than the time frames used in earlier assessments, which had start years of 1966 (e.g., ALBWG 2014). The issues with the data and models for the 1966 – 1993 period have been detailed in the 2014 and 2017 assessments (ALBWG 2014, 2017). Here, a suite of alternative models with a start year of 1966 was developed to help the ALBWG to understand the issues with the models and data prior to 1994. The ALBWG concluded that no model with a start year of 1966 that was investigated during the assessment was satisfactory. However, the ALBWG chose three models with a start year of 1966 to illustrate the qualitative model results and highlight the issues with the models and data. Briefly, the three models were:

1. Start year from 1966 with the inclusion of data from 1966 – 1993. Data prior to 1994 were prepared in the same manner as the base case model and data weighting was done in the same way. The model was also fitted to an adult abundance index in Area 2 and Quarter 1 during the early (pre-1994) period (F13 index; 1976 - 1992). Results indicated that model fits to the size compositions and F13 index were poor. This may be due to data quality being poorer in the early period. In addition, selectivity curves for the F09 and F26 fisheries appeared to be unreasonable, with peak parameters at the upper bounds.
2. In addition to Model 1, a selectivity time block for the Japanese longline fisheries was applied for the 1976-1993 period, when a large proportion of larger fish (>100 cm) were observed in the samples from these fisheries. This was similar to the approach taken in the 2014 assessment. Adding the time block improved model fit to size composition data in the early period. The time block also improved model fit to the late period index (F09 index), but the fit to the early index (F13 index) remained poor. In addition, there were large misfits to the size composition data of the Japanese pole-and-line fisheries in the early period and numerous selectivity parameters were also at parameter bounds.
3. In addition to Model 1, time varying age selectivity was implemented for the Japanese

pole-and-line fisheries. Doing so improved the model fits to the size composition data to the Japanese pole-and-line fisheries, and improved model fits to the early index (F13 index). However, the model did not appear to be converged (Hessian was not positive definite) and was not considered further.

Including the data prior to 1994 and starting the model in 1966 resulted in relatively similar scales and trends in estimated female SSB, spawning biomass depletion, and fishing intensity for the later period (1994 – 2018) and the terminal years (Fig. 5.25). Therefore, the conclusions on the current stock status would have been relatively similar as well. Given the problems with fitting the data during 1966 – 1993, the ALBWG considered these sensitivity model results to be useful in a qualitative manner.

#### **5.6.12 Sensitivity 12 – 2017 base case model structure**

The model structure of the base case model for this assessment had several important changes from the 2017 base case model (Section 2.3). A sensitivity model was developed that followed closely the model structure of the 2017 base case model. Importantly, this sensitivity model had: 1) the same average input sample size for each fishery (~7) and the size composition data for several longline fisheries (F09 – F17; F25 and F26) were down-weighted (0.1x); 2) the Japanese pole-and-line fisheries for Q1 and Q2 (F20 and F22) shared a common selectivity curve, as did the Q3 and Q4 (F22 and F23) fisheries, and did not have time-varying selectivity; and 3) the F10, F11, and F12 Japanese longline fisheries shared a common selectivity curve. Following the model structure of the 2017 base case model resulted in a slightly higher female SSB and spawning depletion, especially in the initial years (Fig. 5.26). The model fits to the F09 index were similar for both models (RMSEs of ~0.17 for both models) (Fig. 5.26) but the base case model in this assessment had substantially better fits to F21 and F22, which are the two largest sources of removals for north Pacific albacore. For example, the harmonic mean of the effective sample sizes for F21 (21.9) and F22 (12.1) in this sensitivity run were substantially smaller than the base case model of this assessment (Table 5.2). The base case model in this assessment included several improvements over the 2017 base case model (Section 2.3) but a model approximating the 2017 model structure was considered to be plausible. Therefore, the ALBWG decided that information from this model would be useful for comparative purposes with the base case model.

### **5.7 Fishery Impact Analysis**

Surface fisheries (primarily troll, and pole-and-line, but including gillnet and other miscellaneous gears), which tend to catch juvenile fish, have generally had a larger impact (approximately 2:1 ratio) on the north Pacific albacore stock than longline fisheries, which tend to remove adult fish (Fig. 5.27).

### **5.8 Future Projections**

The constant fishing intensity and constant catch projection scenarios show that the current fishing intensity ( $F_{2015-2017}$ ) is expected to result in female SSB increasing to 62,873 t (95% CI: 45,123 – 80,622 t) by 2028, with a 0.2 % and <0.01 % probability of being below the LRP by 2020 and 2028, respectively (Fig. 5.28). Similarly, employing the constant catch harvest scenario is expected to lead to an increased female spawning biomass of 66,313 t (95% CI: 33,463 – 99,164 t) by 2028. The probability that female SSB will be below the LRP in the constant catch scenario is higher than the constant  $F_{2015-2017}$  scenario but is still below 0.5% for all years (Fig. 5.29). The probabilities of female SSB falling below the LRP may be higher than estimated in these scenarios because the software does not incorporate all the estimated uncertainty from the base case model into the

projections. It should be noted that the projections, especially the constant  $F_{2015-2017}$  scenario, appear to underestimate the uncertainty due to a fixed  $F$ -at-age over time and a relatively low recruitment variability. Therefore, it is advisable to use the estimated future probabilities of breaching the LRP in a qualitative manner for management purposes until the projection software is improved. It should be noted that the constant catch scenario is inconsistent with current management approaches for north Pacific albacore tuna adopted by the IATTC and the WCPFC.

## 6.0 STOCK STATUS

### 6.1 Current Status

Estimated total stock biomass (males and female at age-1+) declines at the beginning of the time series until 2000, after which biomass becomes relatively stable (Fig. 5.13). Estimated female SSB exhibits a similar population trend, with an initial decline until 2003 followed by fluctuations without a clear trend through 2018 (Fig. 5.13). However, estimated recruitment reached historical lows in 2014 (~125 million fish; 95% CI: 69 – 180 million fish) and 2015 (~113 million fish; 95% CI: 56 – 170 million fish) (Fig. 5.13), which may have contributed to relatively low catches of fisheries catching juvenile albacore in recent years. It is currently unclear if recruitment improved after 2015 because recruitment during the terminal years of the assessment (2016 – 2018) have large uncertainties (Fig. 5.13).

The estimated average SPR (spawners per recruit relative to the unfished population) during 2015 – 2017 is 0.50 (95% CI: 0.36 – 0.64), which corresponds to a moderate fishing intensity (i.e.,  $1-SPR = 0.50$ ). Instantaneous fishing mortality at age ( $F$ -at-age) is similar in both sexes through age-5, peaking at age-4 and declining to a low at age-6, after which males experience higher  $F$ -at-age than females up to age 12 (Fig. 5.14). Juvenile albacore aged 2 to 4 years comprised approximately 70% of the annual catch between 1994 and 2018 (Fig. 5.11). This is also reflected in the larger impact of the surface fisheries (primarily troll, pole-and-line), which remove juvenile fish, relative to longline fisheries, which primarily remove adult fish (Fig. 5.27).

The Northern Committee (NC) of the Western and Central Pacific Fisheries Commission (WCPFC), which manages this stock together with the Inter American Tropical Tuna Commission (IATTC), adopted a biomass-based limit reference point (LRP) in 2014 (<https://www.wcpfc.int/harvest-strategy>) of 20% of the current spawning stock biomass when  $F=0$  ( $20\%SSB_{current, F=0}$ ). The  $20\%SSB_{current, F=0}$  LRP is based on dynamic biomass and fluctuates depending on changes in recruitment. For north Pacific albacore tuna, this LRP is calculated as 20% of the unfished dynamic female spawning biomass in the terminal year of this assessment (i.e., 2018) (<https://www.wcpfc.int/meetings/nc13>). However, neither the IATTC nor the WCPFC have adopted  $F$ -based limit reference points for the north Pacific albacore stock.

Stock status is depicted in relation to the limit reference point (LRP;  $20\%SSB_{current, F=0}$ ) for the stock and the equivalent fishing intensity ( $F_{20\%}$ ; calculated as  $1-SPR_{20\%}$ ) (Fig. 5.15). Fishing intensity ( $F$ , calculated as  $1-SPR$ ) is a measure of fishing mortality expressed as the decline in the proportion of the spawning biomass produced by each recruit relative to the unfished state. For example, a fishing intensity of 0.8 is equivalent to fishing at  $F_{20\%}$  and will result in a SSB of approximately 20% of  $SSB_0$  over the long run. Fishing intensity is considered a proxy of fishing mortality.

The Kobe plot shows that the estimated female SSB has never fallen below the LRP since 1994, albeit with large uncertainty in the terminal year (2018) estimates. Even when alternative hypotheses about key model uncertainties such as growth were evaluated, the point estimate of female SSB in 2018 ( $SSB_{2018}$ ) did not fall below the LRP, although the risk increases with this more



extreme assumption (Fig. 5.15). The  $SSB_{2018}$  was estimated to be 58,858 t (95% CI: 27,751 – 89,966 t) and 2.30 (95% CI: 1.49 – 3.11) times greater than the estimated LRP threshold of 25,573 t (95% CI: 19,150 – 31,997 t) (Table 5.4). Current fishing intensity,  $F_{2015-2017}$  (0.50; 95% CI: 0.36 – 0.64; calculated as  $1 - SPR_{2015-2017}$ ), was at or lower than all seven potential F-based reference points identified for the north Pacific albacore stock (Table 5.4).

Based on these findings, the following information on the status of the north Pacific albacore stock is provided:

1. The stock is likely not overfished relative to the limit reference point adopted by the Western and Central Pacific Fisheries Commission ( $20\%SSB_{current, F=0}$ ), and
2. No F-based reference points have been adopted to evaluate overfishing. Stock status was evaluated against seven potential reference points. Current fishing intensity ( $F_{2015-2017}$ ) is likely at or below all seven potential reference points (see ratios in Table 5.4).

## 6.2 Conservation Information

Two harvest scenarios were projected to evaluate impacts on future female SSB: F constant at the 2015-2017 rate over 10 years ( $F_{2015-2017}$ ) and constant catch<sup>2</sup> (average of 2013-2017 = 69,354 t) over 10 years. Median female SSB is expected to increase to 62,873 t (95% CI: 45,123 - 80,622 t) by 2028, with a low probability of being below the LRP by 2028, if fishing intensity remains at the 2015-2017 level (Fig. 5.28). If future catch is held constant at 69,354 t, the female SSB is expected to increase to 66,313 t (95% CI: 33,463 - 99,164 t) by 2028 and the probability that female SSB will be below the LRP by 2028 is slightly higher than the constant F scenario (Fig. 5.29). Although the projections appear to underestimate the future uncertainty in female SSB trends, the probability of breaching the LRP in the future is likely small if the future fishing intensity is around current levels.

Based on these findings, the following information is provided:

1. If a constant fishing intensity ( $F_{2015-2017}$ ) is applied to the stock, then median female spawning biomass is expected to increase to 62,873 t and there will be a low probability of falling below the limit reference point established by the WCPFC by 2028.
2. If a constant average catch ( $C_{2013-2017} = 69,354$  t) is removed from the stock in the future, then the median female spawning biomass is expected to increase to 66,313 t and the probability that SSB falls below the LRP by 2028 will be slightly higher than the constant fishing intensity scenario.

---

<sup>2</sup> It should be noted that the constant catch scenario is inconsistent with current management approaches for north Pacific albacore tuna adopted by the Inter-American Tropical Tuna Commission (IATTC) and the WCPFC.

## 7.0 KEY UNCERTAINTIES AND RESEARCH RECOMMENDATIONS

The ALBWG noted that the lack of sex-specific size and age data, uncertainty in growth, and the simplified treatment of the spatial structure of north Pacific albacore population dynamics were important sources of uncertainty in the assessment. The following recommendations were developed to improve the future iterations of the stock assessment model:

1. Further investigation of the F01 fishery because there appears to be a mixture of two fisheries (one on juveniles and one adults) in this fishery;
2. Evaluate adult indices from the Japanese longline fisheries in southern areas (Areas 2 and 4), especially with respect to incorporating size data into the standardization process using a spatiotemporal process and/or data from alternative seasons;
3. Evaluate potential juvenile indices from the Japanese longline fisheries in northern areas (Areas 1, 3 and 5), the Japanese pole-and-line and/or EPO surface fisheries;
4. Collect sex-specific age-length samples using a coordinated biological sampling plan to improve current growth curves, and examine regional and temporal differences in length-at-age;
5. Collect sex ratio data by fishery using a coordinated biological sampling plan; and
6. Evaluate and document historical high seas drift gillnet catch by member countries.

## 8.0 LITERATURE CITED

- ALBWG. 2014. Stock assessment of albacore tuna in the North Pacific Ocean in 2014.
- ALBWG. 2016. Report of the Albacore Working Group, 8-14 November 2016, Nanaimo, British Columbia, Canada.
- ALBWG. 2017. Stock assessment of albacore tuna in the North Pacific Ocean in 2017. Page 103. International Scientific Committee for Tuna and Tuna-like Species in the North Pacific Ocean.
- ALBWG. 2019. Report of the Albacore Working Group, 12-18 November 2019, NRIFSF/FRA, Shimizu, Shizuoka, Japan.
- ALBWG. 2020. Report of the Albacore Working Group, 5-14 April, 2020, Webinar.
- Ashida, H., T. Goshio, and H. Kiyofuji. 2016. Sex ratio, spawning season, spawning fraction and size at maturity of North Pacific albacore (*Thunnus alalunga*) caught in subtropical western North Pacific. ISC/16/ALBWG-02/05. Working document submitted to the ISC Albacore Working Group Meeting, 8 - 14 November, 2016, Pacific Biological Station, Nanaimo, BC, Canada.
- Brodziak, J., H. H. Lee, and M. Mangel. 2011. Probable values of stock-recruitment steepness for north Pacific albacore tuna. ISC/11/ALBWG/11. Working Paper submitted to the ISC Albacore Working Group Stock Assessment Workshop, 4-11 June 2011, National Research Institute of Far Sea Seas Fisheries, Shimizu, Japan.
- Chen, C.-Y., and F.-C. Cheng. 2019. Update of albacore CPUE and length distributions of Taiwanese longline fishery in the North Pacific Ocean, 1995-2018. ISC/19/ALBWG-02/11. Working document submitted to the ISC Albacore Working Group Meeting, 12-18 November 2019, National Research Institute of Far Seas Fisheries, Shimizu, Shizuoka Japan.
- Chen, K.-S., P. R. Crone, and C.-C. Hsu. 2010. Reproductive biology of albacore *Thunnus alalunga*. Journal of Fish Biology 77(1):119–136.
- Chen, K.-S., C.-C. Hsu, C.-Y. Chen, F.-C. Cheng, and H. Ijima. 2016. Estimation of sexual maturity-at-length of the North Pacific albacore. Working document submitted to the ISC Albacore Working Group Meeting, 8 - 14 November, 2016, Pacific Biological Station, Nanaimo, BC, Canada.
- Chen, K.-S., T. Shimose, T. Tanabe, C.-Y. Chen, and C.-C. Hsu. 2012. Age and growth of albacore *Thunnus alalunga* in the North Pacific Ocean. Journal of Fish Biology 80(6):2328–44.
- Childers, J., S. Snyder, and S. Kohin. 2011. Migration and behavior of juvenile North Pacific albacore (*Thunnus alalunga*). Fisheries Oceanography 20(3):157–173.
- Chow, S., and H. Ushiyama. 1995. Global population structure of albacore (*Thunnus alalunga*) inferred by RFLP analysis of the mitochondrial ATPase gene. Marine Biology 123(1):39–45.
- Clemens, H. B. 1961. The migration, age, and growth of Pacific albacore (*Thunnus germon*), 1951-1958. Fish Bulletin California Department of Fish and Game 115:1–128.
- Craig, M. T., and J. R. Hyde. 2020. PCR-based sex determination for North Pacific Albacore (*Thunnus alalunga*). ISC/20/ALBWG-01/08. Working document submitted to the ISC Albacore Working Group Meeting, 6-15 April 2020, by Webinar.
- Deriso, R., M. N. Maunder, and J. Skalski. 2007. Variance estimation in integrated assessment models and its importance for hypothesis testing. Canadian Journal of Fisheries and Aquatic Sciences 64(2):187–197.
- Farley, J. H., A. J. Williams, S. D. Hoyle, C. R. Davies, and S. J. Nicol. 2013. Reproductive Dynamics and Potential Annual Fecundity of South Pacific Albacore Tuna (*Thunnus alalunga*). PLoS ONE 8(4).
- Francis, R. I. C. C. 2011. Data weighting in statistical fisheries stock assessment models. Canadian Journal of Fisheries and Aquatic Science 68:1124–1138.

- Fujioka, K., D. Ochi, H. Ijima, and H. Kiyofuji. 2019. Update standardized CPUE of North Pacific albacore caught by Japanese longline data from 1976 to 2018. ISC/19/ALBWG-02/01. Working document submitted to the ISC Albacore Working Group Meeting, 12-18 November 2019, National Research Institute of Far Seas Fisheries, Shimizu, Shizuoka Japan.
- Fujioka, K., D. Ochi, H. Ijima, and H. Kiyofuji. 2020. Estimation of adult and immature abundance indices of North Pacific albacore caught by Japanese longline fisheries over a long period of time, from 1976 to 2018. ISC/20/ALBWG-01/01. Working document submitted to the ISC Albacore Working Group Meeting, 6-15 April 2020, by Webinar.
- Hamel, O. S. 2015. A method for calculating a meta-analytical prior for the natural mortality rate using multiple life history correlates. *ICES Journal of Marine Science* 72(1):62–69.
- Hurtado-Ferro, F., A. E. Punt, and K. T. Hill. 2014a. Use of multiple selectivity patterns as a proxy for spatial structure. *Fisheries Research* 158:102–115.
- Hurtado-Ferro, F., C. S. Szuwalski, J. L. Valero, S. C. Anderson, C. J. Cunningham, K. F. Johnson, R. Licandeo, C. R. McGilliard, C. C. Monnahan, M. L. Muradian, K. Ono, K. A. Vert-Pre, A. R. Whitten, and A. E. Punt. 2014b. Looking in the rear-view mirror: bias and retrospective patterns in integrated, age-structured stock assessment models. *ICES Journal of Marine Science* 72(1):99–110.
- Ichinokawa, M., A. L. Coan, and Y. Takeuchi. 2008. Transoceanic migration rates of young North Pacific albacore, *Thunnus alalunga*, from conventional tagging data. *Canadian Journal of Fisheries and Aquatic Sciences* 65(8):1681–1691.
- Ijima, H. 2020. The test run of future projection for North Pacific albacore stock using the SSfuture C++ and the multivariate normal distribution. ISC/20/ALBWG-01/03. Working document submitted to the ISC Albacore Working Group Meeting, 6-15 April 2020, by Webinar.
- Ijima, H., D. Ochi, and H. Kiyofuji. 2017. Estimation for Japanese catch at length data of North Pacific albacore tuna (*Thunnus alalunga*). ISC/17/ALBWG/04. Working document submitted to the ISC Albacore Working Group Meeting, 11-19 April 2017, Southwest Fisheries Science Center, La Jolla, California, USA.
- Ijima, H., D. Ochi, and K. Satoh. 2016. Japanese catch statistics of North Pacific albacore tuna (*Thunnus alalunga*) for Stock Synthesis 3. ISC/16/ALBWG-02/02. Working document submitted to the ISC Albacore Working Group Meeting, 8 - 14 November, 2016, Pacific Biological Station, Nanaimo, BC, Canada.
- Iwata, S., H. Sugimoto, and Y. Takeuchi. 2011. Calculation of the steepness for the north Pacific albacore. ISC/11/ALBWG/18. Working Paper submitted to the ISC Albacore Working Group Stock Assessment Workshop, 4-11 June 2011, National Research Institute of Far Sea Seas Fisheries, Shimizu, Japan.
- James, K., H. Dewar, and S. L. H. Teo. 2020a. Review of current status of North Pacific albacore (*Thunnus alalunga*) age and growth. ISC/20/ALBWG-01/07. Working document submitted to the ISC Albacore Working Group Meeting, 6-15 April 2020, by Webinar.
- James, K., H. Dewar, and S. L. H. Teo. 2020b. Ideas for future sampling programs of North Pacific albacore (*Thunnus alalunga*). ISC/20/ALBWG-01/09. Working document submitted to the ISC Albacore Working Group Meeting, 6-15 April 2020, by Webinar.
- Kimura, S., M. Nakai, and T. Sugimoto. 1997. Migration of albacore, *Thunnus alalunga*, in the North Pacific Ocean in relation to large oceanic phenomena. *Fisheries Oceanography* 6(2):51–57.
- Kinney, M. J., and S. L. H. Teo. 2016. Meta-analysis of north Pacific albacore tuna natural mortality. ISC/16/ALBWG-02/07. Nanaimo, British Columbia, Canada.
- Kiyofuji, H. 2020. North Pacific albacore catch provided by the WCPFC and IATTC. ISC/20/ALBWG-01/04. Working document submitted to the ISC Albacore Working Group Meeting, 6-15 April 2020, by Webinar.
- Kiyofuji, H., and K. Uosaki. 2010. Revision of standardized CPUE for albacore caught by the Japanese pole and line fisheries in the northwestern North Pacific albacore. ISC/10-3/ALBWG/07.

- Working paper presented at the ISC Albacore Working Group Workshop, 12-19 October 2010, Southwest Fisheries Science Center, NOAA, La Jolla, USA.
- Lee, H. H., M. N. Maunder, K. R. Piner, and R. D. Methot. 2012. Can steepness of the stock-recruitment relationship be estimated in fishery stock assessment models? *Fisheries Research* 125–126:254–261.
- Lee, H. H., K. R. Piner, R. D. Methot, and M. N. Maunder. 2014. Use of likelihood profiling over a global scaling parameter to structure the population dynamics model: AN example using blue marlin in the Pacific Ocean. *Fisheries Research* 158:138–146.
- Mangel, M., J. Brodziak, and G. DiNardo. 2010. Reproductive ecology and scientific inference of steepness: A fundamental metric of population dynamics and strategic fisheries management.
- Matsubara, N., Y. Aoki, and H. Kiyofuji. 2019. Update standardized CPUE of North Pacific albacore caught by Japanese pole and line from 1972 to 2018. ISC/19/ALBWG-02/02. Working document submitted to the ISC Albacore Working Group Meeting, 12-18 November 2019, National Research Institute of Far Seas Fisheries, Shimizu, Shizuoka Japan.
- Matsubara, N., Y. Aoki, and H. Kiyofuji. 2020. Standardized CPUE for North Pacific albacore caught by the Japanese pole and line from 1972 to 2018. Working document submitted to the ISC Albacore Working Group Meeting, 6-15 April 2020, by Webinar.
- Maunder, M. N. 2011. Review and evaluation of likelihood functions for composition data in stock-assessment models: Estimating the effective sample size. *Fisheries Research* 109(2–3):311–319.
- Maunder, M. N., and A. E. Punt. 2013. A review of integrated analysis in fisheries stock assessment. *Fisheries Research* 142:61–74. Elsevier B.V.
- Maunder, M., and K. Piner. 2015a. Contemporary fisheries stock assessment: many issues still remain. *ICES Journal of Marine Science* 72(1):7–18.
- Maunder, M., and K. Piner. 2015b. Contemporary fisheries stock assessment: many issues still remain. *ICES Journal of Marine Science* 72(1):7–18.
- Methot, R. D. 2000. Technical Description of the Stock Synthesis Assessment Program. NOAA Technical Memorandum NMFS-NWFSC-43. Northwest Fisheries Science Center, Seattle, Washington.
- Methot, R. D., and I. G. Taylor. 2011. Adjusting for bias due to variability of estimated recruitments in fishery assessment models. *Canadian Journal of Fisheries and Aquatic Sciences* 68(10):1744–1760.
- Methot, R. D., and C. R. Wetzel. 2013. Stock synthesis: A biological and statistical framework for fish stock assessment and fishery management. *Fisheries Research* 142:86–99. Elsevier B.V.
- Mohn, R. 1999. The retrospective problem in sequential population analysis: An investigation using cod fishery and simulated data. *ICES Journal of Marine Science* 56(4):473–488.
- Montes, I., M. Iriondo, C. Manzano, H. Arrizabalaga, E. Jiménez, M. Á. Pardo, N. Goñi, C. A. Davies, and A. Estonba. 2012. Worldwide genetic structure of albacore *Thunnus alalunga* revealed by microsatellite DNA markers. *Marine Ecology Progress Series* 471:183–191.
- Nishikawa, Y., M. Honma, S. Ueyanagi, and Kikawa S. 1985. Average distribution of larvae of oceanic species of scrombroid fishes, 1956–1981. Far Seas Fisheries Research Laboratory, Shimizu, S Series 12.
- Ochi, D., H. Ijima, J. Kinoshita, and H. Kiyofuji. 2016. New fisheries definition from Japanese longline North Pacific albacore size data. ISC/16/ALBWG-02/03. Working document submitted to ISC Albacore Working Group Meeting, 8 - 14 November, 2016, Pacific Biological Station, Nanaimo, BC, Canada.
- Ochi, D., H. Ijima, and H. Kiyofuji. 2017. Abundance indices of albacore caught by Japanese longline vessels in the North Pacific during 1976-2015. ISC/17/ALBWG/01. Working document

- submitted to the ISC Albacore Working Group Meeting, 11-19 April 2017, Southwest Fisheries Science Center, La Jolla, California, USA.
- Otsu, T., and R. F. Sumida. 1968. Distribution, apparent abundance, and size composition of albacore (*Thunnus alalunga*) taken in the longline fishery based in American Samoa, 1954-65. *Fishery Bulletin* 67(1):47-67.
- Otsu, T., and R. N. Uchida. 1959. Sexual maturity and spawning of albacore in the Pacific Ocean. *Fishery Bulletin* 59(148):287-305.
- Polovina, J. J., E. Howell, D. R. Kobayashi, and M. P. Seki. 2001. The transition zone chlorophyll front, a dynamic global feature defining migration and forage habitat for marine resources. *Progress in Oceanography* 49(1-4):469-483.
- Ramon, D., and K. Bailey. 1996. Spawning seasonality of albacore, *Thunnus alalunga*, in the South Pacific ocean. *Fishery Bulletin* 94(4):725-733.
- Schnute, J. 1981. A versatile growth model with statistically stable parameters. *Canadian Journal of Fisheries and Aquatic Sciences* 38(9):1128-1140.
- Suzuki, Z., Y. Warashina, and M. Kishida. 1977. The comparison of catches by regular and deep tuna longline gears in the western and central equatorial Pacific. *Bulletin Far Seas Fisheries Laboratory* 15:51-89.
- Takagi, M., T. Okamura, S. Chow, and N. Taniguchi. 2001. Preliminary study of albacore (*Thunnus alalunga*) stock differentiation inferred from microsatellite DNA analysis. *Fishery Bulletin* 99(4):697-701.
- Teo, S. L. H. 2016. Spatiotemporal definitions of the US albacore longline fleets in the north Pacific for the 2017 assessment. ISC/16/ALBWG-02/08. Working document submitted to ISC Albacore Working Group Meeting, 8 - 14 November, 2016, Pacific Biological Station, Nanaimo, BC, Canada.
- Teo, S. L. H. 2017. Meta-analysis of north Pacific albacore tuna natural mortality: an update. ISC/17/ALBWG/07. Working document submitted to the ISC Albacore Working Group Meeting, 11-19 April 2017, Southwest Fisheries Science Center, La Jolla, California, USA.
- Teo, S. L. H. 2019. Preliminary catch and size composition time series of the U.S. pelagic longline fleets for the 2020 north Pacific albacore tuna assessment. ISC/19/ALBWG-2/05. Working document submitted to the ISC Albacore Working Group Meeting, 12-18 November 2019, National Research Institute of Far Seas Fisheries, Shimizu, Shizuoka Japan.
- Teo, S. L. H., Y. Gu, and J. Childers. 2019. Preliminary catch and size composition time series of the U.S. and Mexico surface fishery for the 2020 north Pacific albacore tuna assessment. Working document submitted to the ISC Albacore Working Group Meeting, 12-18 November 2019, National Research Institute of Far Seas Fisheries, Shimizu, Shizuoka Japan.
- Then, A. Y., J. M. Hoenig, N. G. Hall, and D. A. Hewitt. 2015. Evaluating the predictive performance of empirical estimators of natural mortality rate using information on over 200 fish species. *ICES Journal of Marine Science* 72(1):82-92.
- Ueyanagi, S. 1957. Spawning of the albacore in the Western Pacific. Report of Nankai Regional Fisheries Research Laboratory 6:113-124.
- Ueyanagi, S. 1969. Observations on the distribution of tuna larvae in the Indo-Pacific Ocean with emphasis on the delineation of the spawning areas of albacore, *Thunnus alalunga*. *Bulletin Far Seas Fisheries Laboratory* 2:177-256.
- Uosaki, K., H. Kiyofuji, and T. Matsumoto. 2011. Review of Japanese albacore fisheries as of 2011. ISC/11/ALBWG/13. Working Paper submitted to the ISC Albacore Working Group Stock Assessment Workshop, 4-11 June 2011, National Research Institute of Far Sea Seas Fisheries, Shimizu, Japan.
- Vaux, F., S. Bohn, J. R. Hyde, and K. G. O'Malley. in prep. Population structure in a highly migratory species, albacore tuna (*Thunnus alalunga*). *Molecular Ecology*.

- Watanabe, H., T. Kubodera, S. Masuda, and S. Kawahara. 2004. Feeding habits of albacore *Thunnus alalunga* in the transition region of the central North Pacific. *Fisheries Science* 70:573–579.
- Watanabe, K., K. Uosaki, T. Kokubo, P. R. Crone, A. L. Coan, and C. C. Hsu. 2006. Revised practical solutions of application issues of length-weight relationship for the North Pacific albacore with respect to stock assessment. ISC/06/ALBWG/14. Report of the ISC Albacore Working Group Workshop, 28 November - 5 December, 2006.
- Waterhouse, L., D. B. Sampson, M. Maunder, and B. X. Semmens. 2014. Using areas-as-fleets selectivity to model spatial fishing: Asymptotic curves are unlikely under equilibrium conditions. *Fisheries Research* 158:15–25.
- WCPFC. 2014. Precautionary management framework for North Pacific albacore. Commission for the Conservation and Management of Highly Migratory Fish Stocks in the Western and Central Pacific Ocean. Northern Committee. Regular Session (10th : 2014 : Fukuoka, Japan). Ten.
- Wells, R. J. D., S. Kohin, S. L. H. Teo, O. E. Snodgrass, and K. Uosaki. 2013. Age and growth of North Pacific albacore (*Thunnus alalunga*): Implications for stock assessment. *Fisheries Research* 147:55–62. Elsevier B.V.
- Williams, A. J., J. H. Farley, S. D. Hoyle, C. R. Davies, and S. J. Nicol. 2012. Spatial and sex-specific variation in growth of albacore tuna (*Thunnus alalunga*) across the South Pacific Ocean. *PLoS ONE* 7(6).
- Xu, Y., T. Sippel, S. L. H. Teo, K. Piner, K. Chen, and R. J. Wells. 2014. A comparison study of North Pacific albacore (*Thunnus alalunga*) age and growth among various sources 1 (April 2014).
- Xu, Y., S. L. H. Teo, and J. Holmes. 2013. An update of standardized abundance index of US and Canada albacore troll fisheries in the North Pacific (1966-2012). ISC/13/ALBWG-03/06. Working paper submitted to the ISC Albacore Working Group Workshop, 5-12 November, 2013.
- Yoshida, H. O. 1966. Early life history and spawning of the albacore, *Thunnus alalunga*, in hawaiian waters. *Fishery Bulletin* 67(2):205–211.
- Zainuddin, M., H. Kiyofuji, K. Saitoh, and S. I. Saitoh. 2006. Using multi-sensor satellite remote sensing and catch data to detect ocean hot spots for albacore (*Thunnus alalunga*) in the northwestern North Pacific. *Deep-Sea Research Part II: Topical Studies in Oceanography* 53(3–4):419–431.
- Zainuddin, M., K. Saitoh, and S.-I. Saitoh. 2008. Albacore (*Thunnus alalunga*) fishing ground in relation to oceanographic conditions in the western North Pacific Ocean using remotely sensed satellite data. *Fisheries Oceanography* 17(2):61–73.

## TABLES



**Table 3.1.** Fishery definitions for the 2020 assessment of north Pacific albacore tuna. Availability of size and abundance index data is indicated in the notes. \* indicates that size or index data were available but were not fitted in the base case model. Two letter country codes are used in the fishery name: JP = Japan; US = United States of America; TW = Chinese-Taipei; KR = Korea; and VU = Vanuatu.

ID	Fishery name	Area	Primary gear	Quarter	Catch unit	Notes
F01	F01_JPLL_A13_Q1_wt	1 & 3	Longline	1	Tonnes	Size, Index*
F02	F02_JPLL_A13_Q2_wt	1 & 3	Longline	2	Tonnes	Size
F03	F03_JPLL_A13_Q3_wt	1 & 3	Longline	3	Tonnes	Size
F04	F04_JPLL_A13_Q4_wt	1 & 3	Longline	4	Tonnes	Size
F05	F05_JPLL_A13_Q1_num	1 & 3	Longline	1	1000s	
F06	F06_JPLL_A13_Q2_num	1 & 3	Longline	2	1000s	
F07	F07_JPLL_A13_Q3_num	1 & 3	Longline	3	1000s	
F08	F08_JPLL_A13_Q4_num	1 & 3	Longline	4	1000s	
F09	F09_JPLL_A2_Q1_wt	2	Longline	1	Tonnes	Size, Index
F10	F10_JPLL_A2_Q2_wt	2	Longline	2	Tonnes	Size
F11	F11_JPLL_A2_Q3_wt	2	Longline	3	Tonnes	Size
F12	F12_JPLL_A2_Q4_wt	2	Longline	4	Tonnes	Size
F13	F13_JPLL_A2_Q1_num	2	Longline	1	1000s	
F14	F14_JPLL_A2_Q2_num	2	Longline	2	1000s	
F15	F15_JPLL_A2_Q3_num	2	Longline	3	1000s	
F16	F16_JPLL_A2_Q4_num	2	Longline	4	1000s	
F17	F17_JPLL_A4_wt	4	Longline	All	Tonnes	Size
F18	F18_JPLL_A4_num	4	Longline	All	1000s	
F19	F19_JPLL_A5_num	5	Longline	All	1000s	Size
F20	F20_JPPL_A3_Q1	3	Pole & line	1	Tonnes	Size
F21	F21_JPPL_A3_Q2	3	Pole & line	2	Tonnes	Size
F22	F22_JPPL_A3_Q3	3	Pole & line	3	Tonnes	Size
F23	F23_JPPL_A3_Q4	3	Pole & line	4	Tonnes	Size
F24	F24_JPPL_A2	2	Pole & line	All	Tonnes	Size
F25	F25_USLL_A35	3 & 5	Longline	All	Tonnes	Size
F26	F26_USLL_A24	2 & 4	Longline	All	Tonnes	Size
F27	F27_TWLL_A35	3 & 5	Longline	All	Tonnes	Size
F28	F28_TWLL_A24	2 & 4	Longline	All	Tonnes	
F29	F29_KRLL	All	Longline	All	Tonnes	
F30	F30_CNLL_A35	3 & 5	Longline	All	Tonnes	Size*
F31	F31_CNLL_A24	2 & 4	Longline	All	Tonnes	Size*
F32	F32_VULL	All	Longline	All	Tonnes	Size*
F33	F33_EPOSF	3 & 5	Surface	All	Tonnes	Size
F34	F34_JPKRTW_DN	All	Drift net	All	Tonnes	
F35	F35_JPTW_MISC	All	Misc	All	Tonnes	

**Table 3.2.** Standardized values and input coefficients of variation (CVs) of north Pacific albacore annual abundance indices developed for the 2020 base case model (F09 index) and sensitivity runs (F01 index). Units are number of fish for both indices. Quarter refers to annual quarters in which the majority of catch was made in the underlying fishery, where 1 = Jan-Mar, 2 = Apr-June, 3 = July-Sept, and 4 = Oct-Dec. A constant of 0.100 (i.e., additional CV) was added to the CVs of the F9 index in the base case model, and 0.165 to the CV of the F1 index in sensitivity model runs, to raise the average CV to 0.2 or the CV of the index relative to a loess smoother, whichever is greater. CV values shown here do not include these additional CVs.

Year	F09 index – Japanese longline in Area 2, Quarter 1		F01 index – Japanese longline in Areas 1 and 3, Quarter 1 (sensitivity runs only)	
	CPUE	CV	CPUE	CV
1996	43.148	0.094	57.896	0.115
1997	50.043	0.096	97.980	0.112
1998	50.614	0.103	79.236	0.110
1999	38.506	0.098	52.345	0.116
2000	53.037	0.096	55.073	0.115
2001	47.347	0.099	34.998	0.124
2002	31.990	0.100	58.925	0.122
2003	35.640	0.100	61.889	0.121
2004	25.644	0.092	30.857	0.110
2005	33.392	0.100	33.002	0.112
2006	36.330	0.091	35.820	0.114
2007	31.747	0.106	51.969	0.109
2008	33.182	0.111	31.225	0.126
2009	34.450	0.094	35.391	0.131
2010	40.304	0.109	34.075	0.117
2011	31.304	0.106	28.535	0.110
2012	31.343	0.092	52.267	0.119
2013	29.238	0.101	34.363	0.109
2014	22.753	0.106	33.818	0.113
2015	41.259	0.095	48.697	0.112
2016	25.922	0.100	26.162	0.114
2017	27.325	0.109	34.664	0.113
2018	31.019	0.100	21.188	0.119

**Table 4.1.** Key life history parameters and model structures used in the base case model.

Parameter	Value	Comments	Source
Natural mortality (M)	Female age-0: 1.36 y <sup>-1</sup> Female age-1: 0.56 y <sup>-1</sup> Female age-2: 0.45 y <sup>-1</sup> Female age-3+: 0.48 y <sup>-1</sup> Male age-0: 1.36 y <sup>-1</sup> Male age-1: 0.56 y <sup>-1</sup> Male age-2: 0.45 y <sup>-1</sup> Male age-3+: 0.39 y <sup>-1</sup>	Fixed parameter.	Teo (2017)
Length at age-1 (L <sub>1</sub> )	Female: 43.504 cm Male: 47.563 cm	Fixed parameter	Xu et al. (2014)
Asymptotic length (L <sub>inf</sub> )	Female: 106.57 cm Male: 119.15 cm	Fixed parameter	Xu et al. (2014)
Growth rate (k)	Female: 0.29763 y <sup>-1</sup> Male: 0.20769 y <sup>-1</sup>	Fixed parameter	Xu et al. (2014)
CV of L <sub>1</sub>	0.06	Non sex-specific, fixed parameter	ALBWG (2014)
CV of L <sub>inf</sub>	0.04	Non sex-specific, fixed parameter	ALBWG (2014)
Weight-at-length – Q1	$W_L$ (kg) = $8.7 * 10^{-5} L$ (cm) <sup>2.67</sup>	Non sex-specific, fixed parameters	Watanable et al. (2006)
Weight-at-length – Q2	$W_L$ (kg) = $3.9 * 10^{-5} L$ (cm) <sup>2.84</sup>	Non sex-specific, fixed parameters	Watanable et al. (2006)
Weight-at-length – Q3	$W_L$ (kg) = $2.1 * 10^{-5} L$ (cm) <sup>2.99</sup>	Non sex-specific, fixed parameters	Watanable et al. (2006)
Weight-at-length – Q4	$W_L$ (kg) = $2.8 * 10^{-5} L$ (cm) <sup>2.92</sup>	Non sex-specific, fixed parameters	Watanable et al. (2006)
Maturity	50% at age-5, 100% age-6+	Fixed parameters	Ueyanagi (1957); Chen et al. (2016);
Fecundity	Proportional to spawning biomass	Fixed parameters	Ueyanagi (1957)
Spawning season	2	Model structure	Ueyanagi (1957); Chen et al. (2010); Ashida et al. (2016)
Spawner-recruit relationship	Beverton-Holt	Model structure	

Parameter	Value	Comments	Source
Spawner-recruit steepness (h)	0.9	Fixed parameter	Brodziak et al. (2011); Iwata et al. (2011); ALBWG (2014)
Log of Recruitment at virgin biomass $\ln(R_0)$	12.1013	Maximum likelihood estimate	
Recruitment variability ( $\sigma_R$ )	0.3	Fixed parameter	
Initial age structure	10 y	Estimated	
Main recruitment deviations	1994-2018	Estimated	
Selectivity	Size selectivity only (splines): F01, F03, & F17 Size selectivity only (dome): F02, F04, F09, F10, F11, F12, F19, F24, F25, F26, & F27 Size and age selectivity: F20, F21, F22, F23, & F33 Shared selectivity: F05, F06, F07, F08, F13, F14, F15, F16, F18, F28, F29, F30, F31, F32, F34, & F35	Estimated (see Table 4.2)	
Catchability		Solved analytically	

**Table 4.2.** Selectivity parameters used in the base case model for fisheries with only size selectivity. Estimated parameters are shown in bold, with estimated standard deviation in parentheses. The optional initial and final parameters for all double-normal selectivity curves were fixed at -999 and ignored by the model. The value for the first knot for all spline selectivity curves were fixed at 0 and values for the second and third knot were estimated relative to that. Knot locations in cm are indicated in parentheses in the years column.

<b>Size selectivity (double-normal)</b>					
Fishery	Years	Parm 1 – Size at peak	Parm 2 – Plateau width	Parm 3 – Ascending slope	Parm 4 – Descending slope
F02	1994 – 2018	<b>79.9 (1.0)</b>	-9	<b>3.85 (0.28)</b>	<b>4.64 (0.28)</b>
F04	1994 – 2018	<b>108.8 (4.0)</b>	<b>-1.45 (2.37)</b>	<b>5.67 (0.21)</b>	<b>2.60 (10.48)</b>
F09	1994 – 2018	<b>109.4 (7.8)</b>	<b>-6.96 (38.57)</b>	<b>5.43 (0.55)</b>	<b>2.83 (4.97)</b>
F10	1994 – 2018	<b>106.3 (2.1)</b>	<b>-7.20 (34.69)</b>	<b>4.43 (0.27)</b>	<b>3.95 (1.11)</b>
F11	1994 – 2018	<b>106.3 (2.2)</b>	<b>-6.89 (38.10)</b>	<b>4.58 (0.26)</b>	<b>3.27 (1.22)</b>
F12	1994 – 2018	<b>109.3 (2.8)</b>	<b>-8.04 (21.96)</b>	<b>4.97 (0.24)</b>	<b>3.07 (1.67)</b>
F19	1994 – 2018	<b>108.6 (40.3)</b>	<b>-0.29 (31.86)</b>	<b>6.15 (1.82)</b>	<b>1.91 (153.98)</b>
F24	1994 – 2018	<b>92.4 (3.2)</b>	-9	<b>4.13 (0.71)</b>	<b>2.28 (2.29)</b>
F25	1994 – 2004	<b>66.6 (13.0)</b>	<b>0.56 (4.34)</b>	<b>2.00 (8.10)</b>	<b>1.72 (156.02)</b>
	2005 – 2018	<b>90.1 (12.4)</b>	<b>0.52 (32.75)</b>	<b>5.49 (1.10)</b>	<b>4.01 (111.37)</b>
F26	1994 – 2004	<b>136.4 (22.9)</b>	<b>0.00 (201.24)</b>	<b>5.74 (0.71)</b>	<b>4.00 (111.80)</b>
	2005 – 2018	<b>133.0 (34.3)</b>	<b>0.00 (201.24)</b>	<b>5.89 (1.15)</b>	<b>4.00 (111.80)</b>
F27	1994 – 2018	<b>91.8 (1.9)</b>	<b>0.71 (54.95)</b>	<b>5.34 (0.15)</b>	<b>4.01 (111.62)</b>
<b>Size selectivity (3-knot spline)</b>					
Fishery	Years (knot locations in cm)	Gradient Low	Gradient High	Value at 2 <sup>nd</sup> knot	Value at 3 <sup>rd</sup> knot
F01	1994 – 2018 (60, 90, 130)	<b>1.05 (0.17)</b>	<b>-1.15 (0.63)</b>	<b>6.95 (1.03)</b>	<b>-3.46 (6.59)</b>
F03	1994 – 2018 (70, 95, 120)	<b>0.666 (0.2)</b>	<b>-0.56 (0.84)</b>	<b>5.32 (3.23)</b>	<b>4.16 (5.01)</b>
F17	1994 – 2018 (60, 90, 140)	<b>0.17 (0.26)</b>	<b>-1.07 (0.88)</b>	<b>6.74 (5.70)</b>	<b>-1.81 (15.44)</b>

**Table 4.3.** Size selectivity parameters used in the base case model for fisheries with selectivity assumed to be a product of size and age selectivity. Estimated parameters are shown in bold, with estimated standard deviation in parentheses. Size selectivity was assumed to follow a double-normal function. The optional initial and final parameters for all double-normal selectivity curves were fixed at -999 and ignored by the model.

<b>Size selectivity (double-normal)</b>					
Fishery	Years	Parm 1 – Size at peak	Parm 2 – Plateau width	Parm 3 – Ascending slope	Parm 4 – Descending slope
F20	1994 – 2018	<b>71.8 (8.3)</b>	<b>-7.01 (8.26)</b>	<b>4.05 (1.50)</b>	<b>2.58 (2.34)</b>
F21	1994 – 2018	<b>71.8 (7.7)</b>	<b>-5.73 (32.4)</b>	<b>4.78 (0.70)</b>	<b>4.56 (0.44)</b>
F22	1994 – 2018	<b>55.4 (1.6)</b>	<b>-2.00 (0.36)</b>	<b>2.51 (0.71)</b>	<b>5.35 (0.34)</b>
F23	1994 – 2018	<b>55.6 (3.3)</b>	<b>-1.05 (0.64)</b>	<b>2.58 (1.86)</b>	<b>3.35 (3.18)</b>
F33	1994 – 2018	<b>58.6 (1.7)</b>	<b>-2.77 (0.73)</b>	<b>2.67 (0.60)</b>	<b>5.34 (0.26)</b>

**Table 4.4.** Age selectivity parameters used in the base case model for fisheries with selectivity assumed to be a product of size and age selectivity. Estimated parameters are shown in bold, with estimated standard deviation in parentheses. Age selectivity was modeled as estimated free parameters for ages-1 to 5, with all other ages fixed at a negligible low value (-9 or -12). Estimated age selectivity parameters at the lower (-9 or -12) or upper (9 or 12) bound were fixed at the bound on the final run to improve model optimization.

<b>Age selectivity (free parameters for ages-1 to 5)</b>						
<b>Fishery</b>	<b>Years</b>	<b>Age-1</b>	<b>Age-2</b>	<b>Age-3</b>	<b>Age-4</b>	<b>Age-5</b>
F20	1994 – 2018	<b>-5.19 (67.1)</b>	<b>-2.86 (34.3)</b>	<b>-6.70 (35.5)</b>	<b>-1.42 (34.9)</b>	<b>7.64 (34.3)</b>
F21	1994	<b>-5.83 (62.4)</b>	<b>-8.06 (49.3)</b>	<b>-9.65 (46.0)</b>	<b>-8.77 (56.5)</b>	<b>11.00 (28.1)</b>
	1995	<b>7.75 (32.8)</b>	<b>-4.22 (32.9)</b>	<b>-5.75 (34.6)</b>	<b>-0.44 (33.4)</b>	<b>-6.61 (48.4)</b>
	1996	<b>-1.87 (9.03)</b>	<b>-3.67 (8.84)</b>	<b>-8.63 (10.4)</b>	<b>8.70 (8.75)</b>	<b>-7.15 (36.3)</b>
	1997	<b>-6.66 (37.6)</b>	<b>-4.82 (9.89)</b>	<b>-8.51 (13.0)</b>	<b>8.66 (9.72)</b>	<b>-6.79 (41.4)</b>
	1998	<b>-7.33 (30.6)</b>	<b>-6.14 (19.4)</b>	<b>-6.65 (19.6)</b>	<b>-5.17 (20.4)</b>	<b>8.30 (19.2)</b>
	1999	<b>-1.76 (41.6)</b>	<b>-3.81 (41.5)</b>	<b>-6.36 (41.6)</b>	<b>7.27 (41.5)</b>	<b>-1.80 (41.7)</b>
	2000	<b>7.15 (45.1)</b>	<b>-5.51 (45.2)</b>	<b>-2.94 (45.1)</b>	<b>-3.80 (45.3)</b>	<b>-2.48 (46.8)</b>
	2001	<b>8.45 (15.2)</b>	<b>-3.90 (15.3)</b>	<b>-4.85 (15.3)</b>	<b>-8.33 (17.5)</b>	<b>-1.38 (15.4)</b>
	2002	<b>7.42 (39.4)</b>	<b>-0.67 (39.7)</b>	<b>-2.90 (39.4)</b>	<b>-1.64 (39.6)</b>	<b>-6.98 (45.8)</b>
	2003	<b>-2.66 (17.8)</b>	<b>-5.28 (17.4)</b>	<b>-7.78 (27.3)</b>	<b>8.39 (17.1)</b>	<b>-7.36 (34.4)</b>
	2004	<b>-2.78 (48.4)</b>	<b>-3.66 (48.4)</b>	<b>-4.14 (48.4)</b>	<b>7.02 (48.4)</b>	<b>-4.12 (49.0)</b>
	2005	<b>-4.00 (25.1)</b>	<b>-2.85 (22.8)</b>	<b>-7.58 (32.0)</b>	<b>8.17 (22.8)</b>	<b>-6.31 (49.8)</b>
	2006	<b>-1.59 (42.9)</b>	<b>-4.85 (42.8)</b>	<b>-5.28 (42.8)</b>	<b>7.27 (42.8)</b>	<b>-3.71 (45.6)</b>
	2007	<b>-1.88 (51.5)</b>	<b>-3.58 (51.0)</b>	<b>-5.43 (51.0)</b>	<b>-0.97 (53.9)</b>	<b>6.79 (51.1)</b>
	2008	<b>7.92 (28.4)</b>	<b>-3.19 (28.4)</b>	<b>-2.04 (28.4)</b>	<b>-2.57 (28.5)</b>	<b>-7.60 (33.4)</b>
	2009	<b>-7.20 (39.2)</b>	<b>-4.38 (32.8)</b>	<b>-3.08 (32.8)</b>	<b>7.71 (32.8)</b>	<b>0.29 (34.8)</b>
	2010	<b>7.43 (39.6)</b>	<b>-5.12 (39.6)</b>	<b>-4.95 (39.6)</b>	<b>-4.97 (39.7)</b>	<b>-1.46 (39.7)</b>
	2011	<b>-5.97 (44.7)</b>	<b>-7.43 (30.8)</b>	<b>-3.00 (27.6)</b>	<b>2.77 (88.4)</b>	<b>7.89 (27.7)</b>
	2012	<b>-6.45 (41.8)</b>	<b>-5.56 (31.6)</b>	<b>-4.91 (31.6)</b>	<b>-1.99 (31.5)</b>	<b>7.80 (31.5)</b>
	2013 – 2014	<b>-4.70 (44.8)</b>	<b>-3.99 (43.8)</b>	<b>-4.71 (43.8)</b>	<b>-2.59 (43.8)</b>	<b>7.25 (43.8)</b>
	2015	<b>8.35 (18.1)</b>	<b>-6.37 (21.2)</b>	<b>-7.72 (28.5)</b>	<b>-1.07 (18.2)</b>	<b>-6.91 (40.9)</b>
	2016	<b>-5.37 (39.1)</b>	<b>-7.25 (24.6)</b>	<b>-6.70 (25.7)</b>	<b>8.30 (19.2)</b>	<b>-6.18 (50.7)</b>
	2017	<b>-5.34 (49.8)</b>	<b>-6.66 (31.2)</b>	<b>-7.94 (25.2)</b>	<b>8.41 (16.8)</b>	<b>-4.98 (64.5)</b>

Age selectivity (free parameters for ages-1 to 5)						
Fishery	Years	Age-1	Age-2	Age-3	Age-4	Age-5
	2018	-5.97 (35.9)	-4.83 (9.63)	-8.56 (11.9)	8.67 (9.31)	-6.75 (41.9)
F22	1994	-12	-12	-11.4 (1.3)	-8.87 (1.1)	1.56 (0.6)
	1995	-4.82 (24.1)	-4.21 (24.0)	-3.96 (24.1)	8.12 (24.0)	-7.60 (32.3)
	1996	-3.79 (46.6)	-4.31 (46.6)	-3.29 (46.6)	7.12 (46.6)	-4.10 (48.2)
	1997	-1.44 (34.3)	-2.86 (34.3)	-3.91 (34.3)	7.68 (34.2)	-7.08 (42.6)
	1998	-2.73 (45.7)	-5.06 (45.9)	7.14 (45.7)	-4.33 (49.2)	-2.86 (49.2)
	1999	-4.32 (29.0)	-2.82 (29.0)	-3.60 (29.0)	7.91 (29.0)	-7.33 (37.5)
	2000	-4.43 (33.0)	-7.06 (33.1)	-1.97 (33.1)	-0.99 (33.7)	7.64 (33.0)
	2001	-3.47 (62.1)	-4.32 (62.1)	-3.06 (62.1)	6.00 (62.2)	2.17 (114.8)
	2002	-1.59 (24.9)	8.06 (24.9)	1.46 (26.3)	-7.67 (31.3)	-6.35 (49.5)
	2003 – 2004	-0.27 (42.7)	-1.45 (42.5)	-2.29 (42.5)	7.25 (42.4)	-6.86 (48.4)
	2005	8.32 (18.6)	-7.97 (24.2)	-6.58 (42.3)	-0.94 (19.1)	-4.23 (74.7)
	2006	-1.90 (29.1)	-7.37 (30.9)	-5.47 (33.2)	7.82 (29.0)	1.17 (113.2)
	2007 – 2008	-4.09 (52.4)	-2.94 (52.3)	2.92 (100.2)	6.71 (52.0)	-5.80 (65.6)
	2009	-7.96 (23.2)	-7.43 (29.3)	-2.50 (16.2)	8.45 (15.4)	-5.38 (59.2)
	2010	8.19 (22.1)	-6.46 (24.5)	-7.05 (35.4)	-6.81 (42.8)	0.14 (34.2)
	2011	-4.35 (33.9)	-3.97 (34.2)	7.74 (33.6)	-6.60 (49.0)	-3.91 (59.7)
	2012 – 2013	-1.90 (8.6)	-8.62 (10.2)	-7.94 (23.3)	-1.81 (9.2)	8.73 (7.9)
	2014	-8.12 (20.3)	-6.38 (19.4)	-4.61 (23.1)	8.47 (14.8)	-6.04 (51.9)
	2015 – 2016	7.24 (40.4)	-5.95 (40.9)	-4.58 (42.2)	4.67 (74.1)	-5.87 (60.3)
	2017 – 2018	-8.44 (14.0)	-6.16 (13.4)	-5.92 (23.6)	8.61 (11.0)	-5.46 (58.4)
F23	1994 – 2018	-1.48 (45.0)	-1.79 (45.0)	-4.11 (45.1)	7.19 (45.0)	-6.12 (58.8)
F33	1994 – 1998	-12	-12	-11.15 (0.5)	-10.12 (1.3)	-0.76 (0.9)
	1999 – 2018	-6.20 (38.5)	-4.60 (38.5)	-3.56 (38.5)	-2.30 (38.5)	7.47 (38.5)



**Table 4.5.** Fisheries without an estimated selectivity were assumed to have size selectivity identical to other fisheries (mirrored selectivity).

<b>Mirrored selectivity</b>			
Fishery without estimated selectivity	Mirrored to	Fishery without estimated selectivity	Mirrored to
F05	F01	F18	F17
F06	F02	F28	F17
F07	F03	F29	F17
F08	F04	F30	F27
F13	F09	F31	F17
F14	F10	F32	F27
F15	F11	F34	F20
F16	F12	F35	F20

**Table 4.6.** Sensitivity analyses conducted on the 2020 base case model for north Pacific albacore.

<b>Sensitivity run number</b>	<b>Sensitivity run name</b>	<b>Description</b>
<b>Sensitivity to biological assumptions</b>		
01	Natural mortality	Use a constant $M$ of $0.3 \text{ y}^{-1}$ for both sexes and all ages (same as 2014 assessment); a constant $M$ of $0.48$ and $0.39 \text{ y}^{-1}$ for female and male albacore of all ages, respectively; and an estimated, single-parameter, female $M$ for all ages, with the prior from Teo et al. (2017), $M_{\text{female}} \sim \log N[-0.7258, (0.457)^2]$ , and a constant logscale offset ( $-0.21258$ ) between male and female $M$ .
02	Stock-recruitment steepness	Use alternative constant values for the steepness parameter ( $h = 0.75; 0.80; \text{ and } 0.85$ ); and an estimated $h$ with the prior, $h \sim N[0.9, (0.05)^2]$ .
03	Growth	CV of $L_{\text{inf}}$ is fixed at higher ( $0.06$ & $0.08$ ) levels. Lower CV levels were not investigated because CV values smaller than the base case model ( $0.04$ ) was considered unreasonable.
<b>Sensitivity to data inputs</b>		
04	Catch estimates for F30, F31 and F32	Change catch time series of F30, F31, and F32 during 1994 – 2015 to catch data from the 2017 assessment.
05	Catch of F33 during 2016 – 2018	Double the catch for the EPO surface fishery (F33) during 2016 – 2018.
06	Extended F09 index	Fit to an extended F09 index (1994 – 2018) that was developed using the same method described in Fujioka et al. (2020).
07	Fit to F01 index	Fit to the F01 index as an index for juvenile/subadult albacore (Section 3.5.2).
08	Size composition weighting	Change the relative weighting of size composition data. Fit size composition data of Japanese longline fishery in Area 2 during Quarter 1 (F09) at natural weight (input sample size multiplier = $0.1625$ ). Down-weight size composition data of each fishery ( $\lambda = 0.1$ ).
<b>Sensitivity to model structure assumptions</b>		
09	US longline asymptotic selectivity	Assume that the US longline fishery in Areas 2 & 4 (F26) has an asymptotic size selectivity.
10	Equilibrium catch	Initial conditions: fit to equilibrium catch of each fishery estimated as the average of 10 years of annual catch during 1984 – 1993. Equilibrium catch of fisheries that were $\leq 50 \text{ t}$ or $\leq 25,000$ fish were assumed to be negligible.

---

<b>Sensitivity run number</b>	<b>Sensitivity run name</b>	<b>Description</b>
11	Start year	Several alternative models with a 1966 start year were developed and examined by the ALBWG. However, all were considered as inadequate as the base case model.
12	2017 base case model structure	Model structure follows the 2017 assessment as close as possible (average input sample size of all fisheries at ~7; down-weight size composition data for Japanese longline fisheries in Areas 2 & 4 and Us longline fisheries; no time varying selectivity for Japanese pole-and-line fisheries; selectivity patterns similar to selectivity patterns in 2017 assessment)

---

**Table 5.1.** Analytical estimates of catchability, mean input variance, variance adjustment, and model fit (root-mean-square-error; RMSE of predictions to observations) for the F9 abundance index in the 2020 base case model.

Index	Years	Catchability	Mean input CV	Variance adjustment	Input CV + Var. Adj.	RMSE
F9	1996 – 2018	2.783E-02	9.99E-02	0.100	0.200	0.169

**Table 5.2.** Mean input variances (input N after variance adjustment) and model estimated mean variance (*effN*) of the size composition data components. Harmonic means of *effN* and ratio of input N to *effN* are also provided. A higher *effN* indicates a better model fit. Number of observations corresponds to the number of quarters in which size composition data were sampled in a fishery.

Fishery	Number of obs.	Var. adj.	Mean input N after var. adj.	Mean effective N ( <i>effN</i> )	Harmonic mean of <i>effN</i>	Harmonic mean <i>effN</i> / mean input N	Francis weighting multiplier
F01	25	0.09756	18.0	68.1	34.3	1.9	1.0
F02	22	0.1626	11.6	55.6	42.7	3.7	2.7
F03	15	0.1626	1.4	45.2	23.9	16.9	7.4
F04	25	0.1626	12.4	129.4	78.8	6.4	2.1
F09	25	0.01626	0.8	99.0	66.6	79.2	17.5
F10	21	0.1626	6.0	135.6	35.0	5.8	4.1
F11	16	0.1626	6.8	229.1	132.0	19.4	13.9
F12	23	0.1626	4.7	102.3	66.9	14.3	4.6
F17	47	0.1626	1.2	96.2	35.1	29.9	9.3
F19	8	0.1626	0.7	50.8	31.9	47.7	19.6
F20	3	0.1626	1.3	57.1	32.6	26.0	22.8
F21	24	0.1626	8.6	144.8	43.6	5.1	13.8
F22	20	0.1626	9.9	85.0	25.9	2.6	32.9
F23	9	0.14634	4.1	12.0	9.9	2.4	1.0
F24	7	0.1626	1.3	13.3	8.5	6.8	5.4
F25	20	0.1626	0.6	67.7	34.0	58.8	40.6
F26	55	0.1626	1.2	106.4	46.7	40.0	40.1
F27	42	0.13008	13.4	60.0	29.7	2.2	1.1
F33	57	0.1626	16.4	255.9	84.2	5.1	3.0

**Table 5.3.** Total biomass (Q1, age-1+), female spawning biomass (Q2), limit reference point adopted by the NC of the WCPFC ( $20\%SSB_{\text{current}, F=0}$ ), recruitment, and fishing intensity (1-SPR) estimated in the base case model. Estimated virgin female spawning biomass ( $SSB_0$ ) and virgin recruitment are 136,833 t and 180 million fish, respectively.

<b>Year</b>	<b>Total biomass age-1+ (t)</b>	<b>Female spawning biomass (t)</b>	<b>Limit reference point (<math>20\%SSB_{\text{current}, F=0}</math>) (t)</b>	<b>Recruitment (x1000 fish)</b>	<b>Fishing intensity (1-SPR)</b>
1994	902,294	81,740	29,123	189,594	0.46
1995	916,529	80,590	28,401	163,714	0.40
1996	905,067	86,715	28,917	170,831	0.48
1997	863,514	83,222	28,807	153,239	0.54
1998	796,695	82,166	29,972	156,442	0.54
1999	743,767	81,895	31,001	256,880	0.71
2000	717,837	67,893	29,768	156,185	0.57
2001	739,902	61,536	28,507	199,342	0.56
2002	745,274	55,030	27,271	139,882	0.62
2003	709,236	54,971	26,155	186,757	0.58
2004	686,419	62,896	28,414	249,480	0.65
2005	712,443	59,876	29,317	170,586	0.46
2006	763,458	59,584	29,068	173,815	0.50
2007	781,779	58,027	28,095	149,597	0.59
2008	749,531	57,404	27,504	187,181	0.45
2009	750,445	71,947	29,950	164,899	0.55
2010	737,662	71,887	30,728	180,860	0.48
2011	742,227	68,172	29,619	137,925	0.52
2012	723,446	64,754	28,167	139,635	0.61
2013	675,066	59,904	27,737	197,952	0.60
2014	660,993	57,602	27,580	124,520	0.60
2015	646,243	55,930	27,432	112,811	0.57
2016	617,363	54,313	26,437	169,108	0.48
2017	617,985	52,466	24,870	175,497	0.45
2018	641,391	58,858	25,573	173,719	0.47

**Table 5.4.** Estimates of maximum sustainable yield (MSY), female spawning biomass (SSB), and fishing intensity (F) based reference point ratios for north Pacific albacore tuna for: 1) the base case model; 2) an important sensitivity model due to uncertainty in growth parameters; and 3) a model representing an update of the 2017 base case model to 2020 data.  $SSB_0$  and  $SSB_{MSY}$  are the unfished biomass of mature female fish and at MSY, respectively. The Fs in this table are indicators of fishing intensity based on SPR and calculated as  $1-SPR$  so that the Fs reflect changes in fishing mortality (e.g.,  $F_{20\%}$  is calculated as  $1-SPR_{20\%}$ ). SPR is the equilibrium SSB per recruit that would result from the current year's pattern and intensity of fishing mortality. Current fishing intensity is based on the average fishing intensity during 2015-2017 ( $F_{2015-2017}$ ).  $20\%SSB_{current, F=0}$  is 20% of the current unfished dynamic female spawning biomass, where current refers to the terminal year of this assessment (i.e., 2018). The model representing an update of the 2017 base case model is highly similar to but not identical to the 2017 base case model due to changes in data preparation and model structure.

Quantity	Base Case	Growth CV = 0.06 for $L_{inf}$	Update of 2017 base case model to 2020 data
MSY (t) <sup>A</sup>	102,236	84,385	113,522
$SSB_{MSY}$ (t) <sup>B</sup>	19,535	16,404	21,431
$SSB_0$ (t) <sup>B</sup>	136,833	113,331	152,301
$SSB_{2018}$ (t) <sup>B</sup>	58,858	34,872	77,077
$SSB_{2018}/20\%SSB_{current, F=0}$ <sup>B</sup>	2.30	1.63	2.63
$F_{2015-2017}$	0.50	0.64	0.43
$F_{2015-2017}/F_{MSY}$	0.60	0.77	0.52
$F_{2015-2017}/F_{0.1}$	0.57	0.75	0.49
$F_{2015-2017}/F_{10\%}$	0.55	0.71	0.48
$F_{2015-2017}/F_{20\%}$	0.62	0.80	0.54
$F_{2015-2017}/F_{30\%}$	0.71	0.91	0.62
$F_{2015-2017}/F_{40\%}$	0.83	1.06	0.72
$F_{2015-2017}/F_{50\%}$	1.00	1.27	0.86

A – MSY includes male and female juvenile and adult fish

B – Spawning stock biomass (SSB) in this assessment refers to mature female biomass only.

## FIGURES

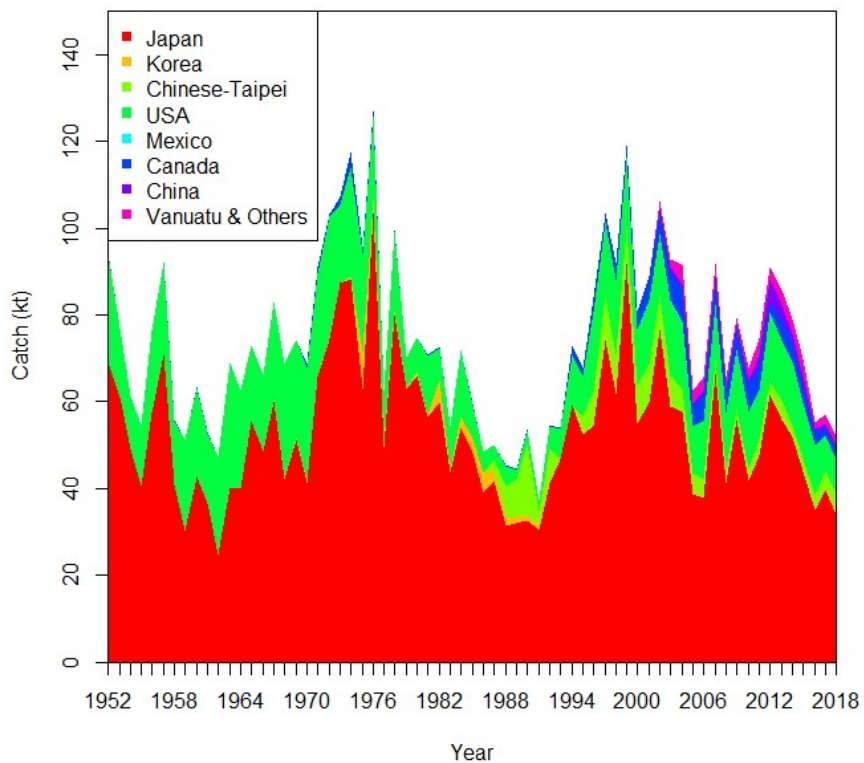


**Figure 2.1.** Total annual reported catch of north Pacific albacore (*Thunnus alalunga*) by ISC member and non-member countries, 1952-2018. Catches by Vanuatu and other countries includes small amounts of catch by other countries such as Tonga, Belize, Cook Islands, and Marshall Islands.



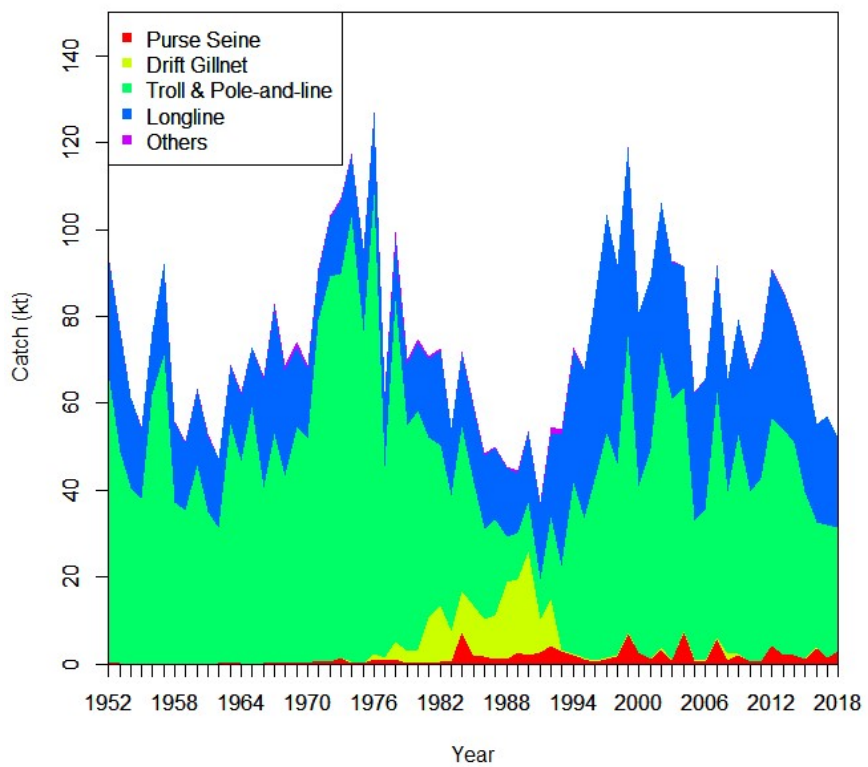


**Figure 2.2.** Total annual reported catch of north Pacific albacore by major gear types, 1952-2018. The Other Gears category includes set nets, recreational, hand line, and harpoon.

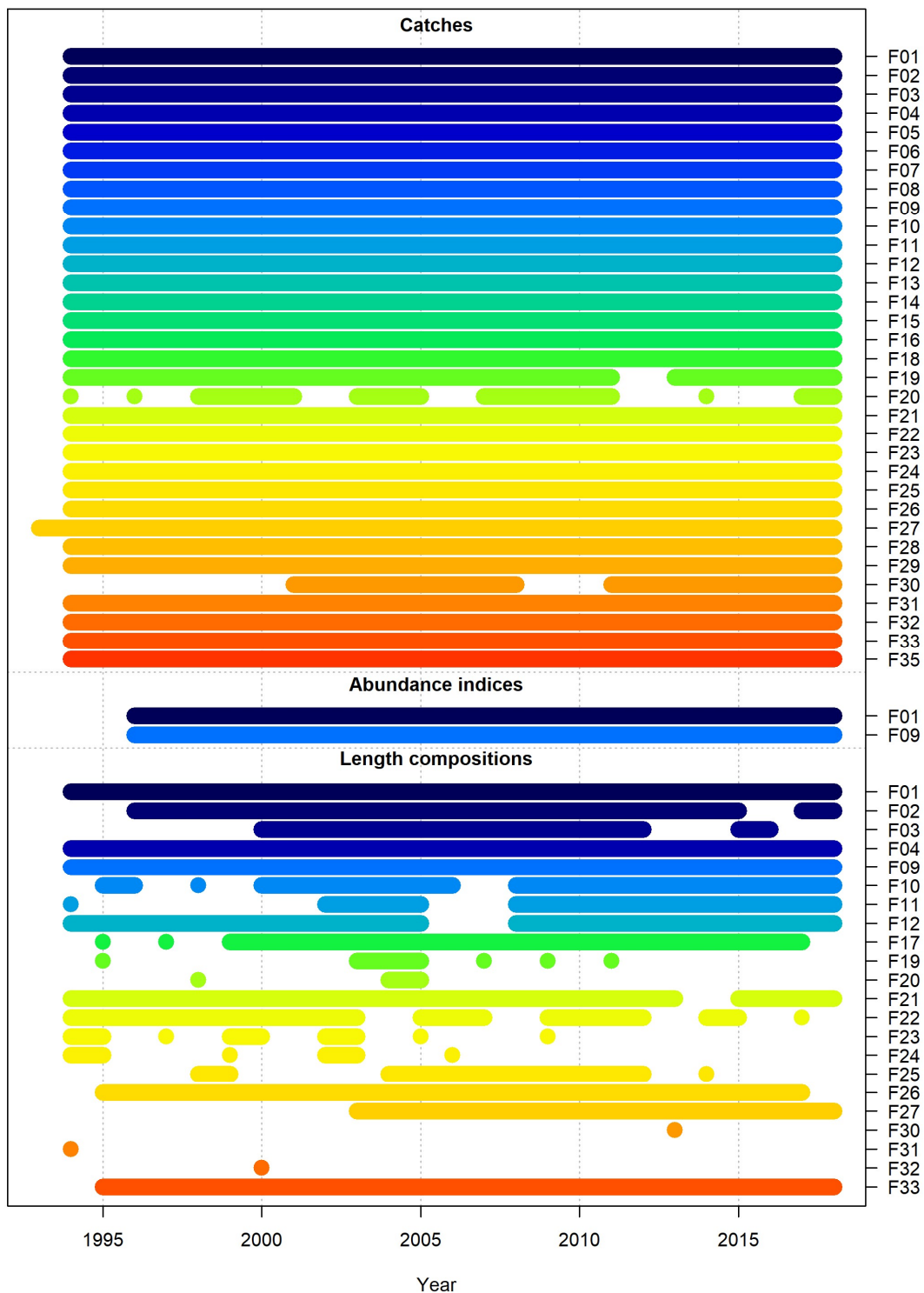


**Figure 3.1.** Temporal coverage and sources of catch, abundance indices, and length composition data by fishery used in the 2020 assessment of north Pacific albacore tuna. See the text and Table 3.1 for detailed descriptions of fishery codes.

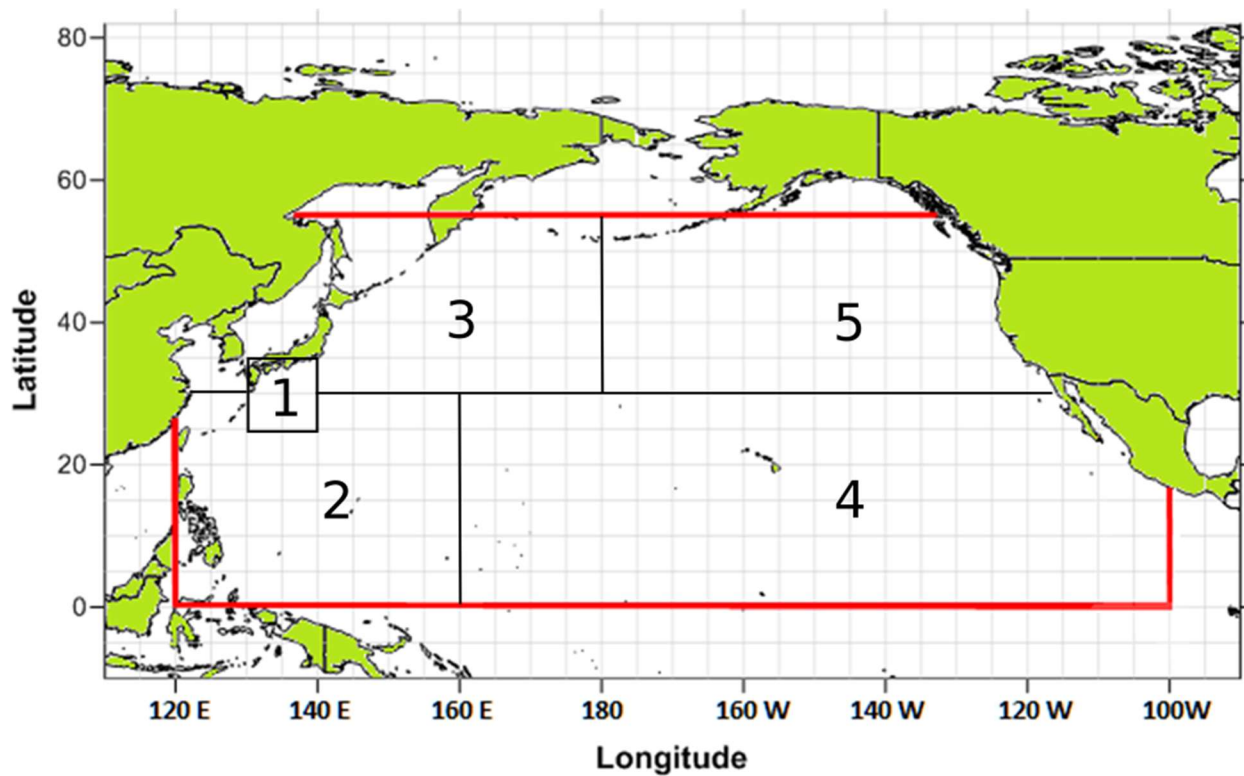


**Figure 3.2.** Spatial domain (red box) of the north Pacific albacore stock (*Thunnus alalunga*) in the 2020 stock assessment. Fishery definitions were based on five fishing areas (black boxes and numbers) defined from cluster analyses of size composition data.

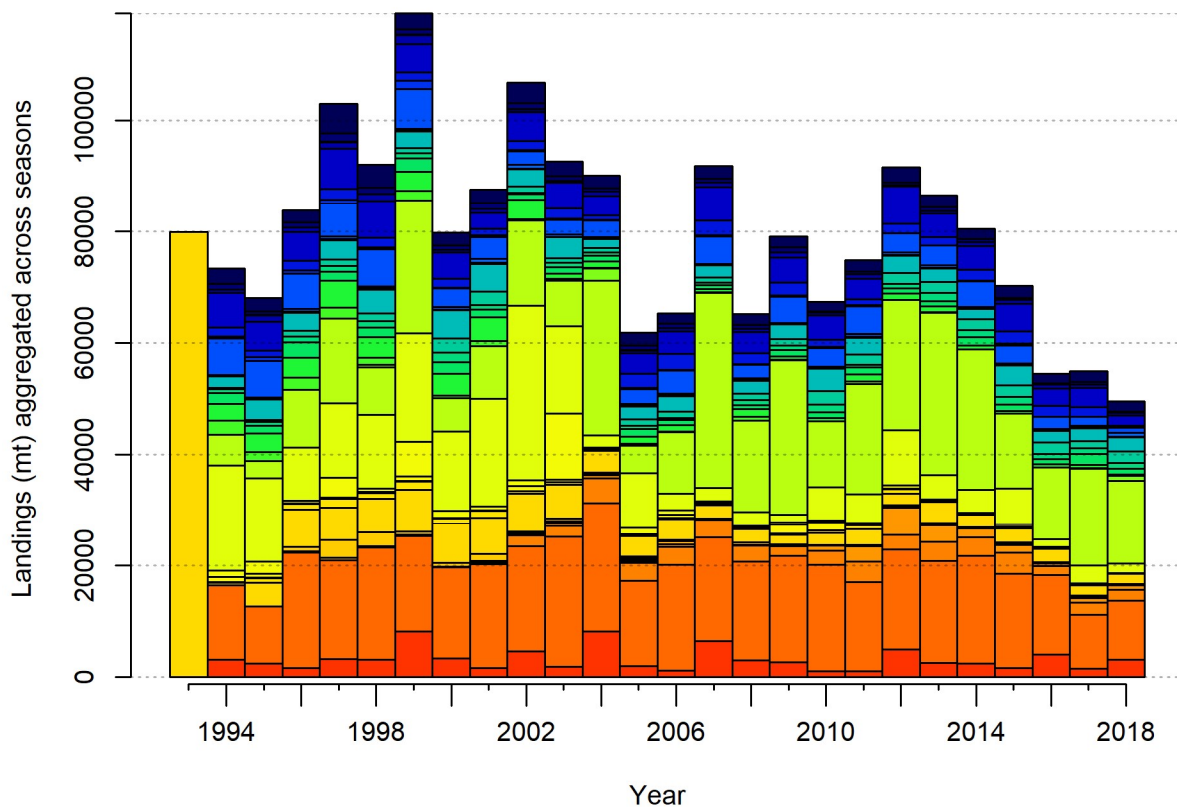


**Figure 3.3.** Annual catch (t) by fishery in the base case model. Color indicates fishery in base case model (Table 3.1) with F1 in dark blue and F35 in dark red. Catch in weight for some fisheries were estimated from catch in numbers. First bar (yellow) indicates the estimated initial catch of F27. Zero catch were recorded for F17 and F34 for the entire modeling period.

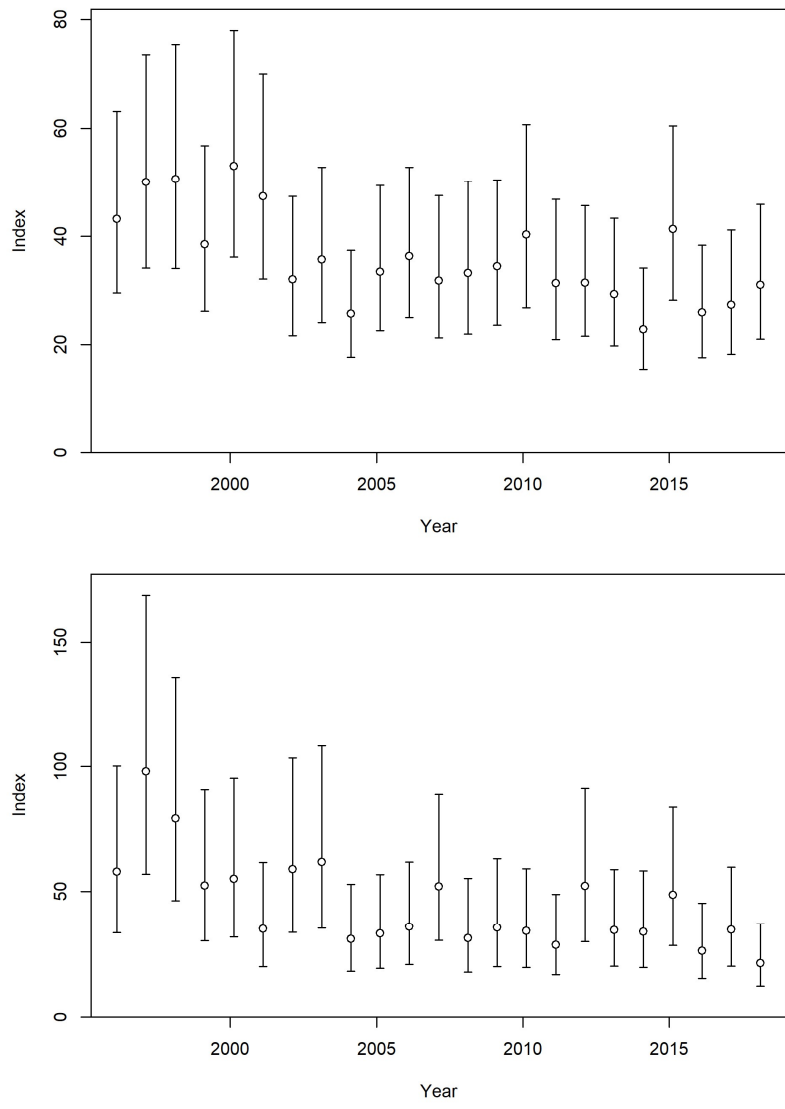


**Figure 3.4.** Trends and 95% confidence intervals of the primary adult index (F9; upper panel) used in the base case model, and the nominally juvenile/subadult index (F1; lower panel) used in sensitivity model runs. Note that the 95% confidence intervals include both input and additional coefficients of variation (CVs). See Table 3.2 for index values and CVs.

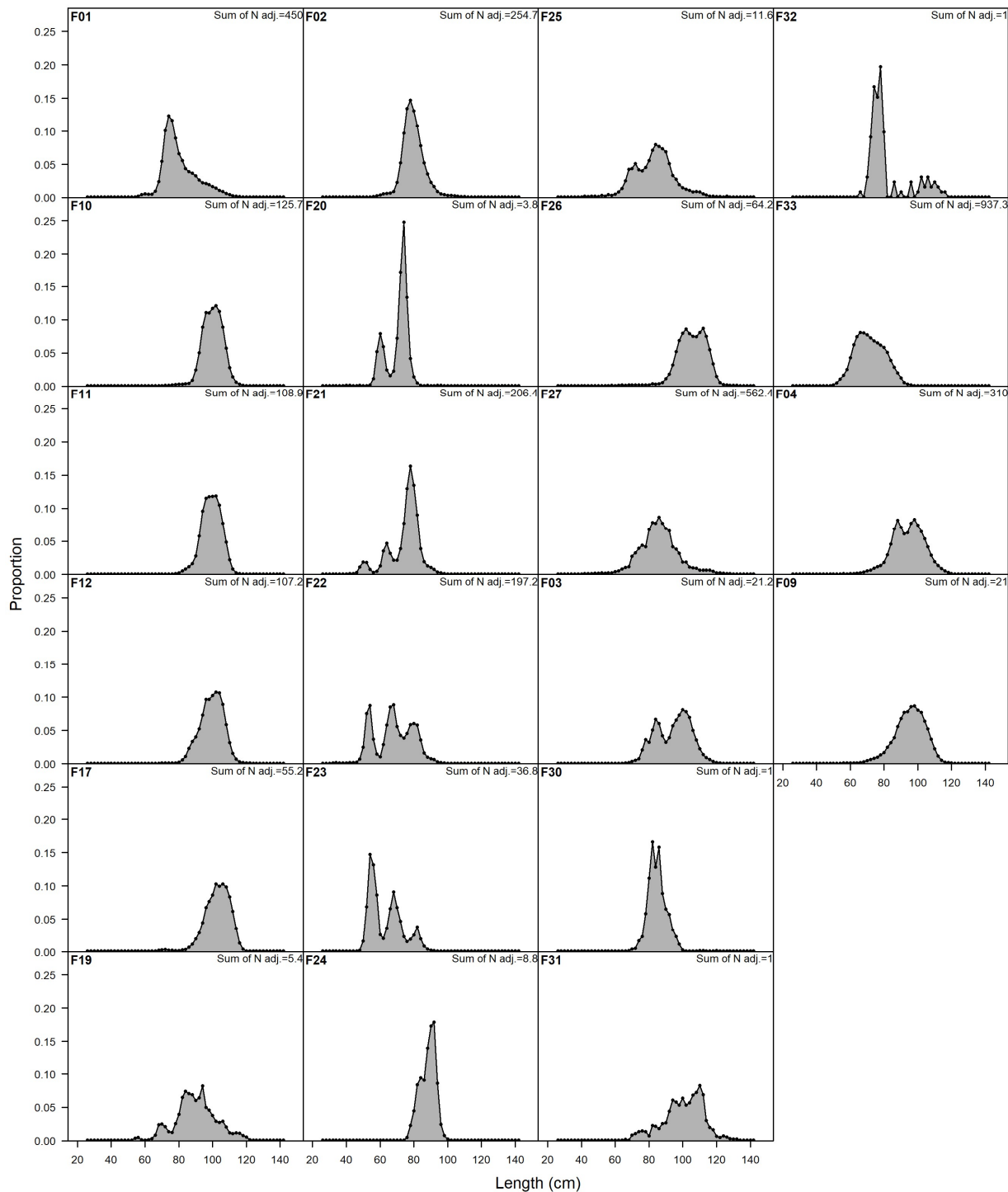


**Figure 3.5.** Aggregated size composition data in the base case model for the 2020 north Pacific albacore stock assessment. Note that size composition data for F30, F31, and F32 were not fitted in the base case model. Sum of N adj indicate the total sample size of the size composition data for each fishery after data reweighting. See Table 3.1 for description of fisheries.

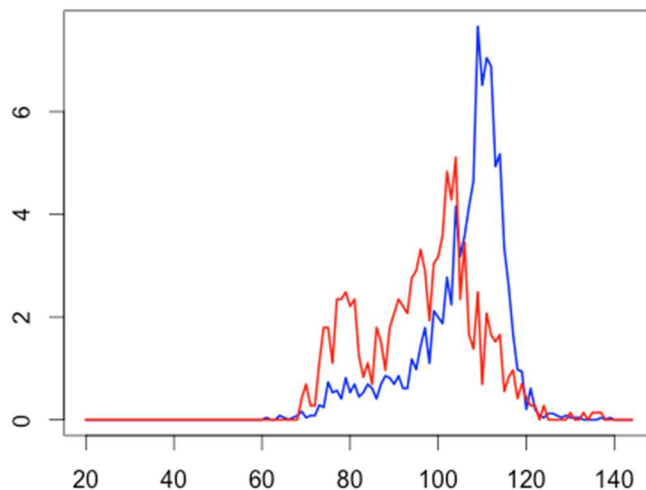


**Figure 3.6.** Proportion of males and females by length (fork length in cm) sampled in Japanese research and training vessel longline catches from 1987 to the present. Data are aggregated across years and fishing areas. Sex composition data are not fitted in the base case model.

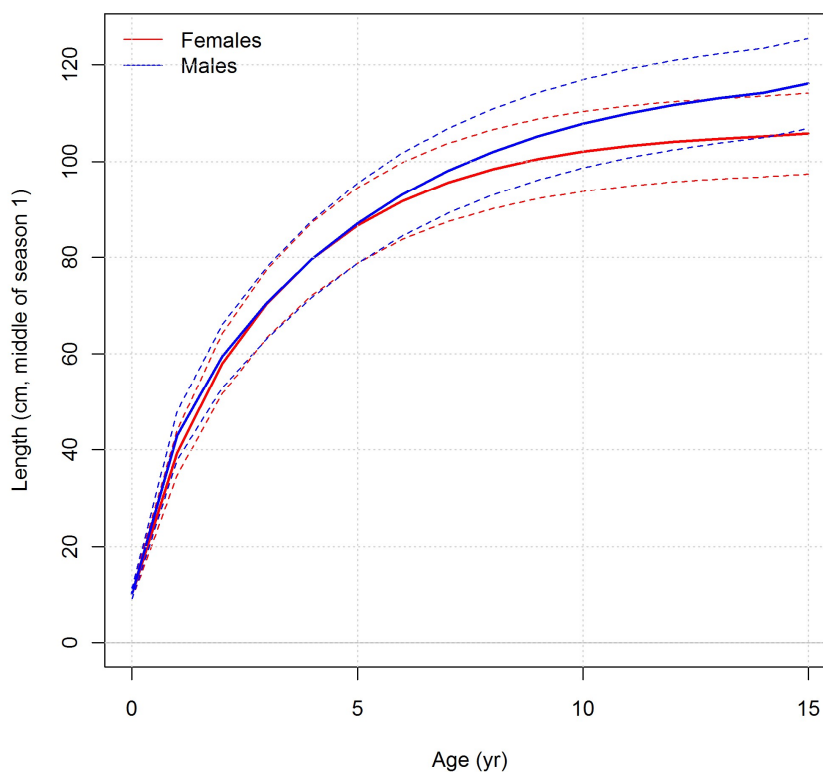


**Figure 4.1.** Growth model of north Pacific albacore used in the 2020 assessment. Dashed lines indicate 95% confidence intervals. Based on sex-specific growth model by Xu et al. (2014). See Table 4.1 for detailed parameters.

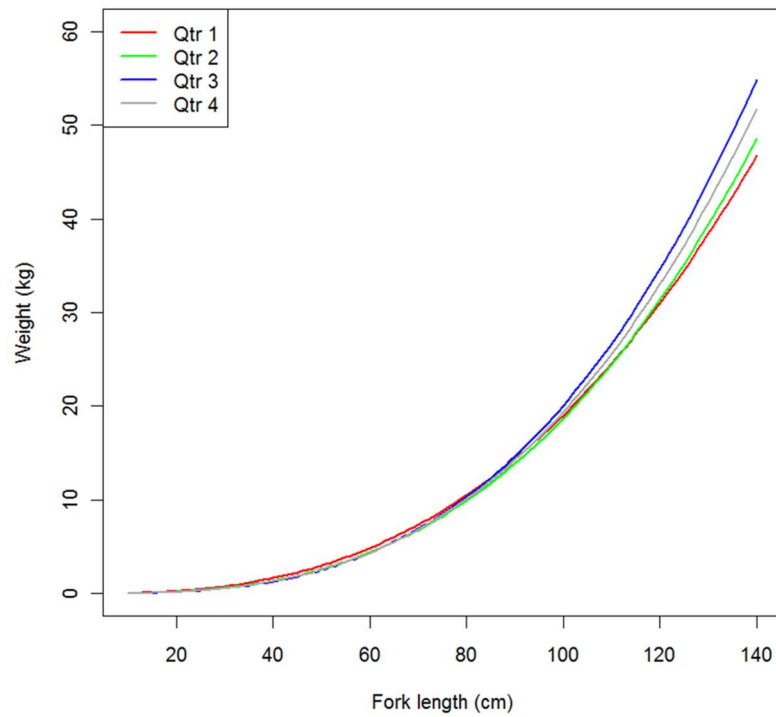


**Figure 4.2.** Seasonal weight-at-length relationships of north Pacific albacore used in the 2020 assessment. Based on Watanabe et al. (2006). Male and female weight-at-length relationships were assumed to be identical. See Table 4.1 for detailed parameters.



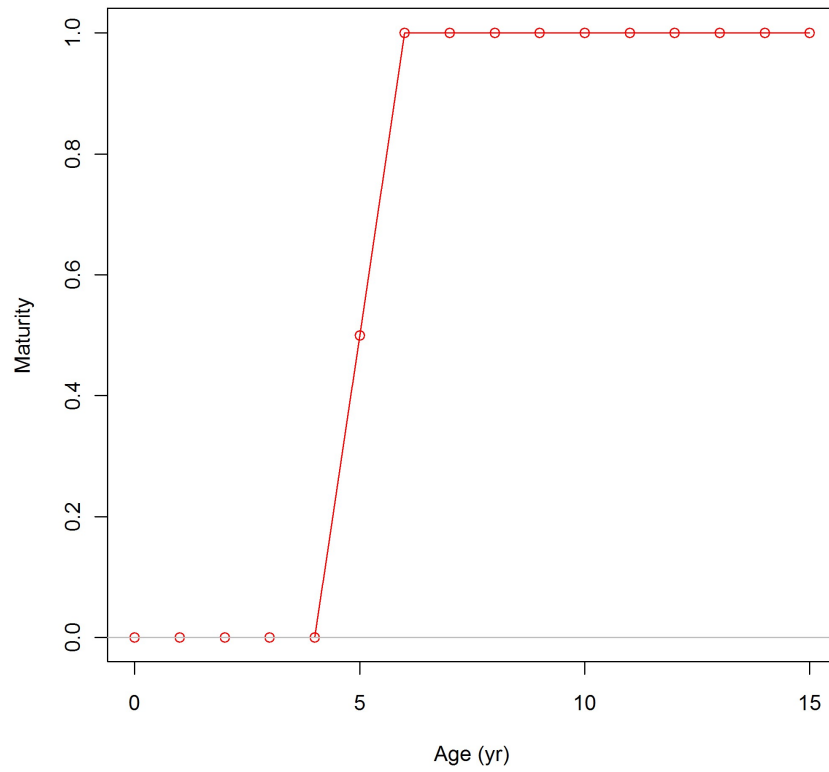


**Figure 4.3.** Maturity-at-age for female north Pacific albacore used in the 2020 assessment. See Table 4.1 for detailed parameters.

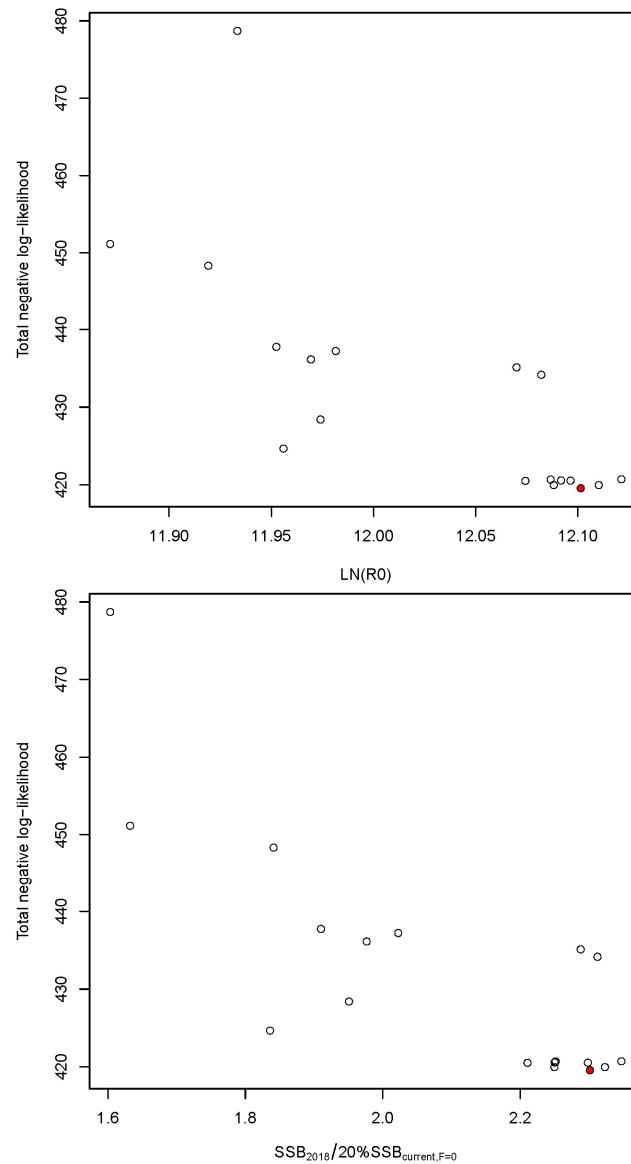


**Figure 5.1.** Total negative log-likelihood versus estimated virgin recruitment in log-scale [ $\ln(R_0)$ ] (upper panel), and the ratio of female spawning biomass in 2018 ( $SSB_{2018}$ ) to the 20% $SSB_{current, F=0}$  biomass-based limit reference point (lower panel) from 50 model runs with different phasing and initial values of  $\ln(R_0)$  and other important parameters, as well as randomly jittered initial values for all estimated parameters in the base-case model. Red closed circle shows results from the model run using initial parameters and phasing corresponding to the 2020 base case model, which had the lowest total negative log-likelihood (419.555) of all 50 model runs.

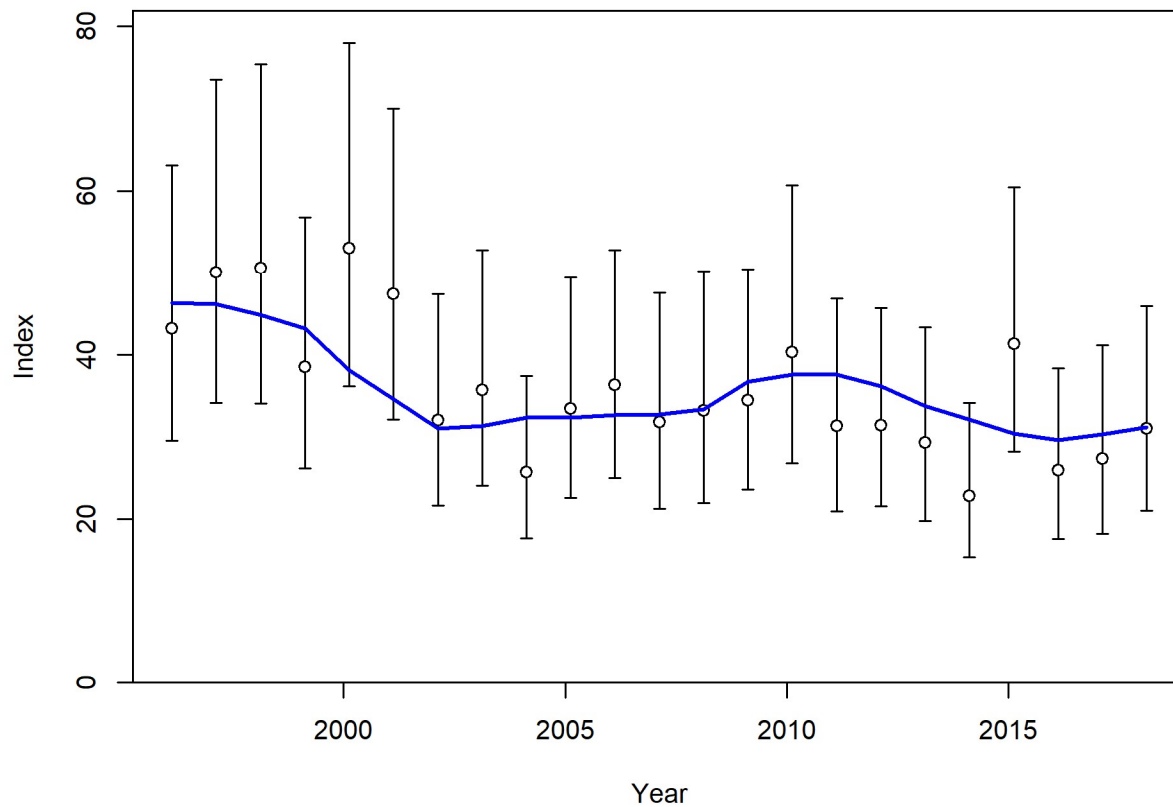


**Figure 5.2.** Observed (open circles) and predicted (blue line) relative abundance from the F9 adult abundance index in the 2020 base case model. Error bars are the 95% confidence intervals.

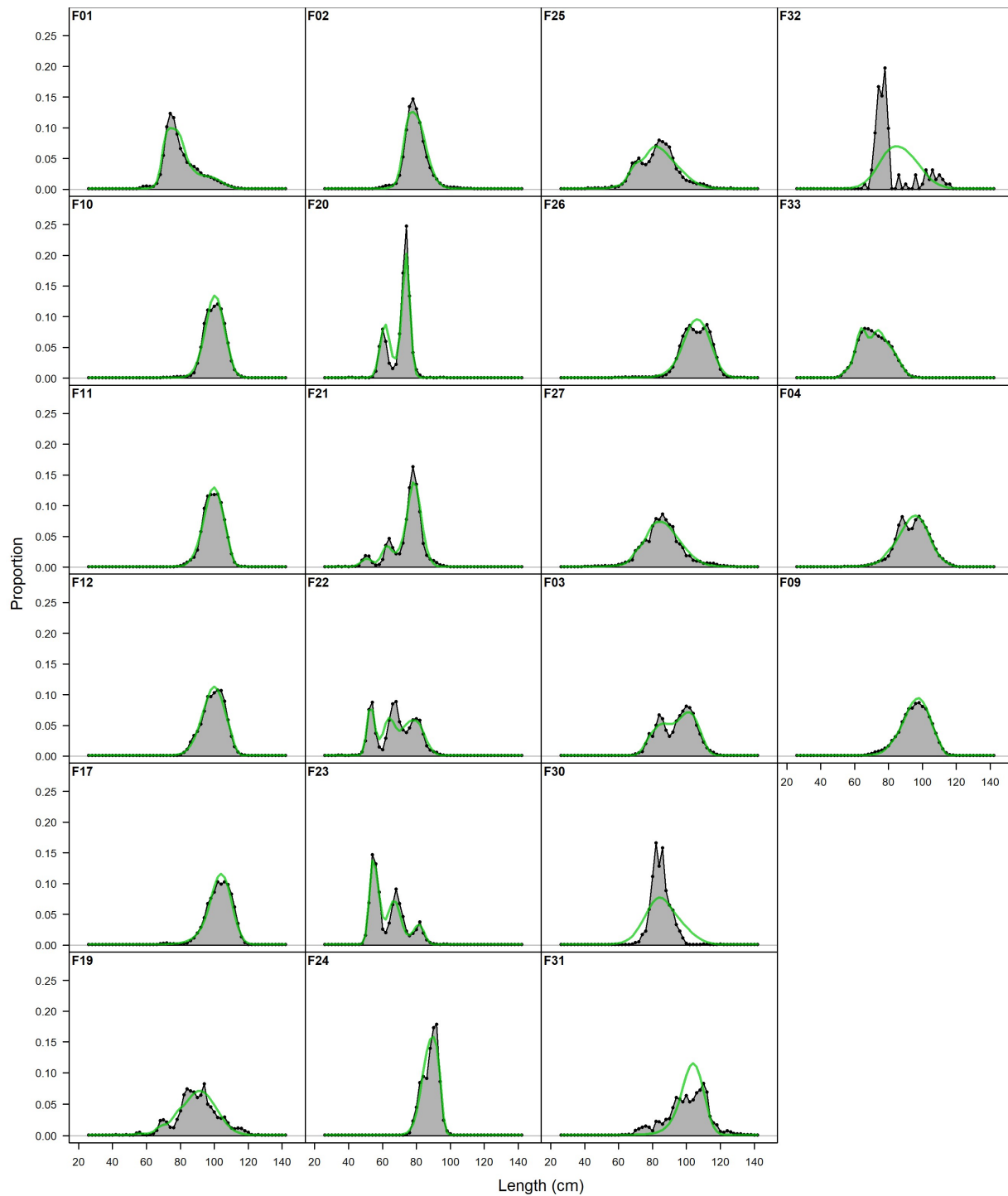


**Figure 5.3.** Observed (grey) and model predicted (green line) aggregated size compositions for fisheries in the 2020 base-case model. F30, F31, and F32 had size composition data available but were not fitted in the base case model because their size composition data were not raised to the catch. See Tables 3.1 and 5.2 for description of fisheries and details of model fit, respectively.

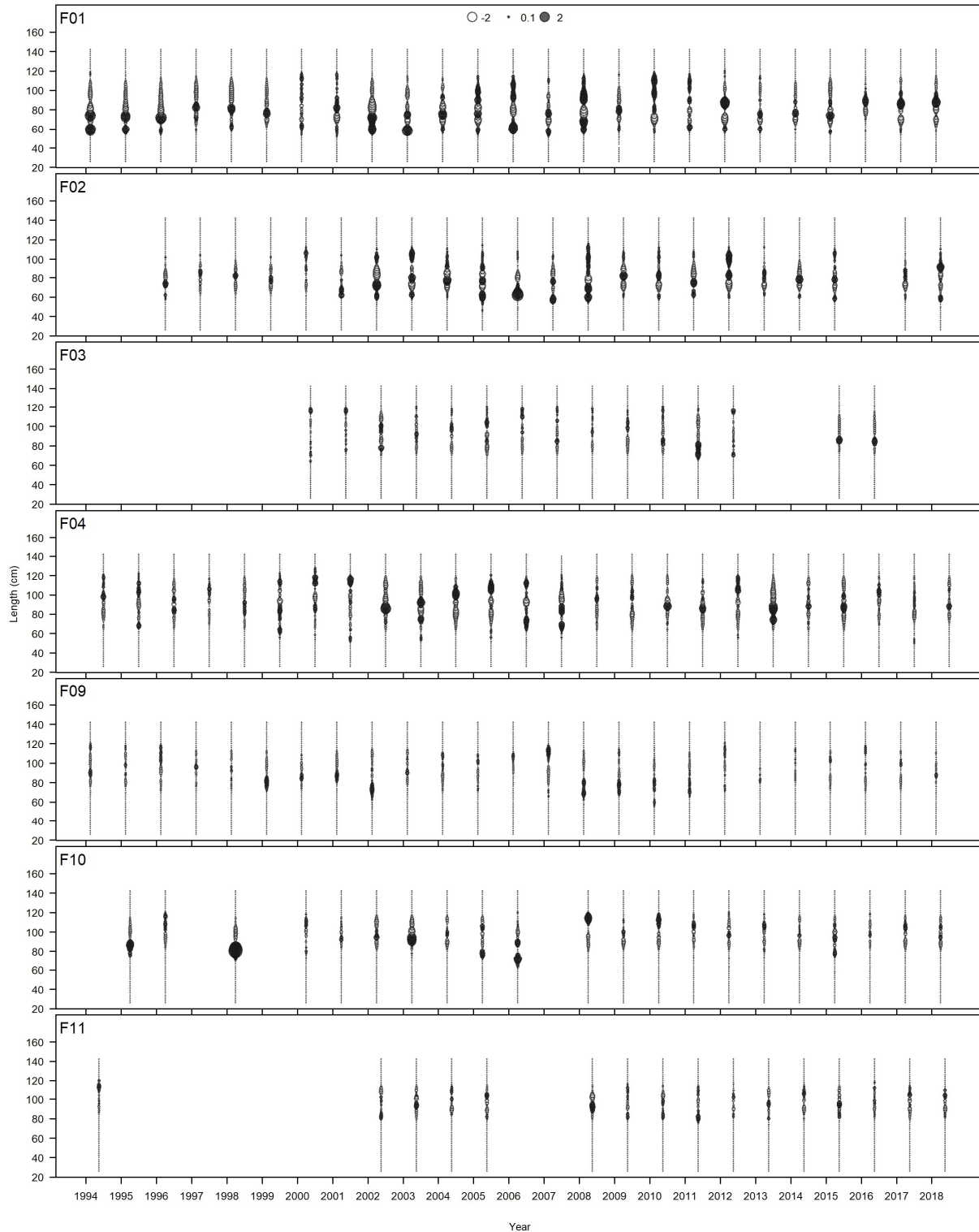


**Figure 5.4.** Pearson residuals of model fit to size composition data from fisheries in the 2020 base case model. Filled and open circles represent observations (i.e., proportions at size) that are larger and smaller than model predictions, respectively. Area of the circle is proportional to absolute values of residuals.

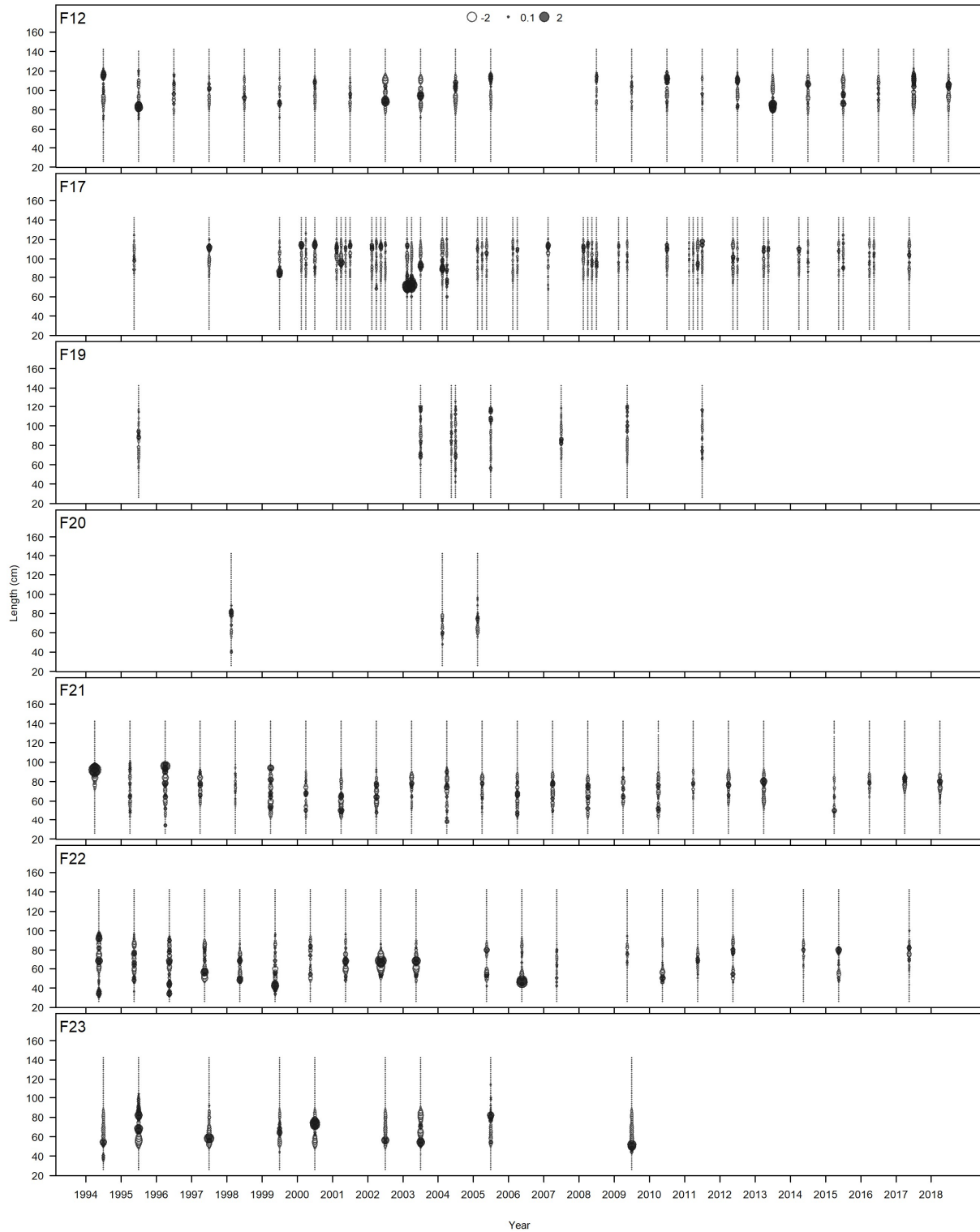


Figure 5.4. continued.

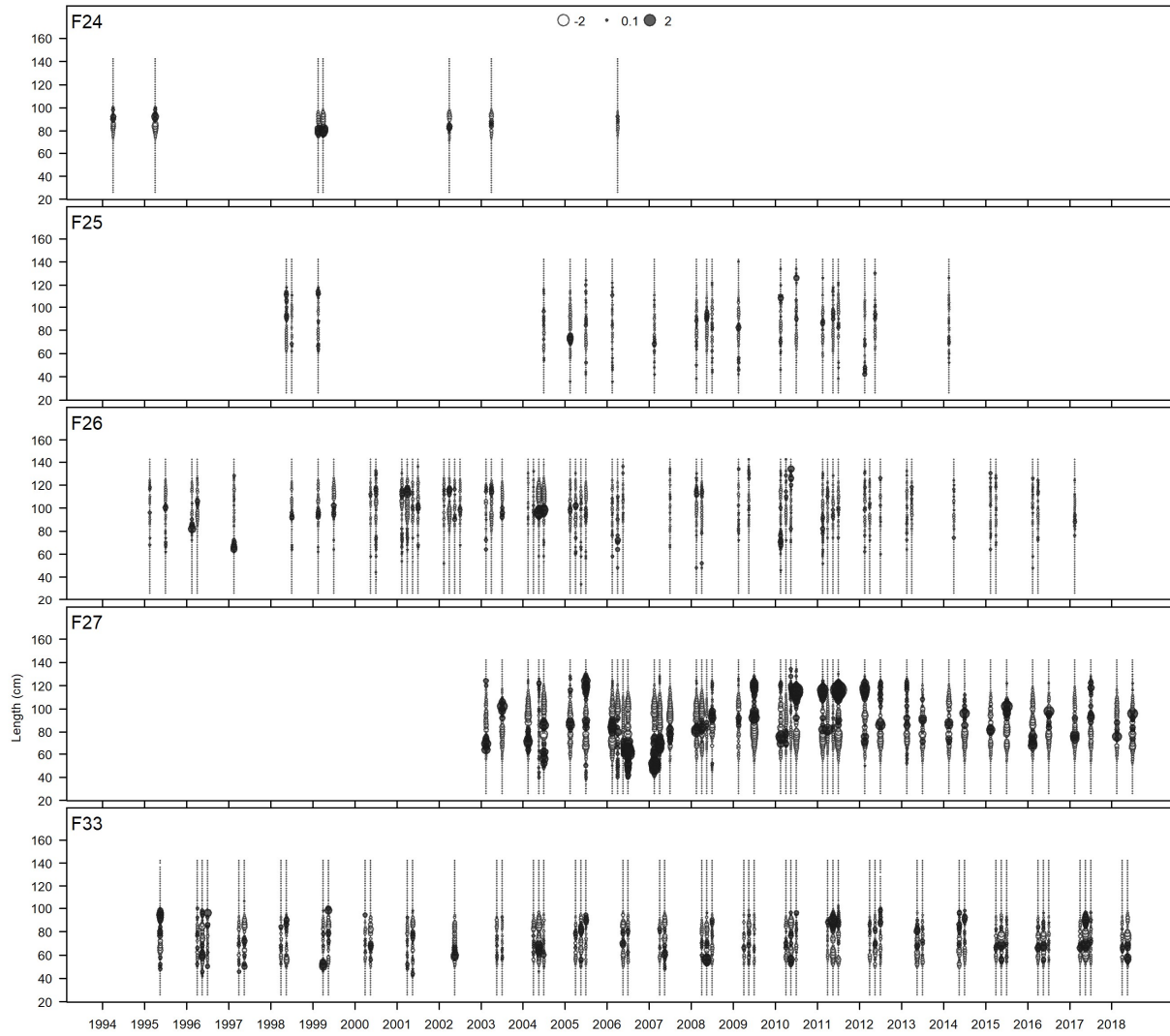
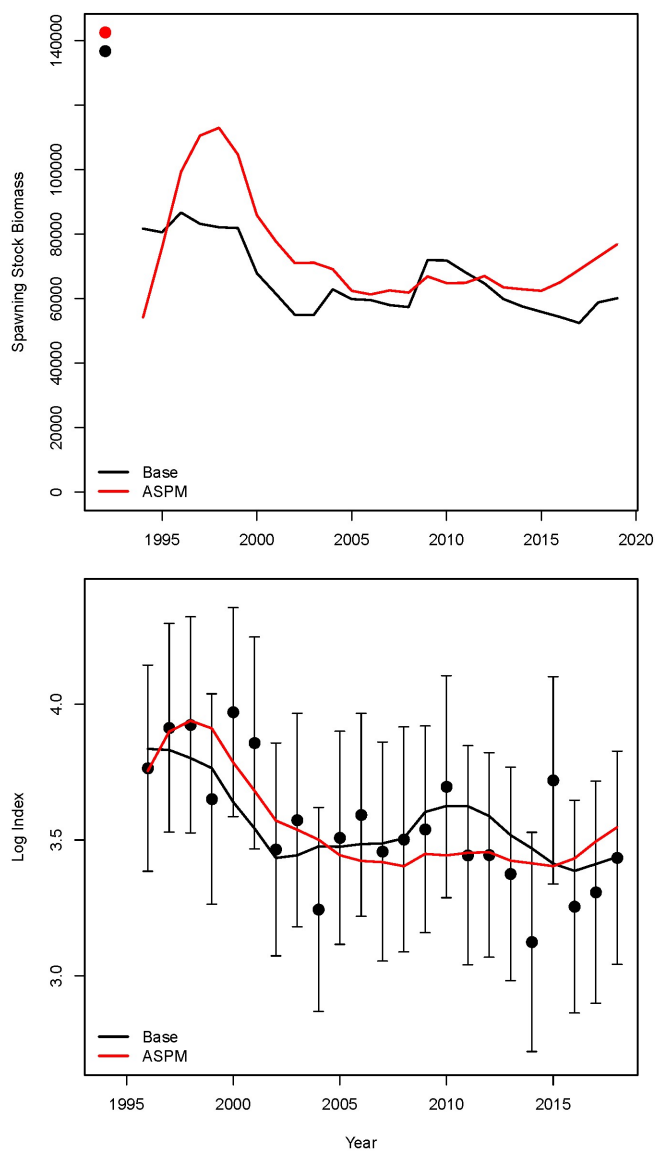
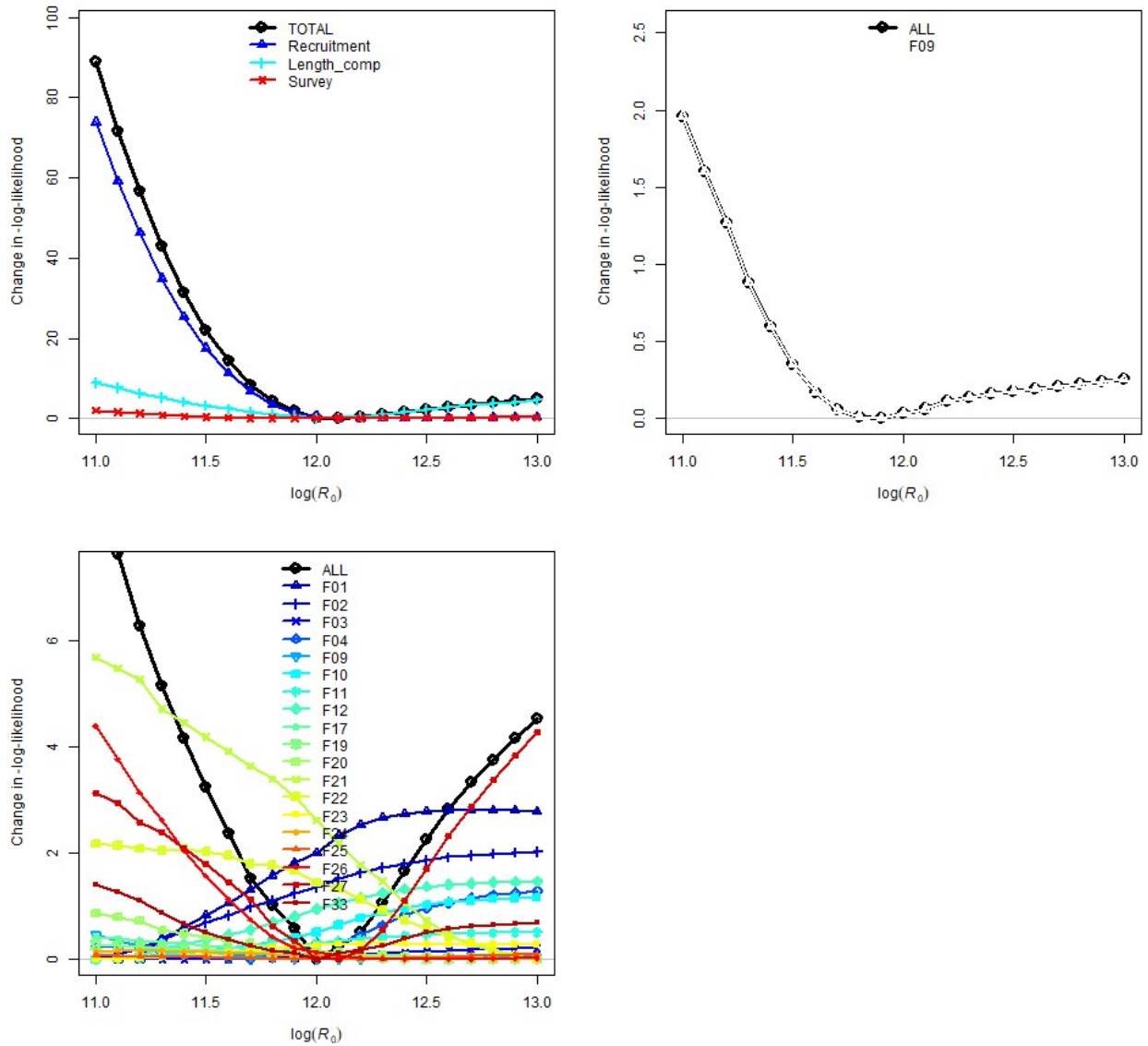


Figure 5.4. continued.



**Figure 5.5.** Estimated female spawning stock biomass (upper panel) and fit to the F09 adult abundance index (lower panel) of the age-structured production model (ASPM; red) and the base case model (blue). Colored circles in upper panel indicate the estimated virgin female spawning stock biomass ( $SSB_0$ ) for each model. Black circles and error bars in the lower panel indicate observations and 95% confidence intervals of the F09 index.





**Figure 5.6.** Likelihood profiles with respect to virgin recruitment [ $\log(R_0)$ ] of the main data components (upper left), F09 abundance index (upper right), and size compositions (lower left) of the 2020 base case model.

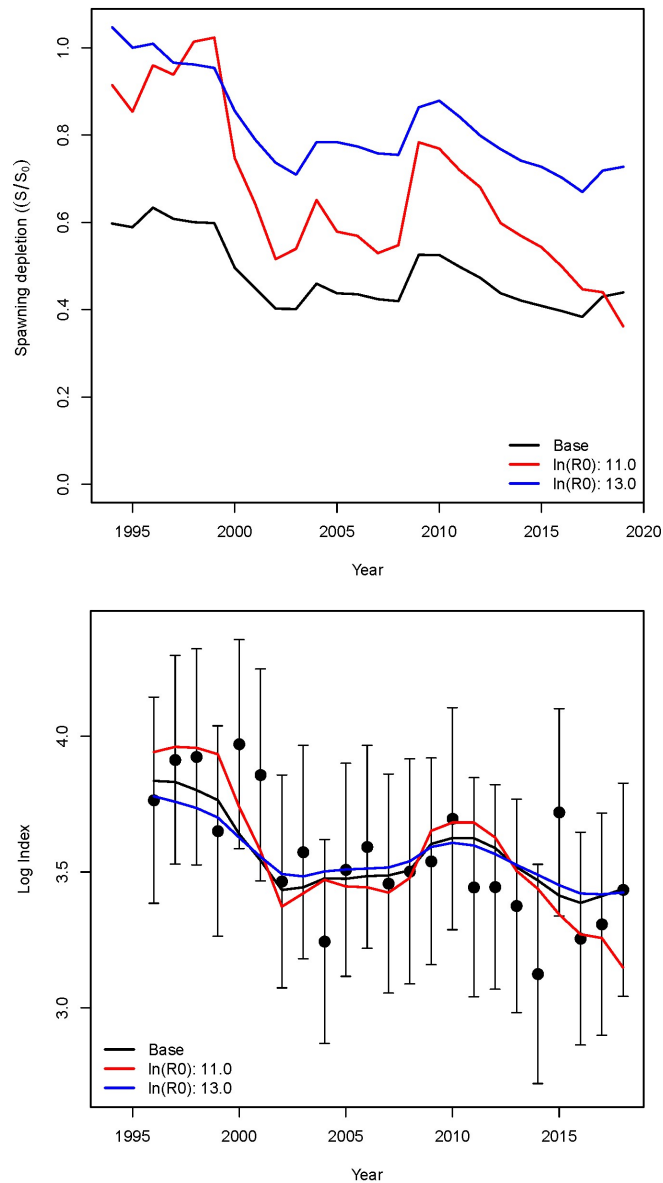


**Figure 5.7.** Estimated female spawning stock biomass (SSB) relative to virgin SSB (upper panel) and fit to the F09 adult abundance index (lower panel) of the base case model (black) and models with virgin recruitment [ $\log(R_0)$ ] fixed at 11.0 (red) and 13.0 (blue). Black circles and error bars in the lower panel indicate observations and 95% confidence intervals of the F09 index.

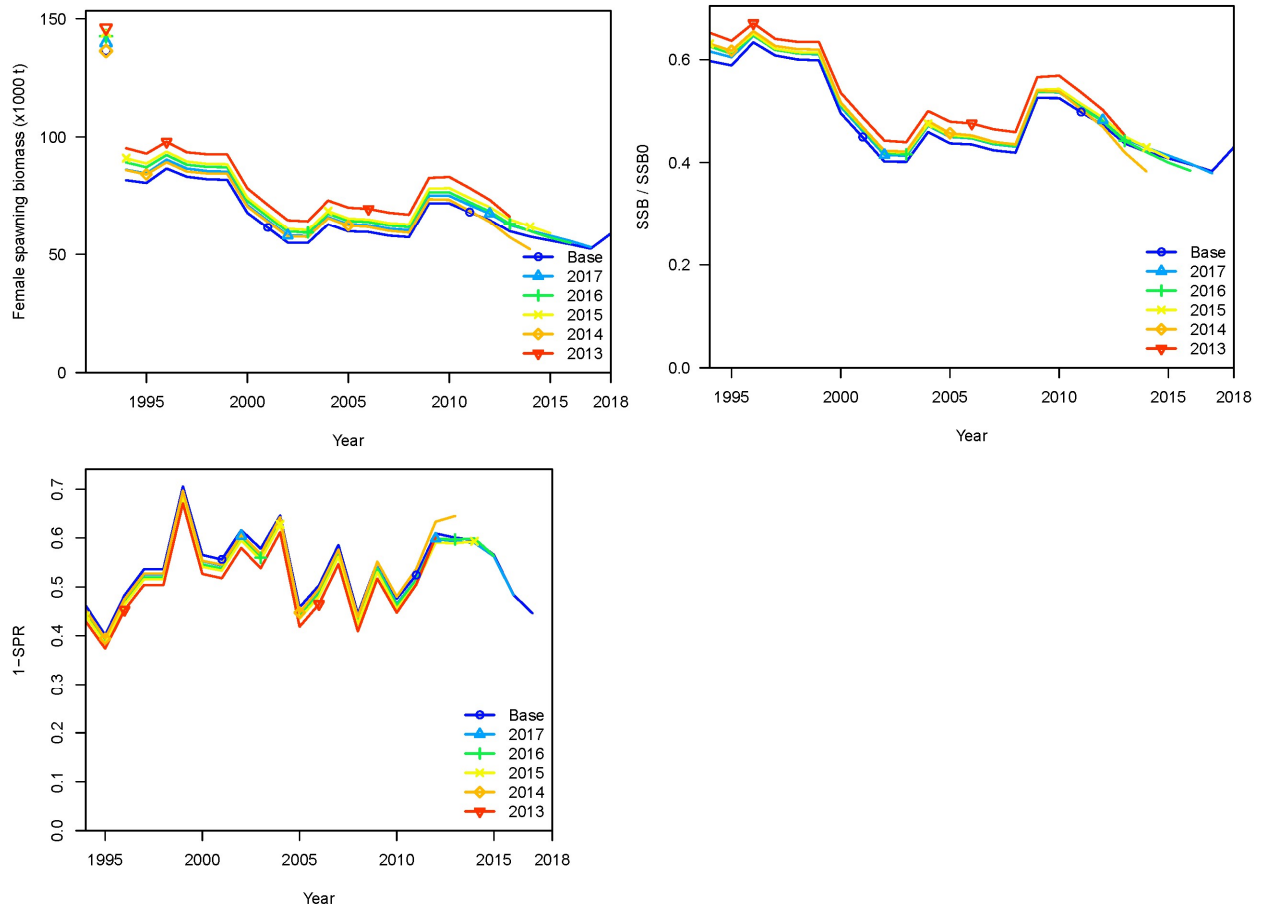


**Figure 5.8.** Estimated female spawning biomass (SSB) (upper left), relative SSB (upper right) and fishing intensity ( $1 - SPR$ ) (lower left) of the base case model (blue) and models with one to five terminal years of data removed.

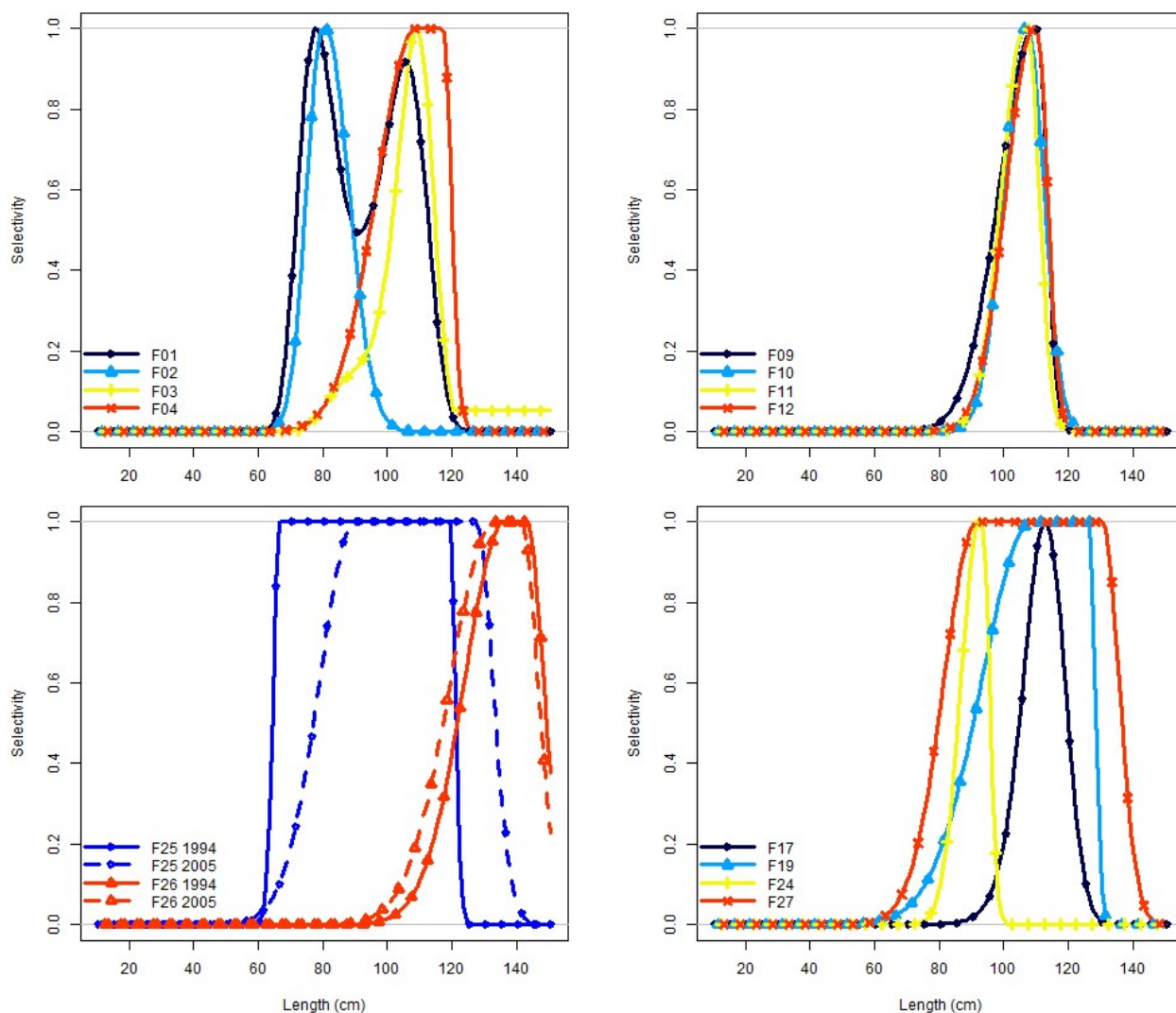


**Figure 5.9.** Estimated selectivity for fisheries with size-only selectivity in the 2020 base case model. Selectivity patterns are grouped by: 1) Japanese longline fisheries in Areas 1 and 3 (upper left panel); 2) Japanese longline fisheries in Area 2 (upper right panel); 3) US longline fisheries (lower left panel); and 4) all other fisheries with size-only selectivities. Years in lower left panel indicates first year of time block. All other panels in this figure have constant selectivity through time. Male selectivity is identical to female selectivity in the base case model. Only fisheries with size composition data fitted in the base case model are shown.

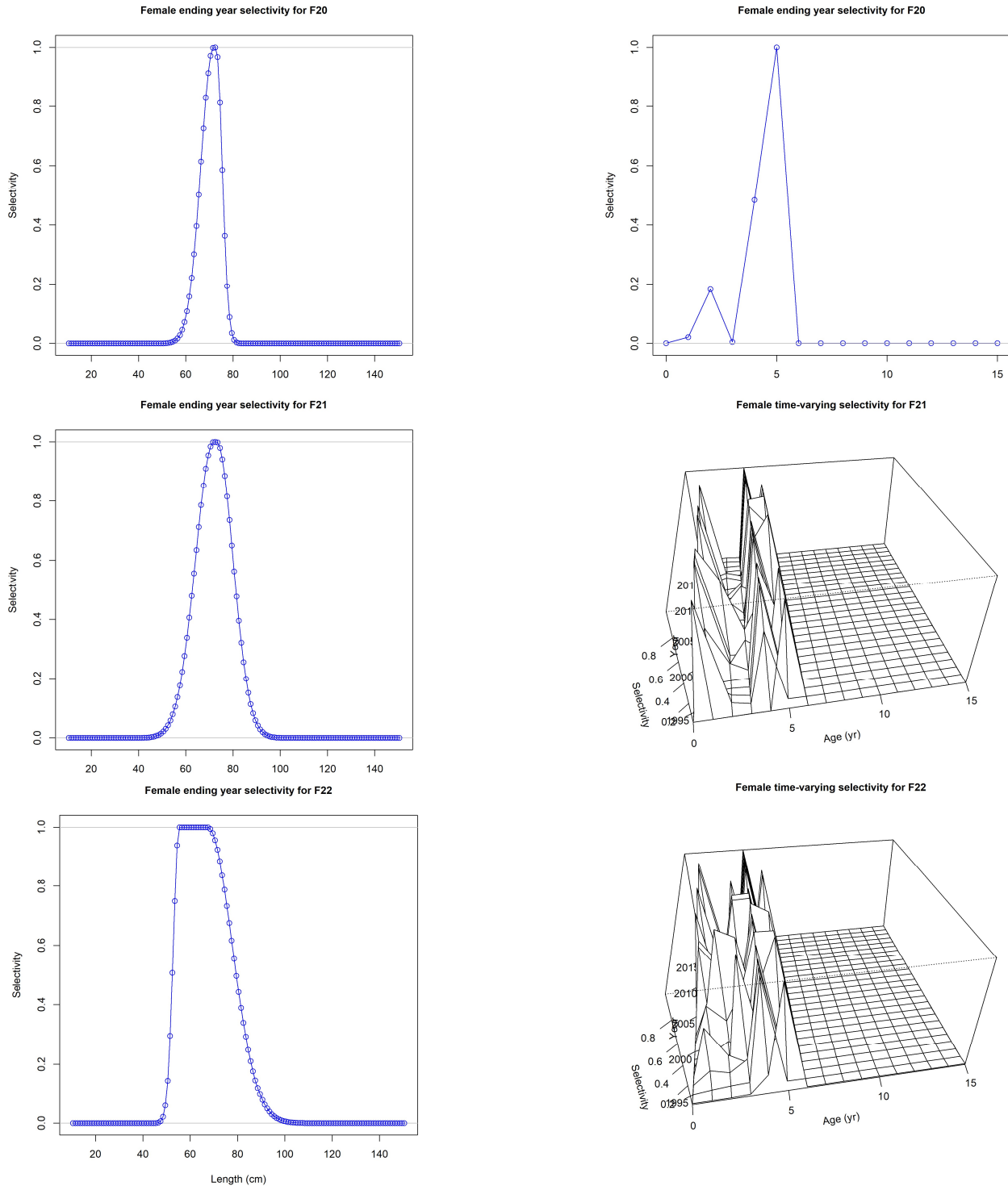


**Figure 5.10.** Estimated selectivity for fisheries with selectivity assumed to be a product of size (left) and age (right) selectivity, in the 2020 base case model. Selectivity patterns displayed as 3-dimensional plots have time-varying selectivity. Male selectivity is identical to female selectivity in the base case model. Only fisheries with size composition data fitted in the model are shown.

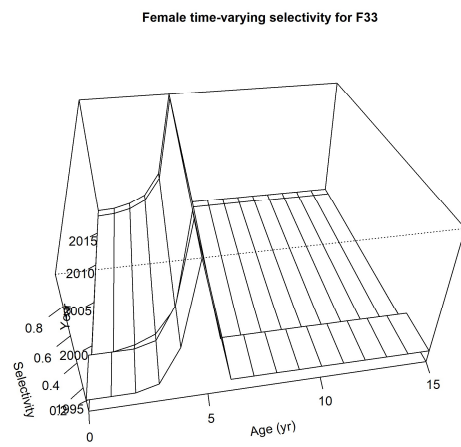
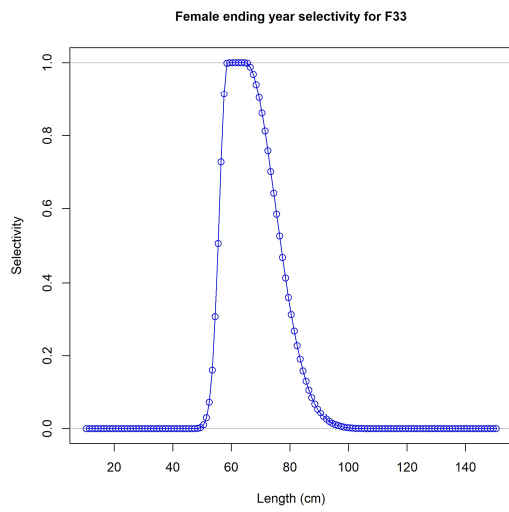
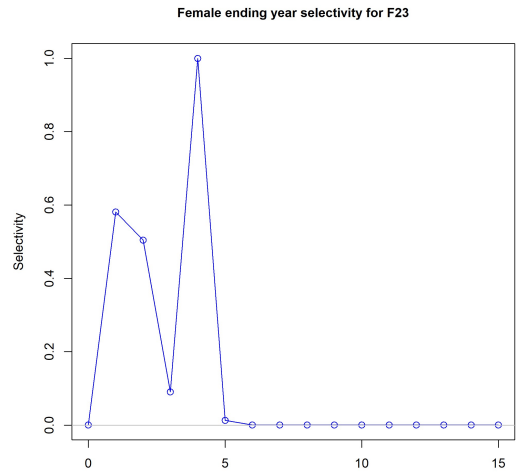
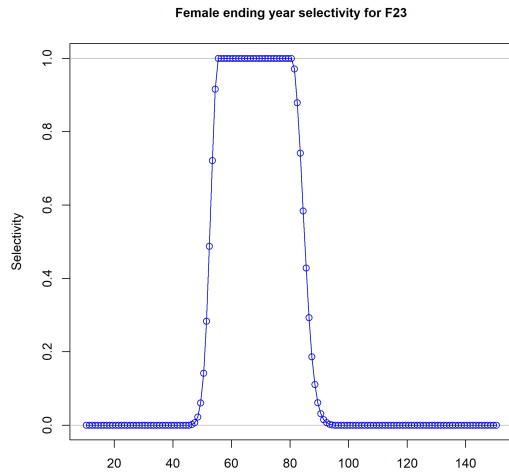
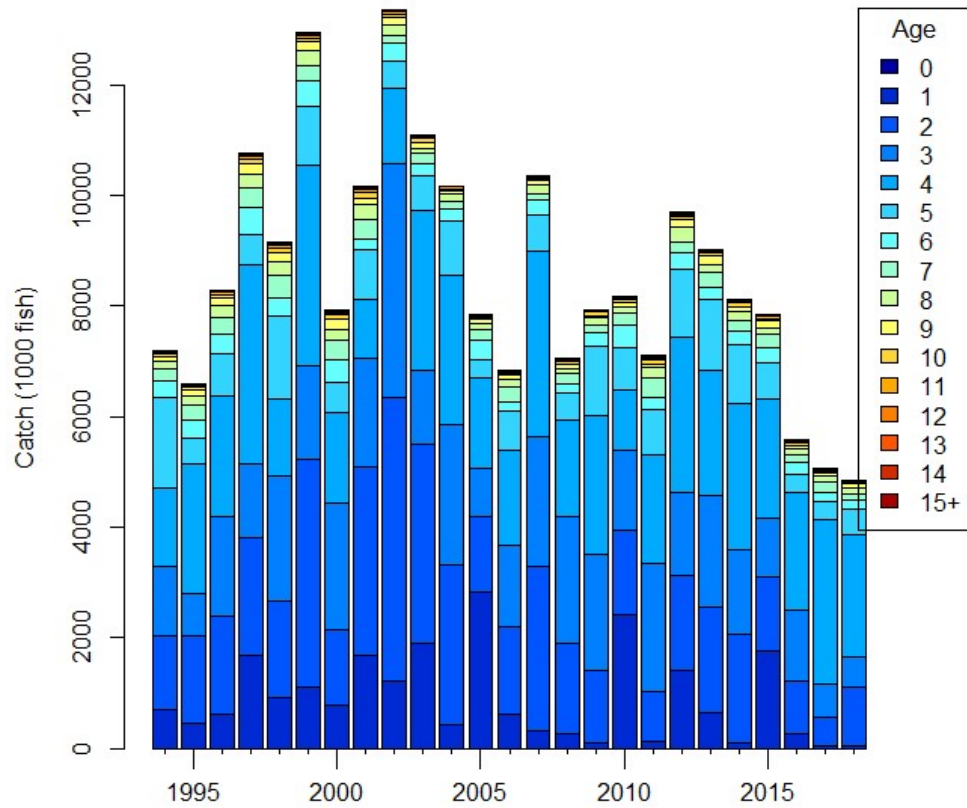
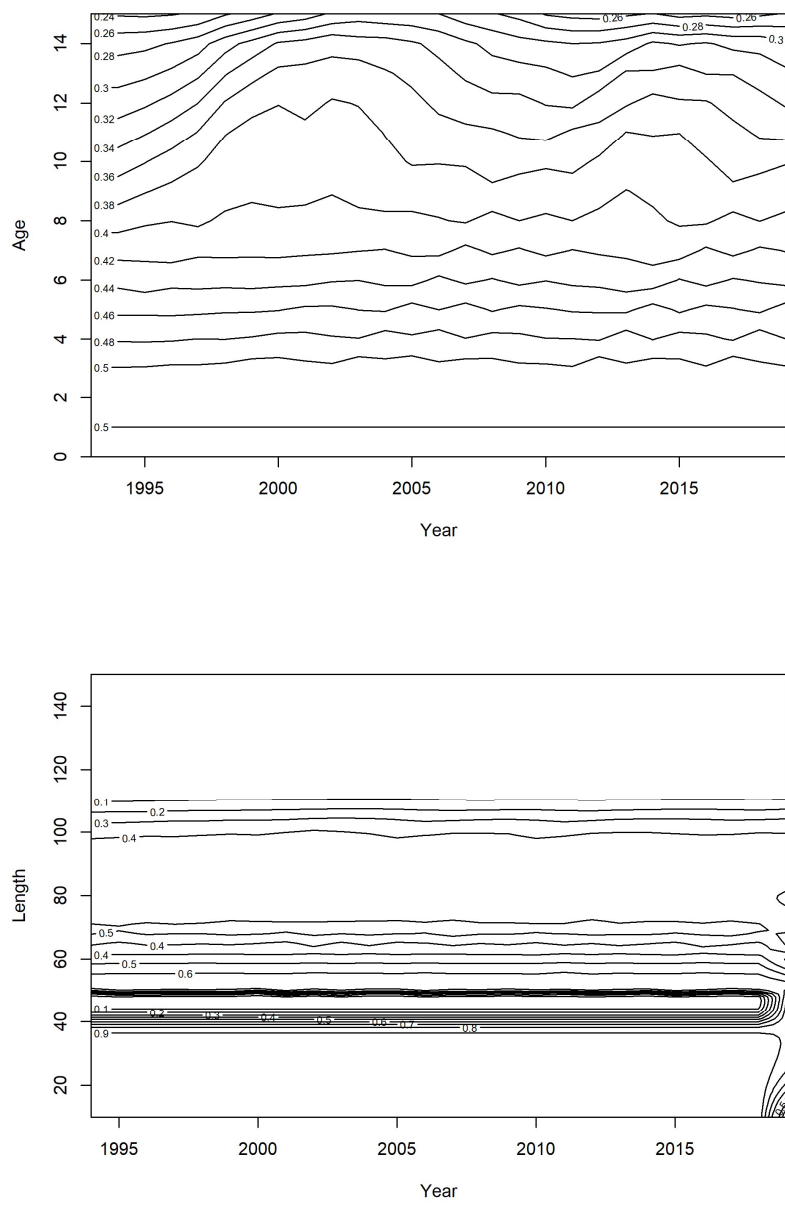


Figure 5.10. Continued.



**Figure 5.11.** Historical catch-at-age of north Pacific albacore (*Thunnus alalunga*) estimated by the 2020 base case model.



**Figure 5.12.** Estimated fraction of females in the population by age (upper) and fork length in cm (lower) in the 2020 base case model.



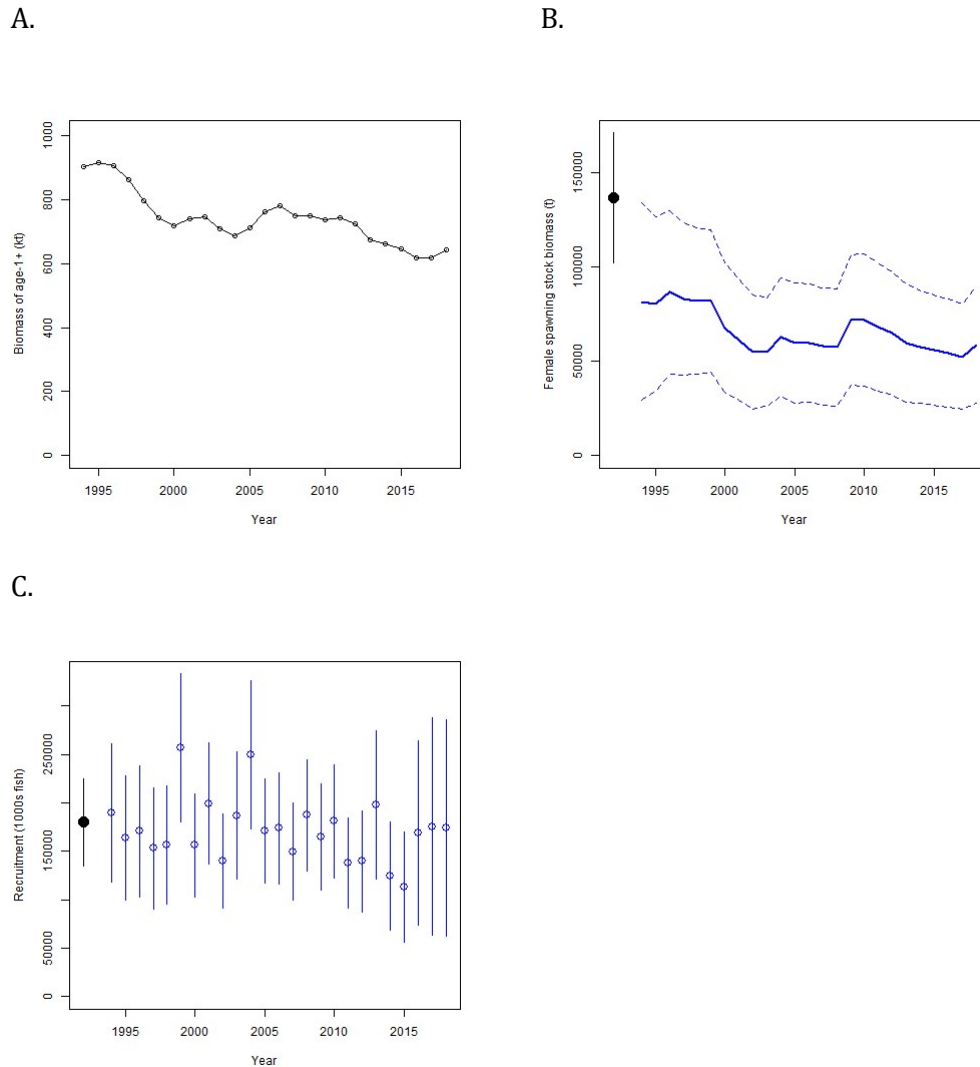


**Figure 5.13.** Maximum likelihood estimates of (A) total age-1+ biomass (open circles) (B), female spawning biomass (SSB) (solid blue line), and (C) age-0 recruitment (open circles) of north Pacific albacore tuna (*Thunnus alalunga*). Dashed lines (B) and vertical bars (C) indicate 95% confidence intervals of the female SSB and recruitment estimates respectively. Closed black circle and error bars in (B) are the maximum likelihood estimate and 95% confidence intervals of unfished female spawning biomass,  $SSB_0$ . Estimates of total biomass (A) are based on estimates from Quarter 1 of each year. Estimates of female SSB (B) and age-0 recruitment (C) are based on estimates from Quarter 2 of each year.

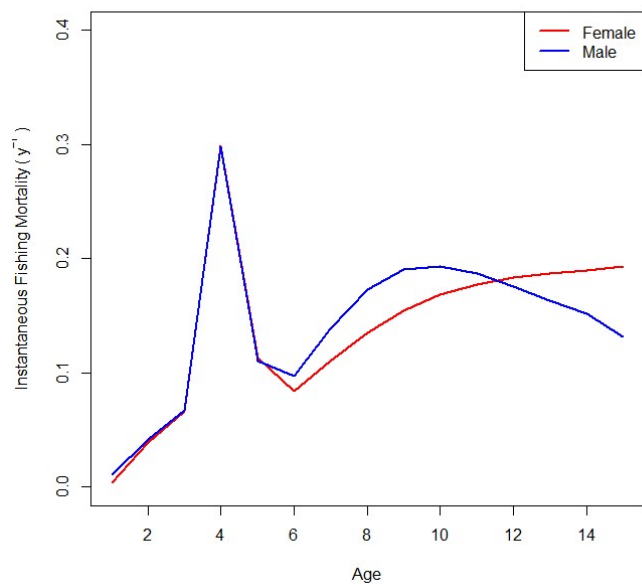


**Figure 5.14.** Estimated sex-specific instantaneous fishing mortality-at-age (F-at-age) for the 2020 base case model, averaged across 2015-2017.

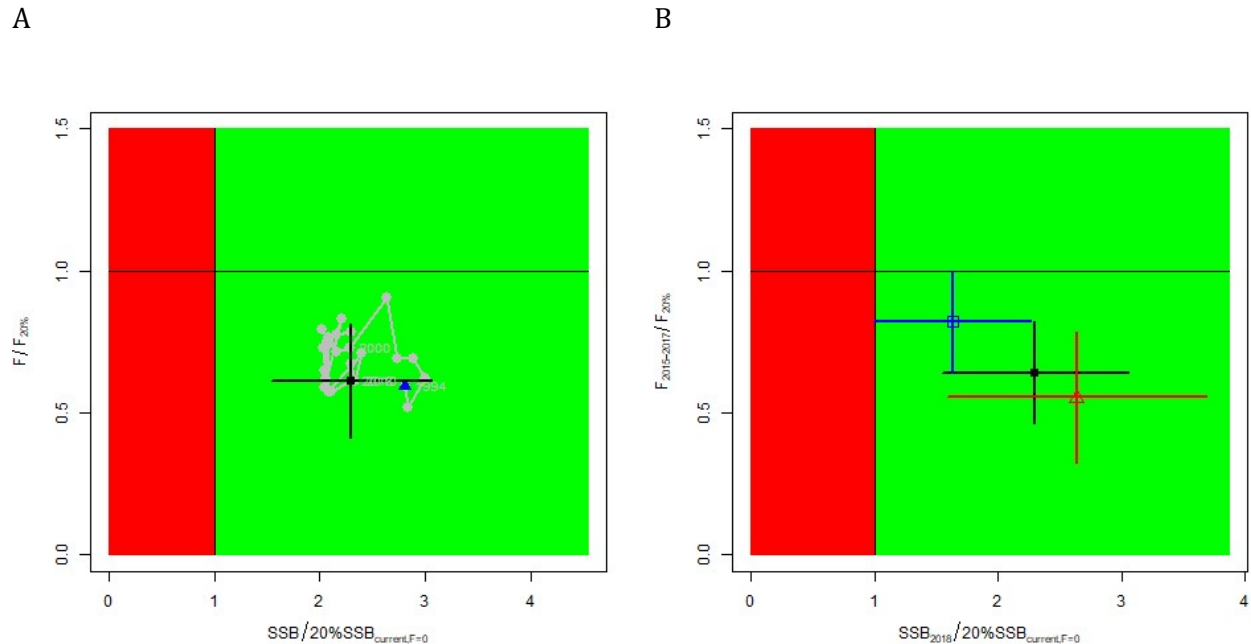


**Figure 5.15.** (A) Kobe plot showing the status of the north Pacific albacore (*Thunnus alalunga*) stock relative to the 20%SSB<sub>current, F=0</sub> biomass-based limit reference point, and equivalent fishing intensity ( $F_{20\%}$ ; calculated as  $1-SPR_{20\%}$ ) over the base case modeling period (1994-2018). Blue triangle indicates the start year (1994) and black circle with 95% confidence intervals indicates the terminal year (2018). (B) Kobe plot showing current stock status and 95% confidence intervals of the base case model (black; closed circle), an important sensitivity run of  $CV = 0.06$  for  $L_{inf}$  in the growth model (blue; open square), and a model representing an update of the 2017 base case model to 2020 data (red; open triangle). The coefficients of variation of the SSB/20%SSB<sub>current, F=0</sub> ratios are assumed to be the same as for the SSB/20%SSB<sub>0</sub> ratios. Fs in this figure are not based on instantaneous fishing mortality. Instead, the Fs are indicators of fishing intensity based on SPR and calculated as  $1-SPR$  so that the Fs reflects changes in fishing mortality. SPR is the equilibrium SSB per recruit that would result from the current year's pattern and intensity of fishing mortality. Current fishing intensity is calculated as the average fishing intensity during 2015-2017 ( $F_{2015-2017}$ ), while current female spawning biomass refers to the terminal year of this assessment (i.e., 2018). The model representing an update of the 2017 base case model is highly similar to but not identical to the 2017 base case model due to changes in data preparation and model structure.

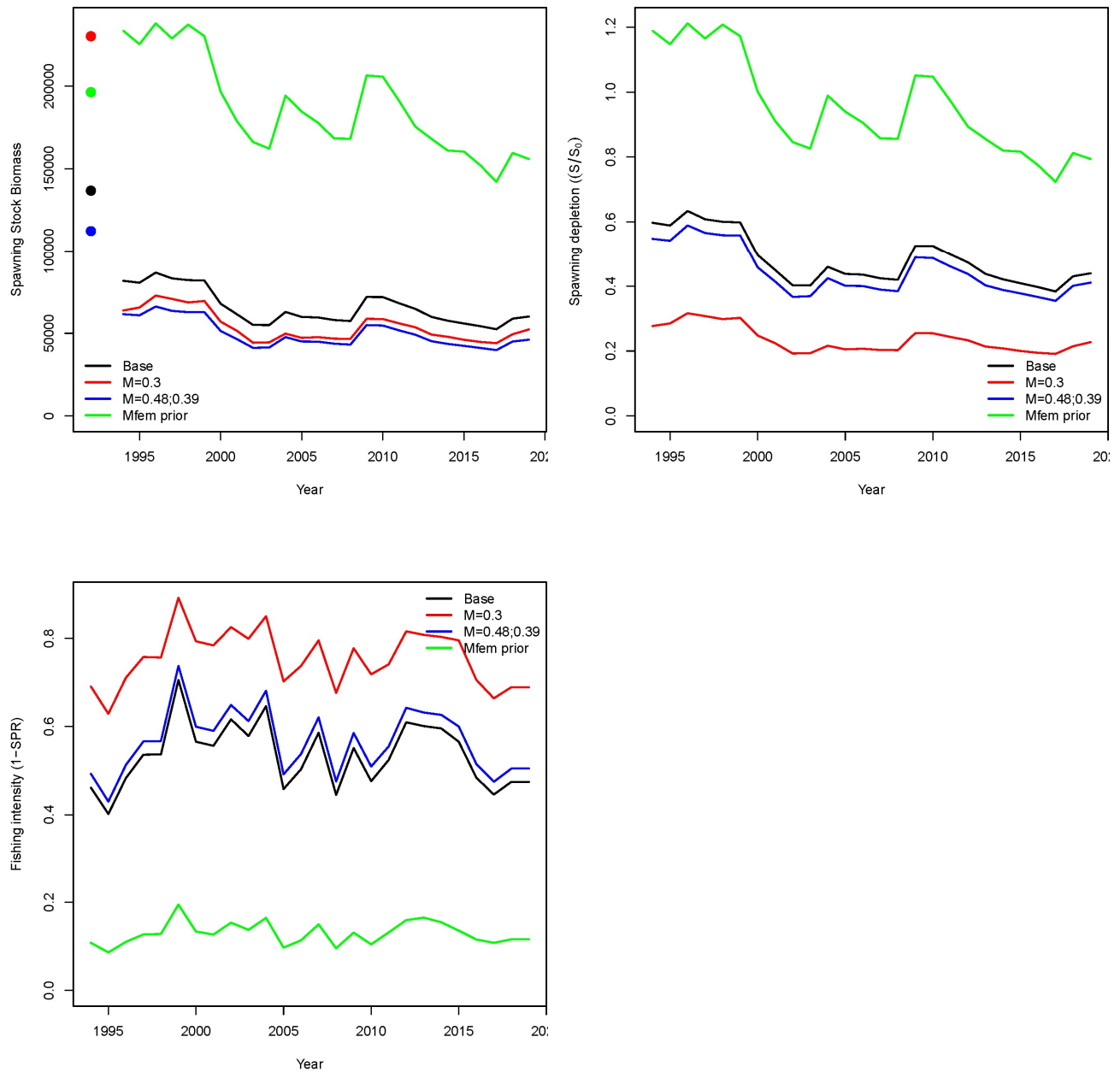


**Figure 5.16.** Estimated female spawning biomass (upper left), spawning biomass depletion (upper right), and fishing intensity (1-SPR) (lower) for the 2020 base case model (black), and three sensitivity runs with alternative natural mortality schedules [constant  $M$  of  $0.3 \text{ y}^{-1}$  for both sexes and all ages (red); constant  $M$  of  $0.38$  and  $0.49 \text{ y}^{-1}$  for males and females, respectively, of all ages (blue); and an estimated, single parameter, female  $M$  for all ages, with the prior from Teo (2017),  $M_{\text{female}} \sim \log N[-0.7258, (0.457)^2]$ , and a constant logscale offset ( $-0.21258$ ) between male and female  $M$  (green)]. See Table 4.6 and Section 5.6.1 for details on sensitivity runs.

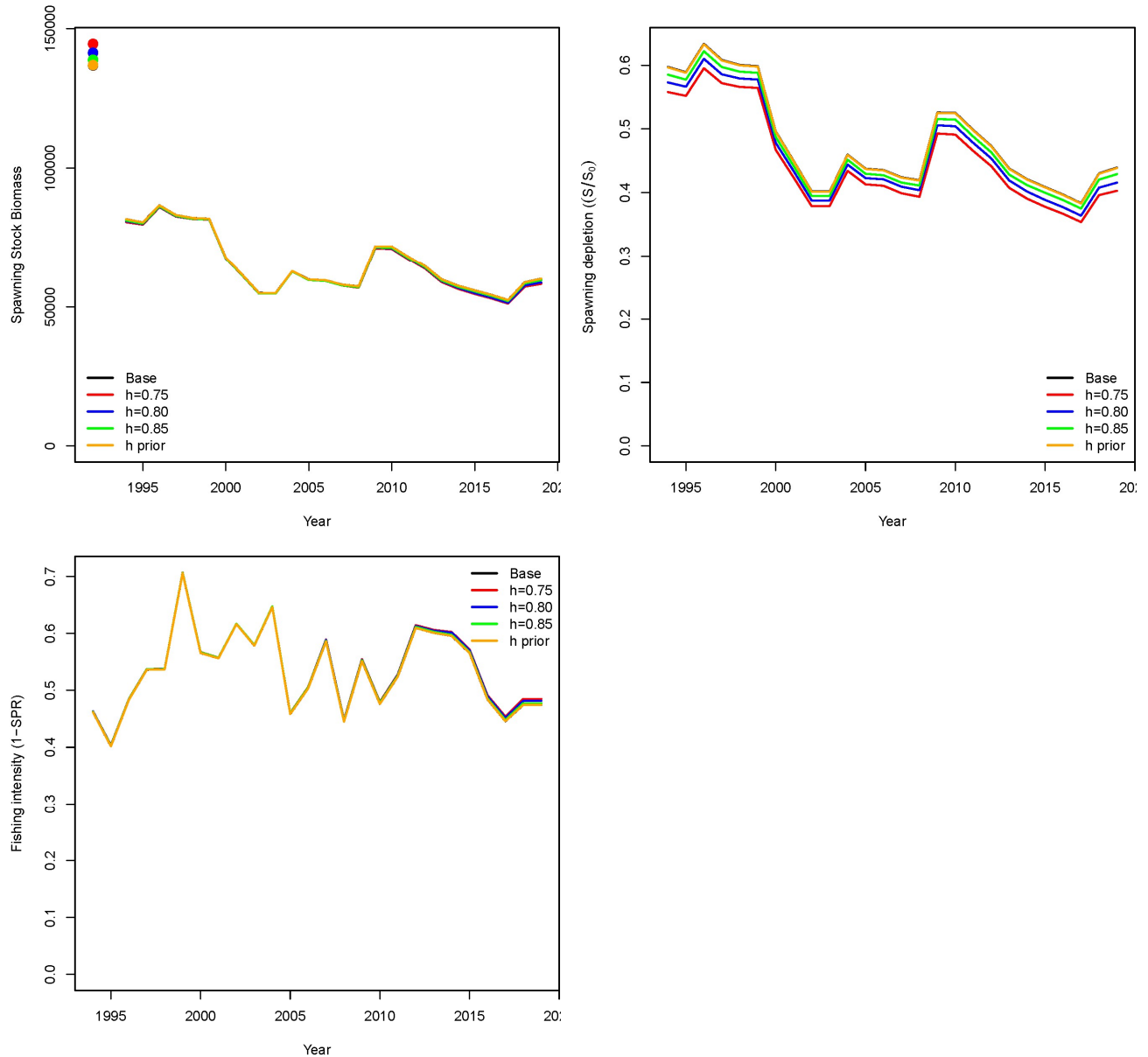


**Figure 5.17.** Estimated female spawning biomass (upper left), spawning depletion (upper right), and fishing intensity ( $1-SPR$ ) (lower) for the 2020 base case model (blue;  $h=0.90$ ) and sensitivity runs using different stock-recruitment steepness ( $h=0.75$ ;  $0.80$ ;  $0.85$ ) values, and an estimated  $h$  using a prior of  $h \sim N[0.9, (0.05)^2]$ . See Table 4.6 and Section 5.6.2 for details on sensitivity runs.

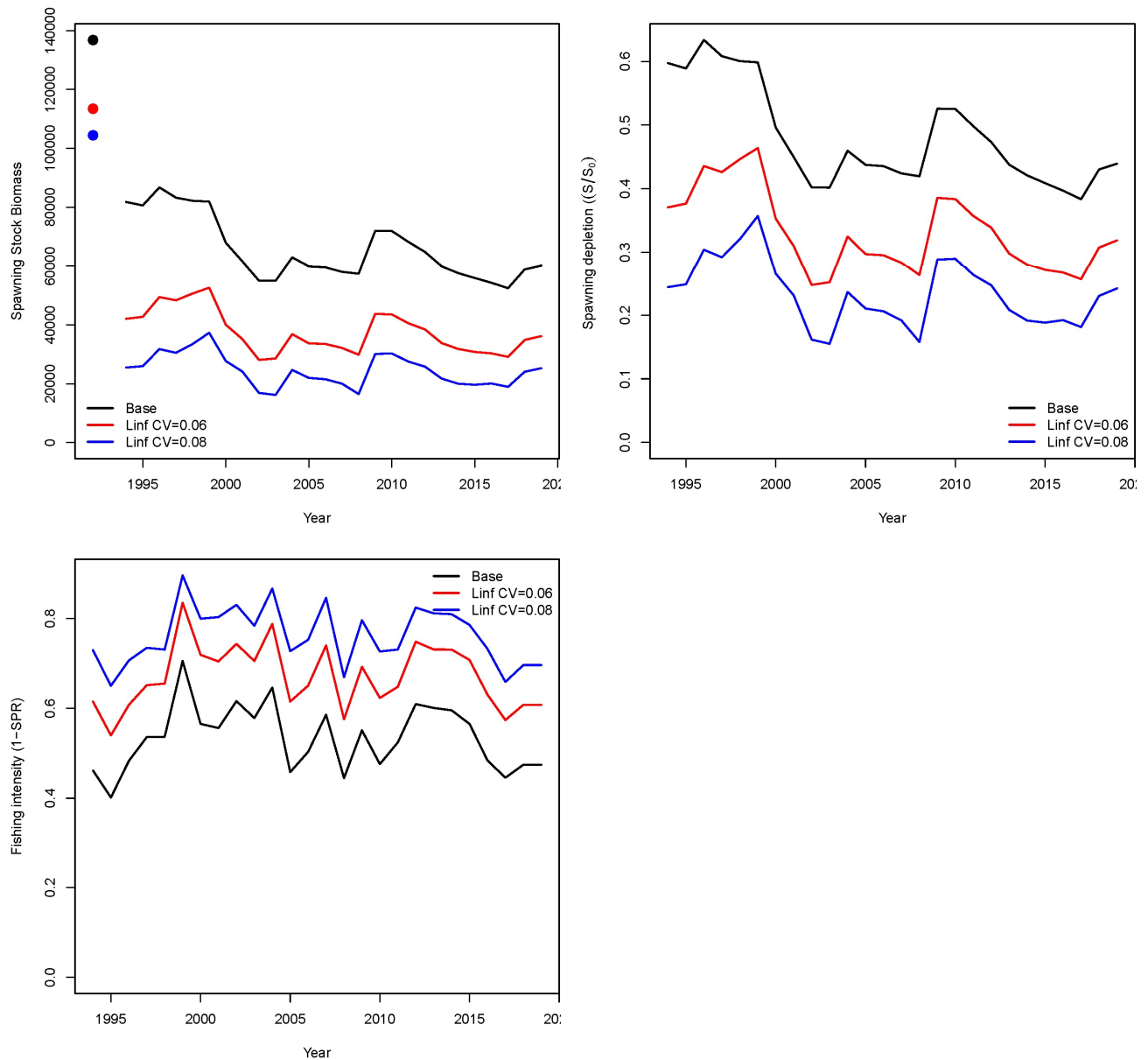


**Figure 5.18.** Estimated female spawning biomass (upper left), spawning depletion (upper right), and fishing intensity (1-SPR) (lower) for the 2020 base case model (blue) and sensitivity runs using different CV values of the  $L_{inf}$  parameter. See Table 4.6 and Section 5.6.3 for details on sensitivity runs.

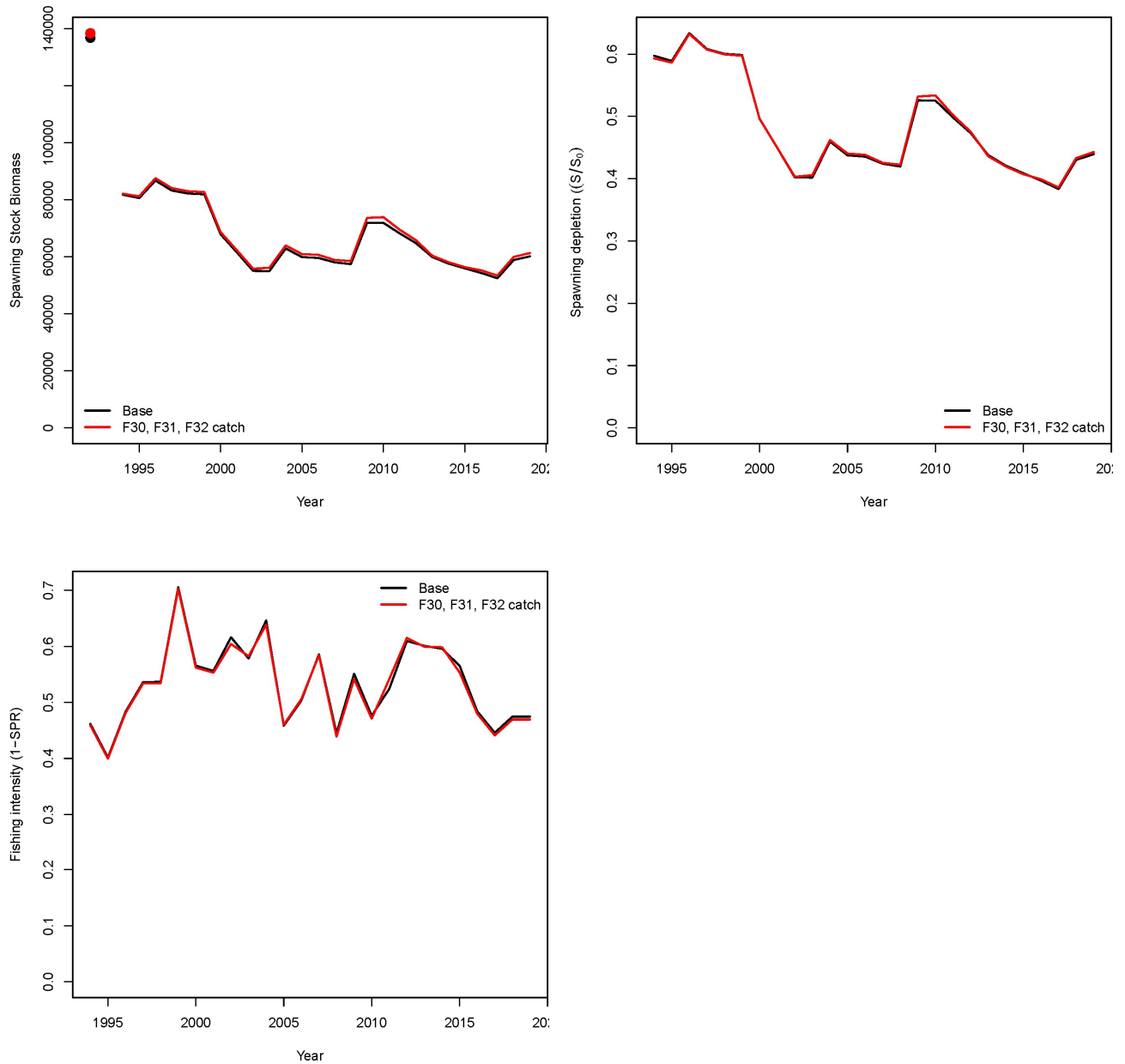


**Figure 5.19.** Estimated female spawning biomass (upper left), spawning depletion (upper right), and fishing intensity (1-SPR) (lower) for the 2020 base case model (blue) and a sensitivity run using catch time series for three fisheries (F30, F31, and F32) from the 2017 assessment for the 1994 – 2015 period. See Table 4.6 and Section 5.6.4 for details on sensitivity runs.

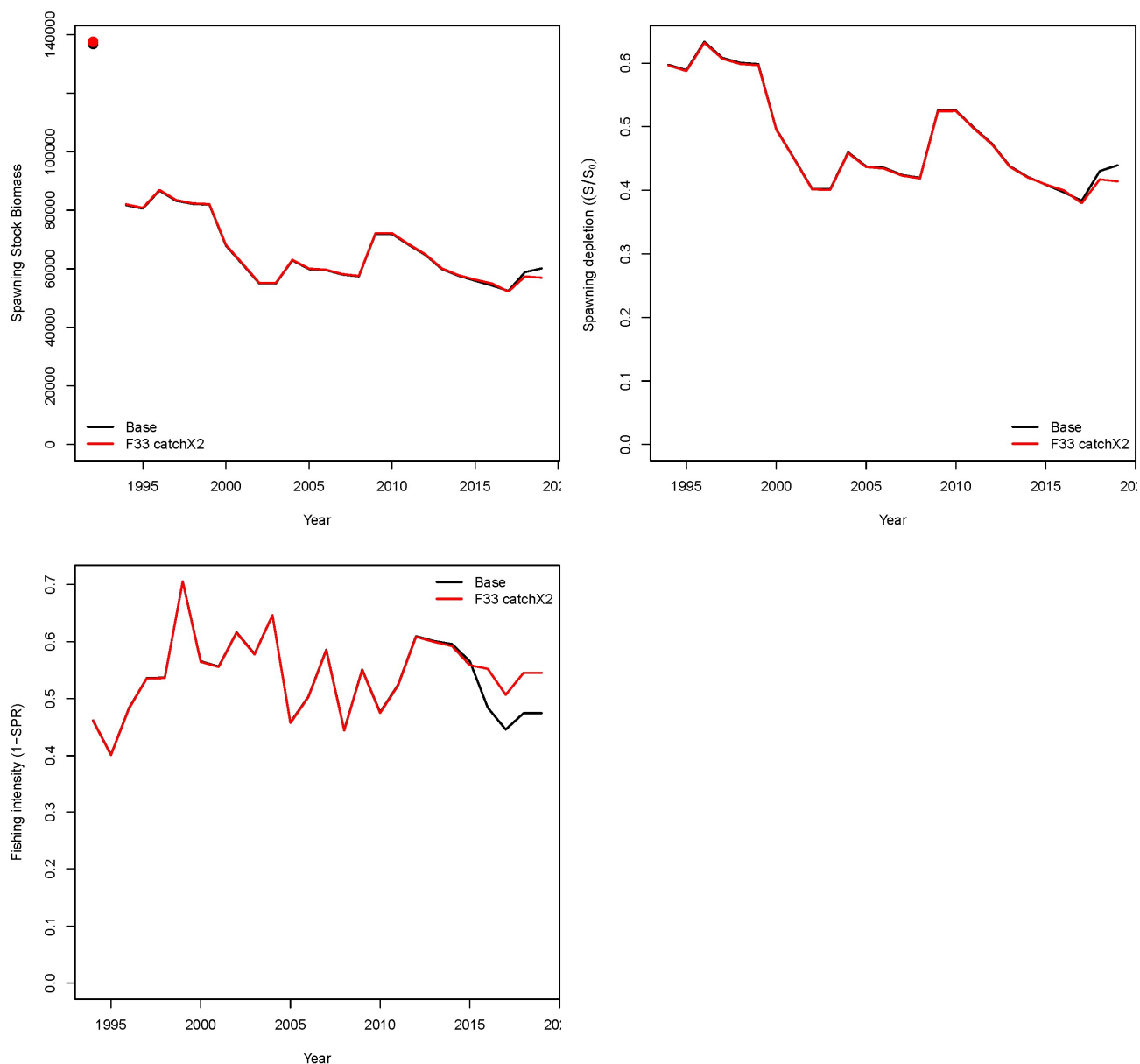


**Figure 5.20.** Estimated female spawning biomass (upper left), spawning depletion (upper right), and fishing intensity (1-SPR) (lower) for the 2020 base case model (blue) and a model run with the catch for F33 being doubled during 2016 – 2018. Note that this model run is not considered a sensitivity run because there is no evidence that the catch of F33 was substantially higher than reported during 2016 – 2018. Instead, this model run is best viewed as a ‘what if’ scenario to help the ALBWG understand what if the catch of F33 was approximately the same as previous years. See Table 4.6 and Section 5.6.5 for details on sensitivity runs.



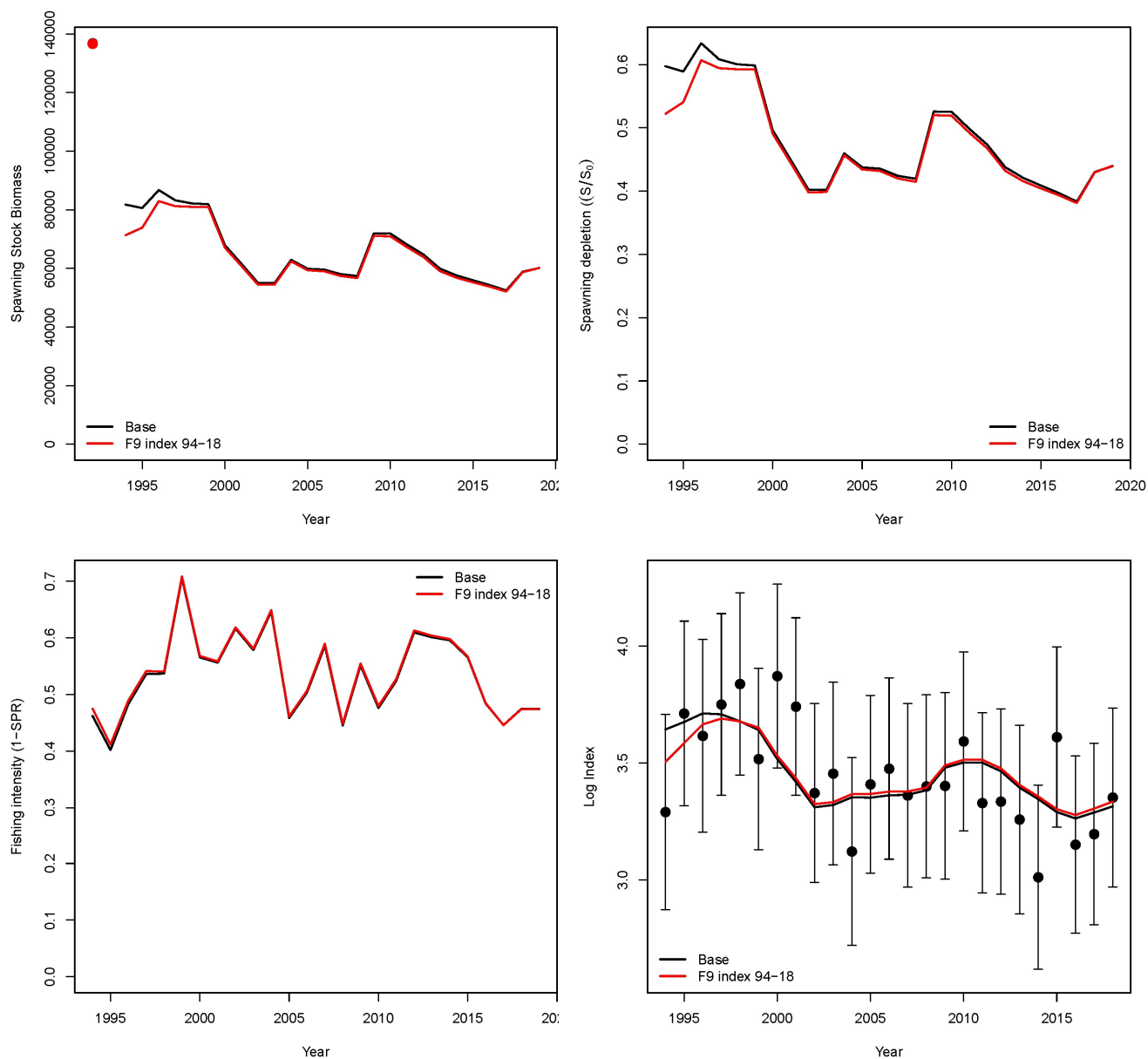


**Figure 5.21.** Estimated female spawning biomass (upper left), spawning depletion (upper right), fishing intensity  $(1-SPR)$  (lower left), and comparison between model predictions and observations of the extended F09 index (1994 – 2018) (lower right) for the 2020 base case model (black), which was fit to the original F09 index (1996 – 2018), and a sensitivity run that fitted to the extended F09 index (red). Black circles, error bars, and colored lines in the lower right panel indicate observations, 95% confidence intervals, and model expectations of the extended F09 index, respectively. See Table 4.6 and Section 5.6.6 for details on sensitivity runs.

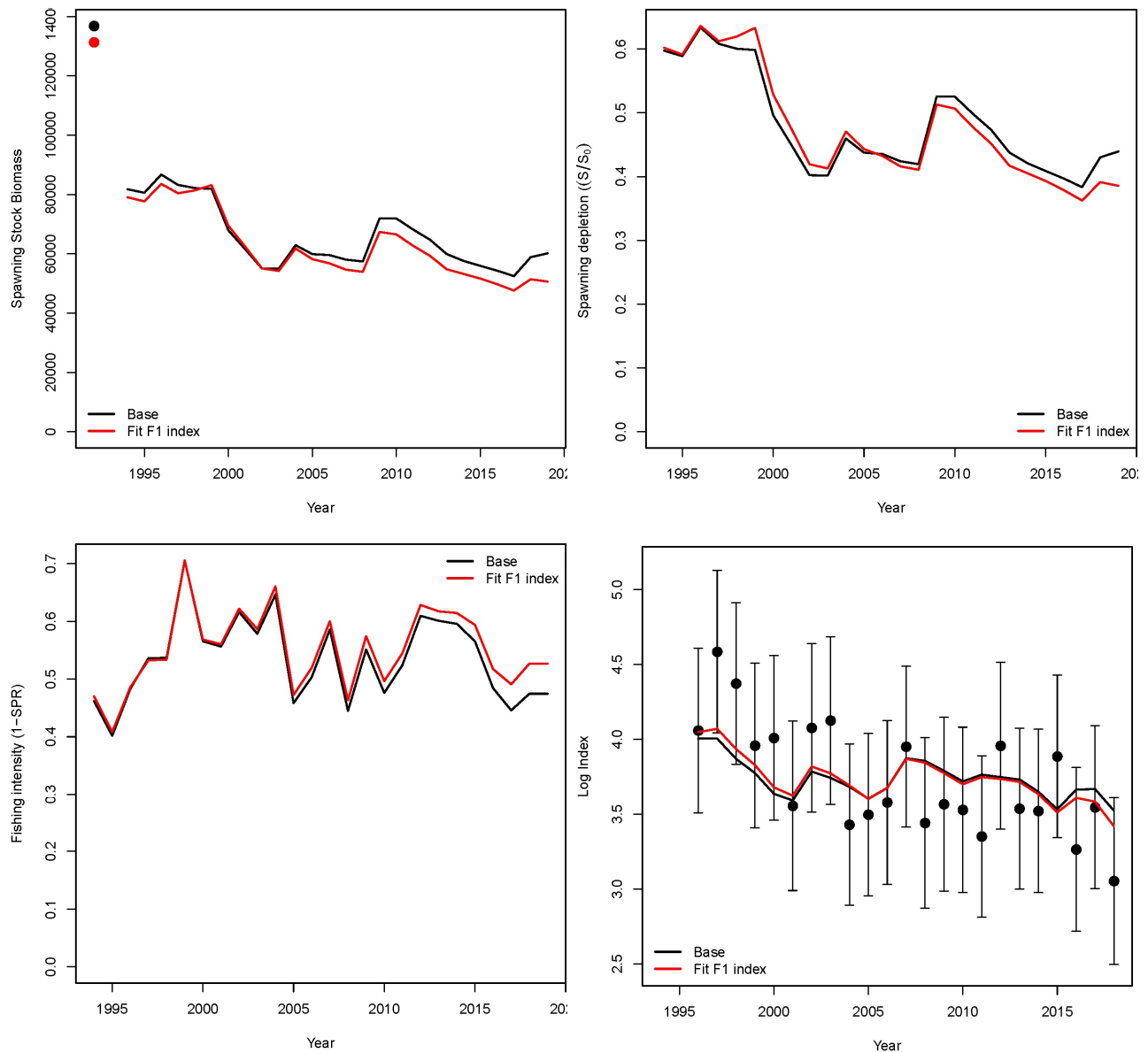


**Figure 5.22.** Estimated female spawning biomass (upper left), spawning depletion (upper right), fishing intensity ( $1-SPR$ ) (lower left), and comparison between model predictions and observations of the F01 index (1996 – 2018) (lower right) for the 2020 base case model (black), which was fitted to the F09 index but not the F01 index, and a sensitivity run that was fitted to both the F09 and F01 indices (red). Black circles, error bars, and colored lines in the lower right panel indicate observations, 95% confidence intervals, and model expectations of the F01 index, respectively. See Table 4.6 and Section 5.6.7 for details on sensitivity runs.

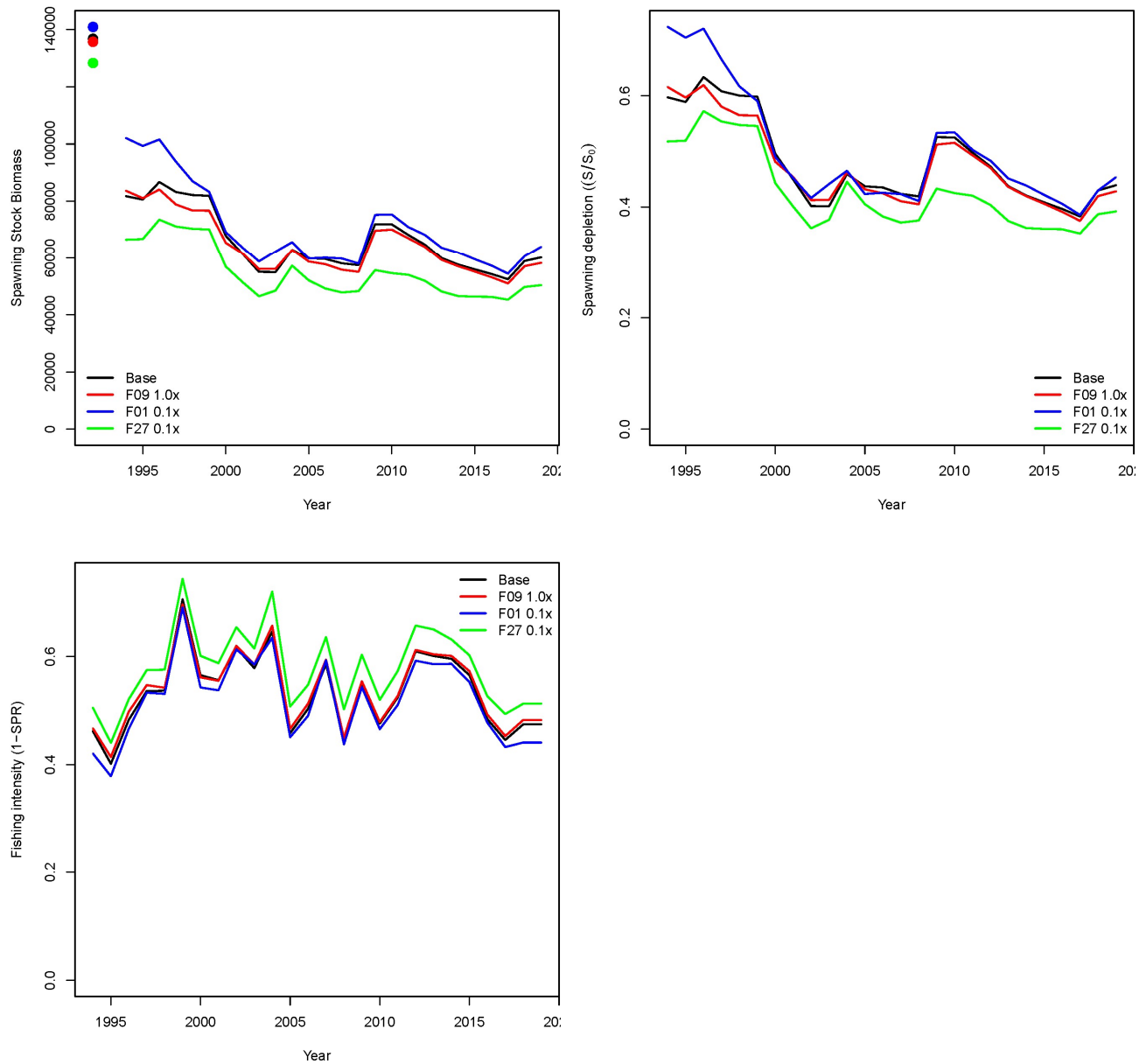


**Figure 5.23.** Estimated female spawning biomass (upper left), spawning depletion (upper right), and fishing intensity (1-SPR) (lower) for the 2020 base case model (black), where the size composition data of the F09 fishery were down-weighted (0.1x), and sensitivity runs where the size composition data from each fishery were either fully weighted (F09: 1.0x) or down-weighted (F01 and F27: 0.1x). See Table 4.6 and Section 5.6.8 for details on sensitivity runs.

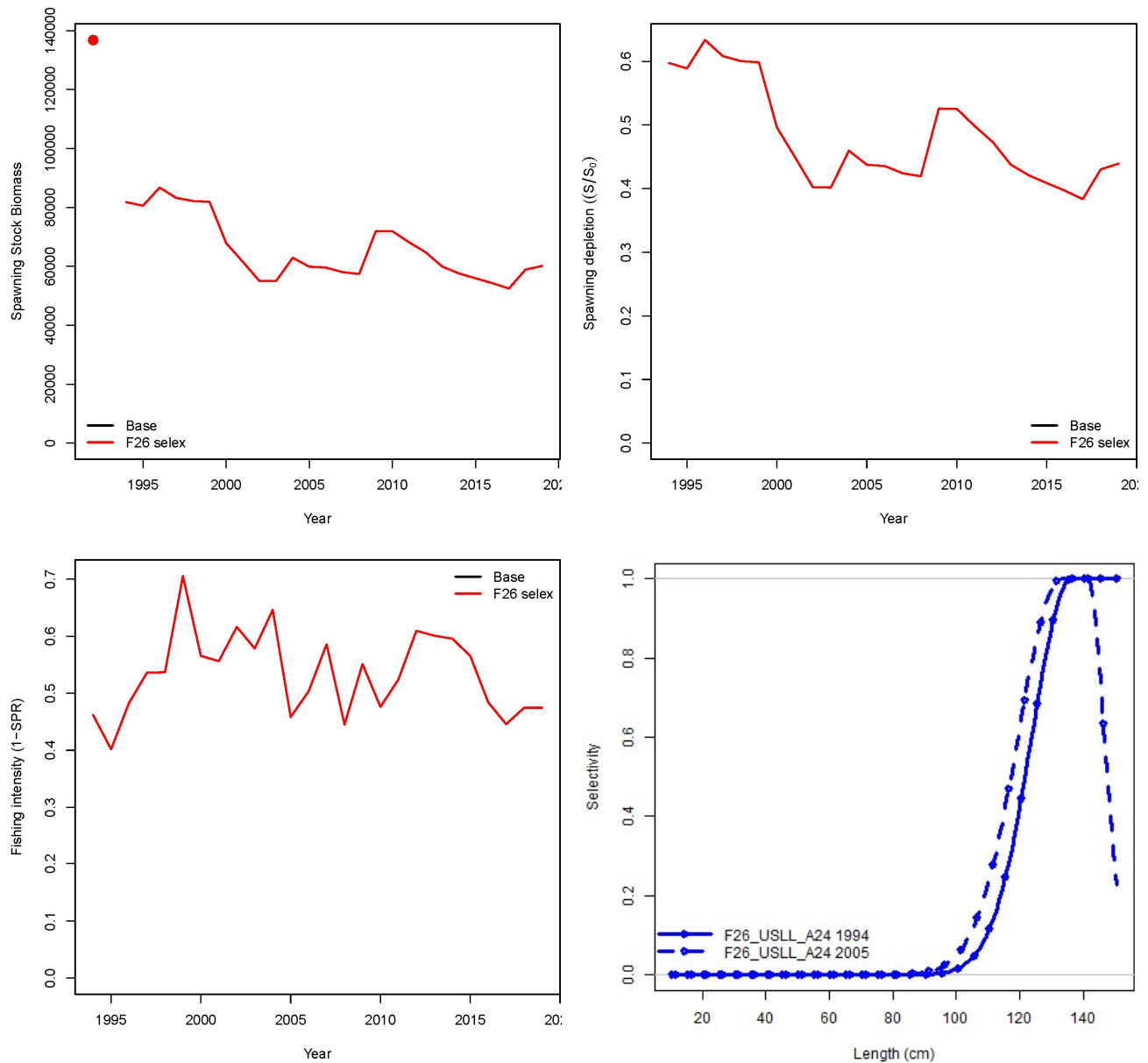


**Figure 5.24.** Estimated female spawning biomass (upper left), spawning depletion (upper right), fishing intensity (1-SPR) (lower left) for the 2020 base case model (black), where the size selectivity of the F26 US longline fishery was allowed to be dome-shaped (see Fig. 5.9), and a sensitivity run where the F26 fishery was forced to have an asymptotic selectivity (lower right). See Table 4.6 and Section 5.6.9 for details on sensitivity runs.

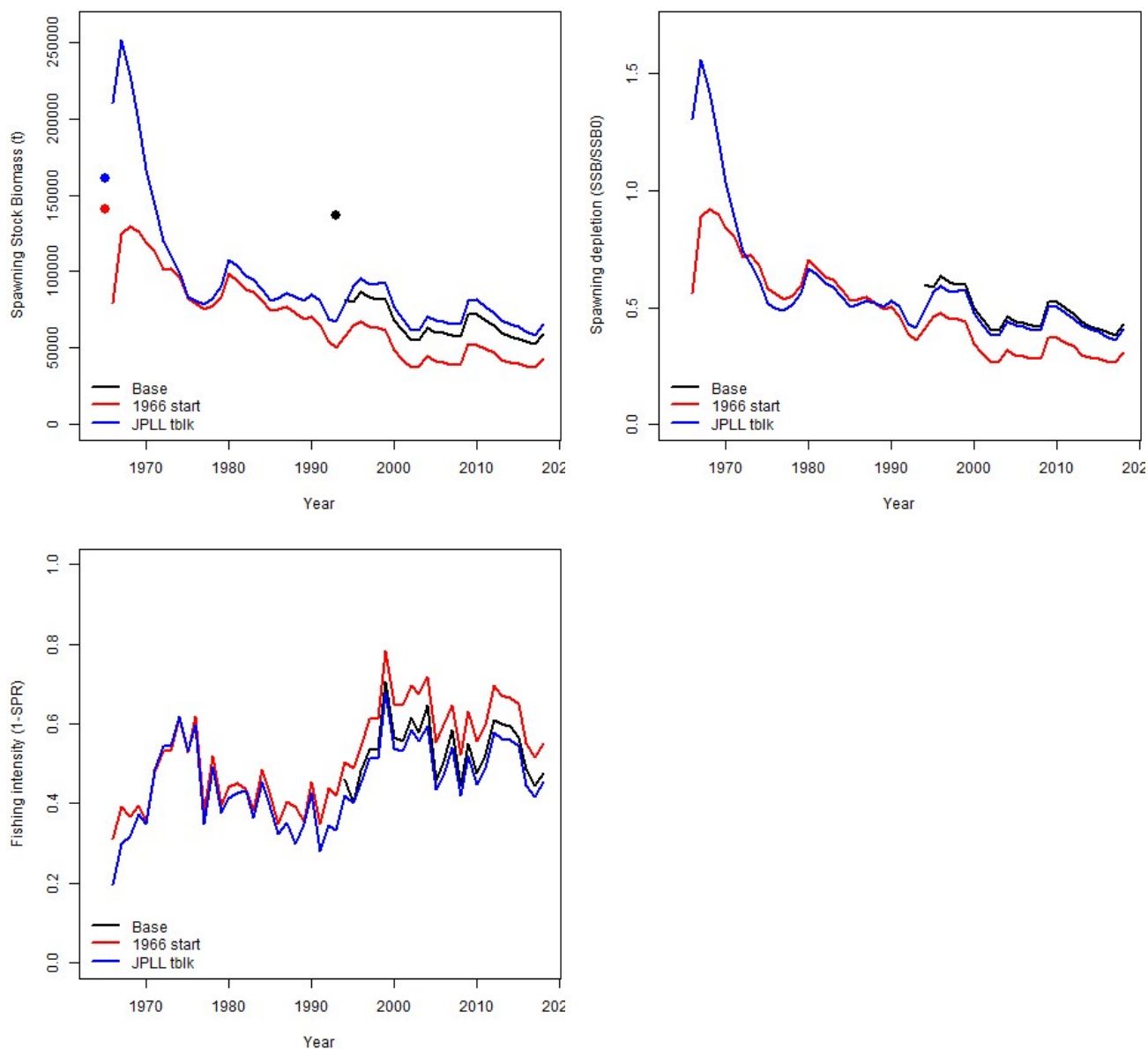


**Figure 5.25.** Estimated female spawning biomass (upper left), spawning depletion (upper right), and fishing intensity (1-SPR) (lower) for the 2020 base case model (black), a sensitivity run with a start year of 1966 (red), and a sensitivity run with a start year of 1966 and a time block for selectivity for Japanese longline fisheries during 1976 – 1993 (blue). See Table 4.6 and Section 5.6.11 for details.

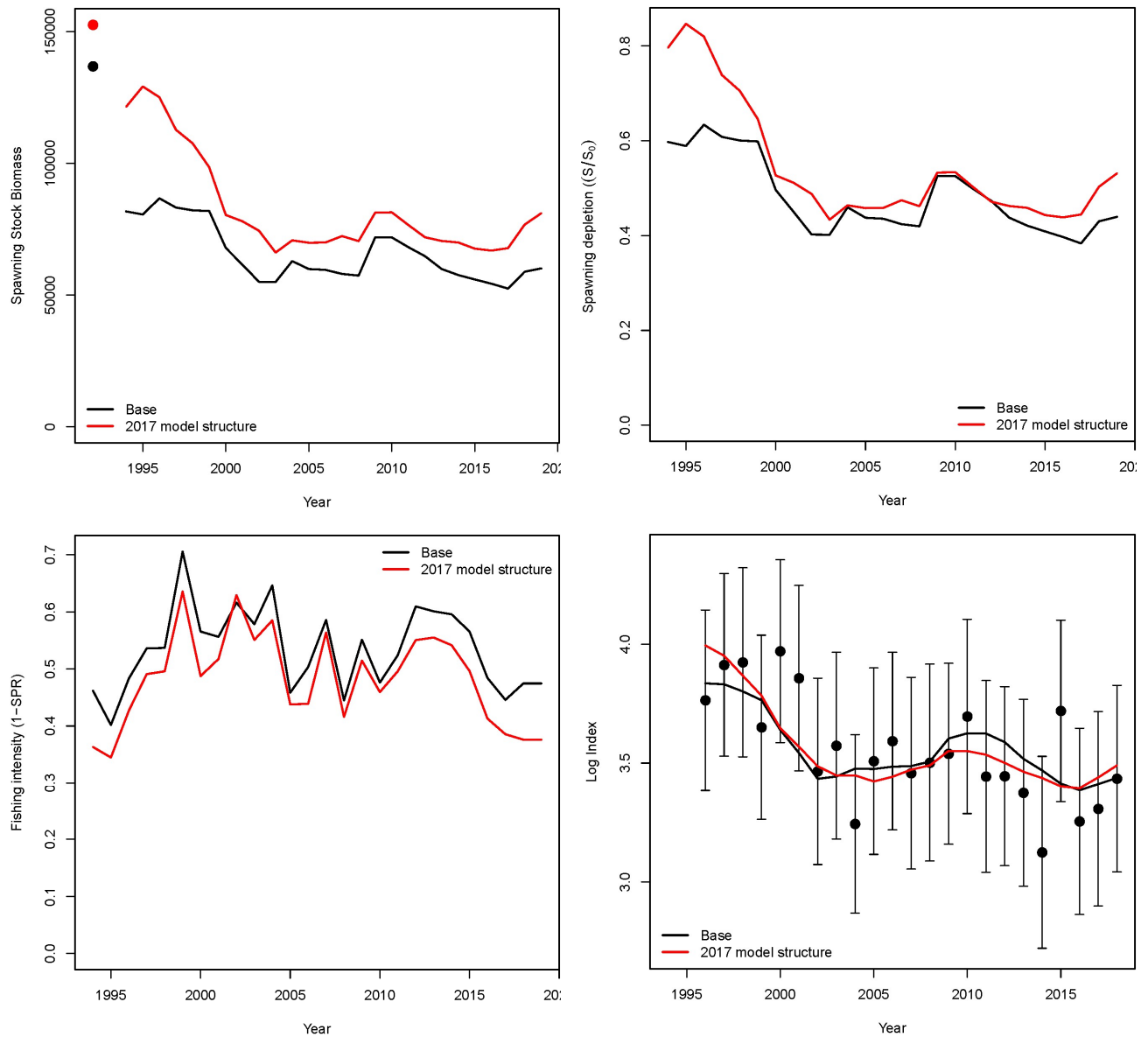


**Figure 5.26.** Estimated female spawning biomass (upper left), spawning depletion (upper right), and fishing intensity (1-SPR) (lower) for the 2020 base case model (black), and a sensitivity run that followed closely the model structure of the 2017 base case model. See Table 4.6 and Section 5.6.11 for details on sensitivity runs.

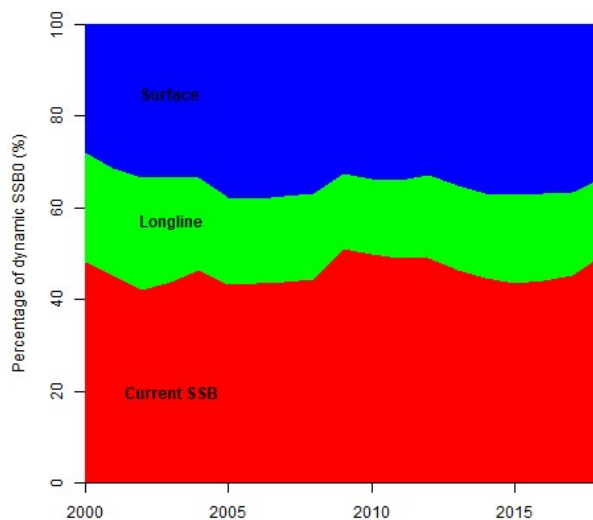


**Figure 5.27.** Fishery impact analysis on north Pacific albacore (*Thunnus alalunga*) showing female spawning biomass (SSB) (red) estimated by the 2020 base case model as a percentage of dynamic unfished female SSB (SSB<sub>0</sub>). Colored areas show the relative proportion of fishing impact attributed to longline (USA, Japan, Chinese-Taipei, Korea, China, Vanuatu and others) (green) and surface (USA, Canada, and Japan) fisheries (primarily troll and pole-and-line gear, but including all other gears except longline).

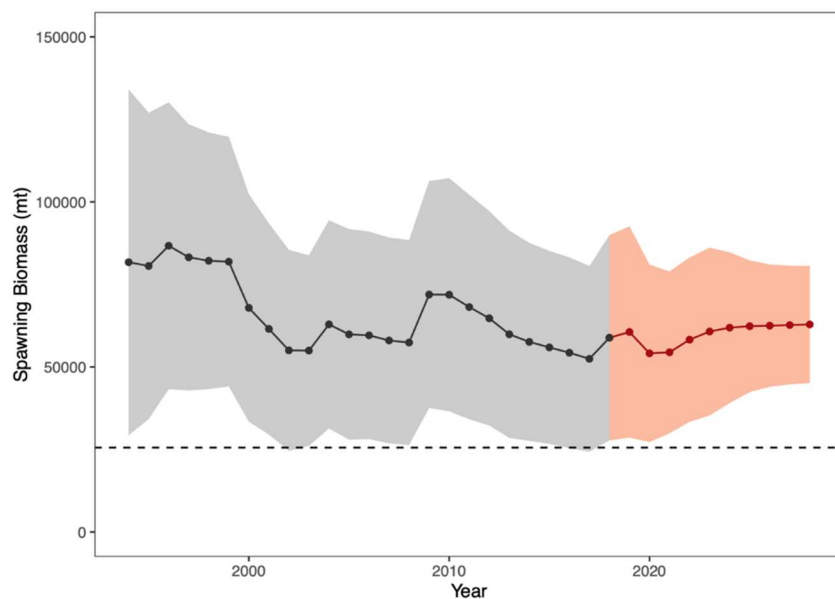


**Figure 5.28.** Historical and future trajectory of north Pacific albacore (*Thunnus alalunga*) female spawning biomass (SSB) under a constant fishing intensity ( $F_{2015-2017}$ ) harvest scenario. Future recruitment is based on the expected recruitment variability. Black line and gray area indicates maximum likelihood estimates and 95% confidence intervals (CI), respectively, of historical female SSB, which includes parameter uncertainty. Red line and red area indicates mean value and 95% CI of projected female SSB, which only includes future recruitment variability and SSB uncertainty in the terminal year. Dashed black line indicates the  $20\%SSB_{\text{current } F=0}$  limit reference point for 2018 (25,573 t).



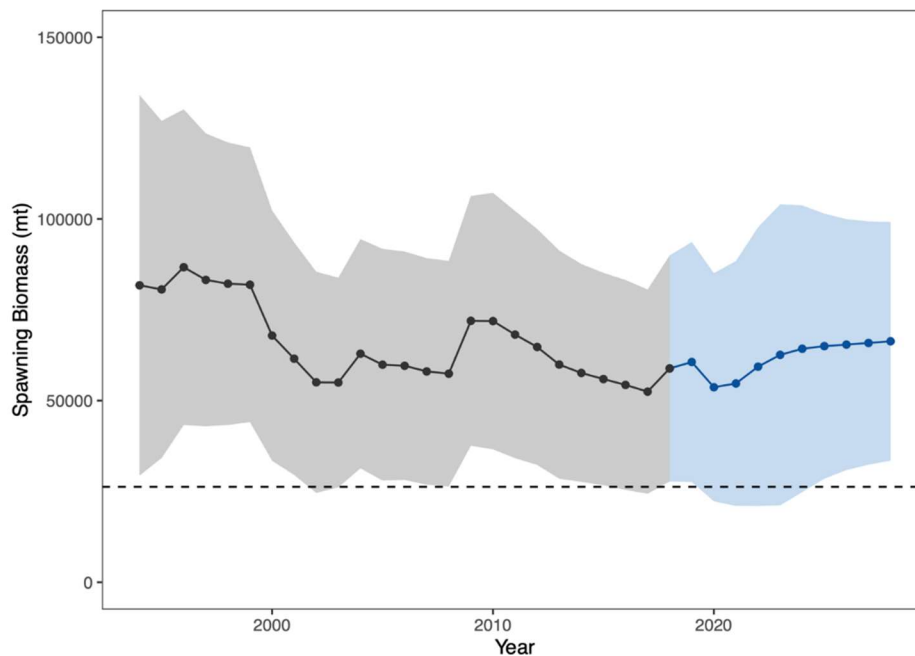


**Figure 5.29.** Historical and future trajectory of north Pacific albacore (*Thunnus alalunga*) female spawning biomass (SSB) under a constant catch (average 2013-2017 = 69,354 t) harvest scenario. Future recruitment is based on the expected recruitment variability. Black line and blue area indicates maximum likelihood estimates and 95% confidence intervals (CI), respectively, of historical female SSB, which includes parameter uncertainty. Blue line and blue area indicates mean value and 95% CI of projected female SSB, which only includes future recruitment variability and SSB uncertainty in the terminal year. Dashed black line indicates the 20%SSB<sub>current F=0</sub> limit reference point for 2018 (25,573 t).